Cupriavidus metallidurans and the biomineralization of gold

The role of bacteria in the formation of secondary gold on grains in the Australian regolith

Lintern Fairbrother

A thesis submitted for the degree of Doctor of Philosophy of

The Flinders University of South Australia

June 2013

Statement of Originality

'I certify that this thesis does not incorporate without acknowledgment any material previously submitted for a degree or diploma in any university; and that to the best of my knowledge and belief it does not contain any material written by another person except where due reference is made in the text.

Chapters 3 and 4 are published as Fairbrother *et al.*, 2013 and 2012 respectively. The co-authors provided advice and helped to write the manuscripts.

Lintern Fairbrother

June 2013

Published journal articles from this thesis

Fairbrother, L., Brugger, J., Shapter, J., Laird, J.S., Southam, G., Reith, F., 2012. Supergene Gold Transformation: Biogenic Secondary and Nano-particulate Gold from Arid Australia. Chemical Geology, 320,17-31.

Fairbrother, L., Etschmann, B., Brugger, J., Shapter, J., Southam, G., Reith, F., 2013. Biomineralization of Gold in Biofilms of *Cupriavidus metallidurans*. Environmental Science & Technology, 47(6), 2628-2635.

Acknowledgements

It takes a village. I owe my deepest thanks to many people for the guidance, friendship and encouragement I've received. During my candidature many of the following have not only helped me learn the craft but have been present during turning points and provided memorable moments that I will carry with me forever. I truly believe that without you all I wouldn't have been able to submit this thesis.

Firstly I'd like to thank my supervisory "family". Frank, you pushed me when I needed it and challenged me to rise to the level that was required. Thank you for that. It was a happy circumstance that saw you were present that night at Adelaide Microscopy, where SEM revealed the results that comprise the meat of Chapter 3. Joe, your friendly nature and ability to instill confidence in students is a gift. You have been a stream of confidence-boosting, no-nonsense advice that made the process seem much more surmountable. When I was at my most "wobbly" it was your few words of encouragement across a (free!) lunch that proved all the difference in getting me on my way. Carla, you came to our little family with a smile and a fresh take on how things should be done. I feel like your presence greased the wheels of progress for us all. A pint at the pub, a friendly chat (and a couple tricks of the trade) several years ago gave me much needed momentum that kept me rolling for a long time after. Barb and Joël, the sound of both of you laughing is a sound I don't think I will ever forget. Chocolate, cheese, coffee

and all things good often reminds me of you both and to remember to enjoy the good things in life no matter the circumstances (*i.e.,* during days and days of beamtime). Christine, it has been an absolute pleasure sharing the ups and downs of Ph.D. life with you. Your “don’t forget to smile” is still written on the whiteboard and I look at it every day.

The friends I have made at the Waite campus have taken great care of me and kept me sane. Greggs, not only did you take me under your wing in the lab, shown tremendous patience while I picked your brain about 1001 things but you have listened to me rant and rave for the better part of five years. Trying to figure you out over coffees has provided me with a world of laughs. Deb, your positivity is infectious and I swear just being around you has helped me stay upbeat in defeating the thesis monster. Szarvas, if you ever consider a career change please go into standup, the world deserves to share in your side splitting antics. I’m sitting here giggling just thinking of you. Hai, thankyou for being our master of ceremonies. You are always the one to actually organize a get together. To fellow Ph.D. students Brett and Jenna, hearing the difficulties you’ve experienced and watching you rise above them is inspirational. The late night talks have been fun and therapeutic. It’s always nice to have a laugh in the middle of the night with another “ghost-student”. To Ram and Wakelin, your words of advice had an impact greater then you could know.

This work has been supported by many institutions and as such there are too many to thank here. However it would be remiss of me if I were to not make special mention of Ben, Ken, Aoife, Angus, and the rest of the staff at

Adelaide Microscopy. You provide a professional service with a friendly air that made the basement all the more bearable.

To my family, I hope I make you half as proud as I am to be part of you. Mum, your unfathomable confidence in everything I do is a paradox in that it challenges me to reach up to your expectations and provides me the confidence to do so. Dad, you have always been there late at night to provide counsel and I always leave with the determination to just keep going. Chezza, you are a menace and I wouldn't want you any other way. I love you all to the moon and back.

Finally to my sweetheart, Gemma. You have patiently sat with me while I have stressed and brooded providing the pats, back rubs and belly scratches that are the cornerstone of my mental health. I can't imagine what it must be like to live with a Ph.D. student but you my dearest have done-so while leaving me with that feeling that at the end of the day, I will still be loved no matter how grumpy I come home.

I want to live,

I want to give,

I’ve been a miner

For a heart of gold

...

Neil Young

Abstract

Cupriavidus metallidurans dominates bacterial communities in sheet-like biofilms on Australian gold grains. This organism has the capability to take up aqueous gold-complexes (Au-complexes), precipitating gold nanoparticles and is likely a main driver of gold biomineralization in the Australian regolith. Existing biogeochemical models for the formation of placer grains have placed importance on the role bacterial biofilms play in their genesis, and in the dispersion of gold throughout the environment. However, the importance of *C. metallidurans* remains to be adequately shown. This study demonstrates the ability of *C. metallidurans* to play a key role in the geomicrobiological cycle of gold by precipitating Au-complexes in planktonic and biofilm modes of growth in regolith-simulating experiments. Active versus inactive states of cell metabolism were compared in order to define the active uptake (*i.e.*, the definable removal of gold from solution by bacteria) and passive sorption (*i.e.*, retention) of Au-complexes across a pH range. In batch experiments with Au(I)-complexes a biologically active pure culture of planktonic *C. metallidurans* cells, over 144 hours, took up a maximum of 68.9 % of the gold, present as Au(I)-thiosulfate in media that contained the minimal nutrients possible for colony growth. In contrast, 17.5 %, 7.9 % and 3.6 % was passively adsorbed by the inactive, sterile and abiotic controls respectively under identical conditions. The gold complexes, Au(I)-thiomalate, and Au(I)-cyanide were also investigated however Au(I)-thiosulfate showed the greatest variation of uptake across cell states. Thus,

columns experiments designed to optimally support microbial growth (via the use of “full” media; a largely undefined, non-selective medium comprising of all the elements most bacteria need for growth) on sand grains, saw metabolically active biofilms of *C. metallidurans* take up ~100 wt.% of gold from increasing concentrations of aqueous Au(I)-thiosulfate solutions over 84 days. This uptake of gold from Au(I)-thiosulfate by active biofilms of *C. metallidurans* resulted in the formation of gold particles associated with cells and the associated exopolymeric layer. The formation of gold occurred as isolated nano-particles, conglomerates of nano-particles directly associated with cells, and as larger (> 1 µm) extracellular spheroidal and framboidal particles. Larger particles were rod-shaped and hollow confirming assumptions that cellular processes lead to the encapsulation and replacement of cells whilst preserving their morphology. Biofilm growth of *C. metallidurans* resulted in minimum bactericidal concentrations (MBC) six times that of planktonic *C. metallidurans* cells in aqueous Au(I)-thiosulfate. This capacity to take up and precipitate Au-complexes makes *C. metallidurans* a good fit for modeling supergene gold grain genesis that also encompasses the dispersion of gold. To determine the applicability of such a model and confirm the influences of (bio)geochemical processes on the transformation of gold grains in arid Australian environments, supergene grains from eight arid sites in three Australian gold provinces, *i.e.*, Lawlers (Western Australia), Tanami (Northern Territory), and Flinders Ranges (South Australia) were collected and characterized. Collection was based on contrasting deposit styles, *i.e.*, primary underground and epithermal deposits

as well as secondary elluvial-, colluvial- and alluvial placers at increasing distances from primary mineralization. Gold grains from all surface environments displayed supergene transformation features, including spheroidal and bacteriomorphic gold, which developed and increased with distance to source. While viable biofilms and gold nano-particles and spheroidal gold µ-crystals were detected on all grains from the Flinders Ranges, gold grains from the Lawlers and the Tanami provinces were found to be covered by a polymorphic layer in which nano-particulate, spheroidal and bacteriomorphic gold was dispersed. These polymorphic layers consist of materials suggestive of remnant biofilms and due to the similarities seen on grains from the field and within biofilms in the laboratory it is concluded that biofilms capable of transforming gold grains develop periodically on gold grains in arid environments. This study shows that microbial processes, particularly those of biofilms and *C. metallidurans*, play a critical role in the transformation of supergene gold grains and contribute to the dispersion of gold and geochemical anomalies in arid environments.

Table of Contents

List of Figures

List of Tables

List of Abbreviations

at.%	Atomic percent
BSE	Back scatter electron
CAS	Chemical abstracts service
CFU	Cell forming units
CPD	Critically point dried
DGGE	Denaturing gradient gel electrophoresis
dH_2O	MilliQ water
DNA	Deoxyribonucleic acid
EBSD	Electron backscatter diffraction
EDX/S	Energy dispersive X-ray/spectroscopy
EMPA	Electron microprobe analysis
EPS	Extracellular polymeric substances
FIB	Focused ion beam
GWB	Geochemist's workbench
HPLC	High performance liquid chromatography
ICPMS	Inductively coupled mass spectroscopy
ICPOES	Inductively coupled optical emission spectrometer
ICPQ	Inductively coupled plasma quantometer
MBC	Minimum bactericidal concentrations
MIC	Minimal inhibitory concentration
MME	Minimal media
^oC	Degrees Celsius
OD	Optical density
OM	Optical microscopy
PCR	Polymerase-chain reaction
PGE	Platinum group element
PIXE	Particle induced X-ray emission
PME	Peptone meat extract
RMS	Root mean square roughness
rRNA	Ribosomal ribonucleic acid
SEM	Secondary electron microscopy
SRB	Sulfate reducing bacteria
STM	Scanning tunneling microscopy
SXRF	Micro synchrotron x ray fluorescence
TEM	Transmission electron microscopy
TOF-SIMS	Time of flight secondary ion mass spectrometry
wt.%	Weight percent
XANES	X-ray absorption near edge spectroscopy
XAS	X-ray absorption spectroscopy
XRD	X-ray diffraction
XRF	X-ray fluorescence

Chapter 1: Introduction

Metallophillic bacteria have been shown to solubilize and precipitate metals in the supergene environment. Similarly microorganisms, specifically bacteria have demonstrated the ability to solubilize and precipitate gold-complexes (Au-complexes; chemical forms of gold will be abbreviated hereon) leading to the unification of formation theories for supergene gold grains. However, for the proposed driving role that metallophillic bacteria play in gold grain formation to be conclusively demonstrated, gold uptake and precipitation by bacteria, most likely to be present around gold mineralization, needs to be shown in arid settings as it has for more temperate climes.

1.1. Gold and its presence in the supergene

Gold is a precious metal that is valued for its beauty as well as being conductive and malleable. These properties make gold valued both in industry and in economics. Gold has a rarity in the lithosphere of 5 $ng.g^{-1}$ (average) and 0.197 $mg.L^{-1}$ in natural water bodies, (average; Goldschmidt, 1954; McHugh, 1988). However, due to the stable nature of gold, despite being widely scattered throughout the environment it is not uniformly spread. Gold is commonly found in deposits, which form *in situ*, via metal rich

hydrothermal fluids permeating rocks and cooling, forming primary gold deposits (Morteani, 1999) in skarn- and vein-type deposits, igneous, volcanic and sedimentary rock as well as quartz (conglomerates and quartzite), pyrite and arsenopyrite (Boyle, 1979). In this process a number of other metals, such as copper, aluminum, iron, bismuth, lead, zinc, palladium and platinum, are incorporated but the most common minerals of gold are native gold (*i.e.*, electrum, porpezite, rhodite) and gold tellurides (Boyle, 1979). Native primary gold is typically found with gold grain concentrations ranging from 50 to 80 wt.% (Boyle, 1979). Gold is mined from both primary and secondary deposits with secondary gold found to be principally alluvial and elluvial placer deposits (Boyle, 1979). Native gold in placers, commonly occurs as grains (< 500 μm) and nuggets (> 4 mm or > 1 g; Hough *et al.*, 2007) with gold of primary origin often consisting of 5 to > 50 % silver and thus easily differentiated from most secondary gold (< 1% silver) (Boyle 1979; Webster and Mann 1984; Freyssinet and Butt 1988; Freyssinet *et al.*, 1989, 2005). Gold in surface conditions is found as metallic gold (0) or aurous (+1) and auric (+3) gold complexes (Boyle, 1979). The existence of free gold ions is thermodynamically unfavorable due to standard redox potentials of Au^{+} (1.68 V) and Au^{3+} (1.23 V) exceeding that of water (Boyle 1979; Vlassopoulos *et al.*, 1990a). Gold(I/III)-complexes with thiosulfate, halides and cyanide appear to be the most important in waters that contain little dissolved organic matter based on thermodynamic calculations and natural abundances (Boyle, 1979; Mann, 1984; Vlassopoulos *et al.*, 1990a; Benedetti and Boulegue, 1991; Gray, 1998). Thiosulfate readily solubilizes gold, with the resulting Au(I)-

thiosulfate complex $[Au(S_2O_3)_2]^{3-}$ stable from mildly acid to highly alkaline pH, and moderately oxidizing to reducing conditions (Mineyev, 1976; Goldhaber, 1983; Webster, 1986; Aylmore and Muir, 2001). Produced during the oxidation of sulfide minerals, thiosulfate is likely to dominate in groundwater surrounding gold-bearing sulfide deposits (Stoffregen, 1986). Although the general stability of gold-halide complexes follows the trend of I^- >Br^- >Cl^- (Boyle, 1979) natural abundance of Cl^- means that Au-chloride complexes are assumed to be more important than other halogens (Groen *et al.*, 1990; Gray, 1998). Oxidizing groundwater with high dissolved chloride contents, common in arid and semi-arid zones, may solubilize gold, leading to the formation of Au(I/III)-chloride complexes ($[AuCl_2]^-$, $[AuCl_4]^-$; Krauskopf, 1951; Gray, 1998). The Au(I)-chloride complex is not stable under oxidizing conditions (Farges *et al*., 1991; Pan and Wood, 1991; Gammons *et al*., 1997). In natural systems, certain microorganisms and plants form and release cyanide (Sneath, 1972; Lakin *et al.*, 1974; Campbell *et al.*, 2001). Commonly used in heap and leach operations to extract gold from the host rock, Au(I) forms a very strong complex with cyanide $[Au(CN)_2]^-$. Cyanide is present in the soil via the hydrolysis of cyanogenic plants, animals and fungi to result in the solution of gold in an oxygenated environment (Lakin *et al.*, 1974).

Group IB metals strongly bind to organic matter (Boyle, 1979; Vlassopoulos *et al*., 1990b; Gray *et al*., 1998). As such, in soil solutions with high concentrations of dissolved organic matter organic Au-complexes may be important with organic acids such as humic and fulvic acids, amino acids

and carboxylic acids shown to promote the solubilization of native gold (Freise, 1931; Baker, 1973, 1978; Boyle *et al*., 1975; Korobushkina *et al*., 1983; Varshal *et al*., 1984).

1.2. Microbially mediated solubilization and mobilization of gold in supergene environments

Solubilization is the result of oxidation of gold and complexation with suitable ligands, either present in the soil systems or excreted by microorganisms (Stone, 1997; Ehrlich, 2002; Lloyd, 2003). These stable Au-complexes can be transported to surrounding areas in a number of ways and are best summarized in Aspandiar *et al*., (2004) where mechanisms capable of Au-complex transport, such as capillary action, rising water tables and uptake by plants, are discussed.

An example of a Au-complexing ligand is thiosulfate which in the presence of oxygen leads to gold oxidation and complexation (Aylmore and Muir, 2001). In arid, surficial environments (down to 500 m below the land surface; Enders *et al*., 2006) chemolithoautotrophic iron- and sulfur-oxidizing bacteria, such as *Acidithiobacillus ferrooxidans* and *A. thiooxidans*, and archaea obtain metabolic energy by oxidizing the metal sulfides, such as gold-bearing pyrites and arsenopyrites, on which they are found (Nordstrom and Southam, 1997; Friedrich *et al*., 2005; Southam and Saunders, 2005).

These sulfide minerals are oxidized, via the formation of microbial (e.g., *A. ferrooxidans*) biofilms which provide sulfuric acid for proton hydrolysis and keep Fe(III) in the oxidized, reactive state. The valence bonds of the sulfides are then attacked by the high concentrations of Fe3+ and protons, degrading by the main intermediate, thiosulfate (Sand *et al*., 2001) resulting in the release of associated metals, *i.e.*, gold, (Southam and Saunders, 2005):

$$2FeAsS[Au] + 7O_2 + 2H_2O + H_2SO_4 \rightarrow Fe_2(SO_4)_3 + 2H_3AsO_4 + [Au] \quad (1)$$

Some iron and sulphur oxidizers (*i.e.*, *A. ferrooxidans* and *A. thioparus)* excrete thiosulfate during this process and can also be produced by other microbial processes involving different groups of microorganisms, promoting gold solubilization in other environmental zones. An example of this is sulfate reducing bacteria (SRB), which form thiosulfate during the reduction of sulfite with H_2 and formate common in anoxic metal rich sulfate-containing zones, *i.e.*, acid sulfate soils (Fitz and Cypionka, 1990). Also a common soil actinomycete, *Streptomycetes fradiae*, produces thiosulfate as a result of the metabolization of sulfur from cystine (Kunert and Stransky, 1988). In the presence of oxygen this leads to the complexation of gold (Aylmore and Muir, 2001):

$$Au + \tfrac{1}{4}O_2 + H^+ + 2S_2O^{2-}_3 \rightarrow [Au(S_2O_3)^{3-}_2] + \tfrac{1}{2}H_2O \quad (2)$$

In a study from the Tomakin Park Gold Mine in temperate New South Wales, Australia, functional and molecular community structure analyses suggested a link between the solubilization of gold and the turnover of amino acids by a heterotrophic microbial community (Reith and Rogers, 2008). The dissolution of gold by amino acids and the formation of Au-amino-acid complexes, biotic or otherwise, has been observed (Boyle, 1979; Korobushkina *et al*., 1983). Amino acids, such as glycine and aspartic acid function as metabolic precursors for the formation of cyanide (Korobushkina *et al*., 1983; Reith and McPhail, 2006). Cyanide is produced by many common soil microorganisms, such as bacteria (e.g., *Pseudomonas* sp.), algae (e.g., *Chlorella vulgaris*), and fungi (e.g., *Marasmius oreades*, *Stemphylium loti*, *Gloeocercospora sorghi*; Knowles, 1976; Basile *et al.*, 2008). Common soil bacteria such as *Chromobacterium violaceum*, *P. aeruginosa* and *P. fluorescens* are capable of producing cyanide (Knowles, 1976; Blumer and Haas, 2000; Campbell *et al*., 2001; Faramarzi and Brandl, 2006) and are common in organic-matter-rich soils such as the auriferous soils at the Tomakin Park Gold Mine. These bacteria have been shown to readily solubilize gold via cyanidation in *in-vitro* studies (Knowles, 1976; Rodgers and Knowles, 1978; Blumer and Haas, 2000; Campbell *et al*., 2001; Faramarzi *et al*., 2004; Faramarzi and Brandl, 2006; Fairbrother *et al*., 2009).

The study by Fairbrother *et al*. (2009) showed that *C. violaceum* was capable of affecting the roughness of ultra-flat gold surfaces, by solubilizing gold through the formation of free cyanide that then interacts with the gold. The production of cyanide was found to be at a maximum under growth

limiting conditions (*i.e.*, low concentrations of readily available carbon and nitrogen sources) resulting in a maximum of 15 $\mu g.mL^{-1}$ of free cyanide (based on levels in 24 and 48 hour experiments). After 56 days of incubation 125 $ng.mL^{-1}$ of gold was detected in solution or associated with *C. violaceum* cells (Fairbrother *et al*., 2009). Root mean square roughness (RMS) measured via scanning tunnelling microscopy (STM) and calculated by the software package WSxM (Nanotec Electronica, Spain; Horcas *et al*., 2007), was observed to be often double that of negative controls e.g., 0.40 and 0.21 nm respectively for 100 nm scans after 28 days incubation (Fairbrother *et al*., 2009). Gold solubilization and cyanide formation was not observed in negative controls. Thus, a possible microbial mechanism for gold solubilization in auriferous soils is the oxidation and complexation of gold with cyanide (excreted by cyanogenic microbiota) leading to the formation of dicyanoaurate complexes (Rodgers and Knowles, 1978; Faramarzi *et al*., 2004; Faramarzi and Brandl, 2006).

Biogeochemical solubilization and mobilization of gold via the formation of stable Au-complexes has been proven (Korobushkina *et al.*, 1983; Rawlings and Silver, 1995; Faramarzi *et al*., 2004; Faramarzi and Brandl, 2006; Reith and McPhail, 2006, 2007) and with an understanding of these processes the aims of this thesis, being the microbial precipitation of Au-complexes and the formation of secondary gold, similar to those observed on native gold grains, can be discussed.

1.3. Microbial precipitation of gold complexes

Gold-complexes can be highly toxic to organisms and as such microorganisms need to able to detect, and subsequently reduce gold (Witkiewicz and Shaw, 1981; Karthikeyan and Beveridge, 2002). The ability of microorganisms to actively precipitate gold may result in advantages for the survival of microbial populations by being able to detoxify the immediate cell environment, gain metabolic energy using the complexing ligands or use gold as a micronutrient (Reith *et al.*, 2007). Cell death due to toxicity will begin to occur at even very low levels of gold (Nies, 1999), however the mechanisms of gold toxicity are poorly understood. Concentrations in auriferous soils can reach more than 100 $ng.g^{-1}$ gold (McPhail *et al*., 2006; Reith and McPhail, 2006) and microorganisms may exhibit toxic effects at these concentrations.

Thus, laboratory studies have been conducted to elucidate the interactions of Au-complexes with microorganisms, Nakijima (2003), conducted a series of maximal gold accumulation experiments involving the addition of Au(I/III)-complexes to pure strains of micro-organisms and measuring gold content before and after with an inductively coupled plasma quantometer (ICPQ). It was found that bacteria demonstrated higher abilities of gold accumulation from Au(I/III)-complexes in solution than other groups of microorganisms. Tsuruta (2004), studied Au(III)-chloride bioaccumulation in 75 different species (25 bacteria, 19 actinomycetes, 17 fungi and 14 yeasts), confirmed the work of Nakjima (2003) and found that gram-negative bacteria,

such as *Actinobacter calcoaceticus* and *P. aeruginosa*, have the highest ability to accumulate gold. When fungi and algae species are exposed to Au-complexes, passive biosorption is often observed (Savvaidis *et al*., 1998; Khoo and Ting, 2001; Nakajima, 2003) with passive absorption defined as being mediated by the matrix or external organic framework of the organism. In contrast, an active mechanism is the result of metabolic activity through which a metal becomes concentrated within the tissue (Erlich, 1996; Mossman 1999; Das *et al*., 2008). Some bacteria appear to be able to selectively and/or actively precipitate gold, which suggests that gold bioaccumulation in these organisms may be part of a metabolic process. The study of gold uptake involves the exposure of bacteria to Au-complexes in microbial growth media with quantification of gold in aqueous Au-complexes typically achieved via spectroscopy (inductively coupled mass spectroscopy (ICPMS), inductively coupled plasma optical emission (ICPOES) and time of flight secondary ion mass spectroscopy (TOF-SIMS)) before and after exposure to determine uptake, while electron microscopy (transmission electron microscopy (TEM), secondary electron microscopy (SEM) and back scatter electron (BSE) microscopy) and X-ray techniques (energy dispersive X-ray/spectroscopy (EDX/S), X-ray absorption spectroscopy (XAS) and X-ray diffraction (XRD) analysis) are used to qualify resultant precipitates.

Historically laboratory studies to elucidate the formation of metallic gold by microbial uptake of gold have focused on Au(III)-chloride. Beveridge and Murray (1976) studied the uptake of Au(III)-chloride by cell wall fragments of *Bacillus subtilis.* Precipitates resulting from uptake formed with

areas of the cell walls acting as nucleation sites for the growth of microscopic gold crystals (Figure 1.1A.). These precipitates were seen to grow, exhibiting definite geometrical shapes, until they extended beyond the limits of the wall (Figure 1.1B.). This reduction and precipitation of Au(III)-chloride by *B. subtilis* was shown to be selective as a similar process did not occur for silver(I)-complexes (Beveridge and Murray, 1976). Exposure of *B. subtilis* to Au(III)-chloride in low-temperature diagenesis experiments, to simulate sediments, resulted in the immobilization of gold (Southam and Beveridge, 1994, 1996) as fine grained intracellular colloids (5-50nm; Figure 1.1C) whereupon hexagonal-octahedral gold crystals formed (20 μm; Figure 1.1D). This crystalline, octahedral gold was found to be comprised of 85.4 atomic % (at.%) gold, 0.8 at.% sulfur and 10.3 at.% phosphorus (Southam and Beveridge, 1996) and the organic phosphate compounds apparent role in the development of octahedral gold was found to be suggestive of indirect bacteria involvement, *i.e.*, the release of gold complexing agents (Southam and Beveridge, 1996).

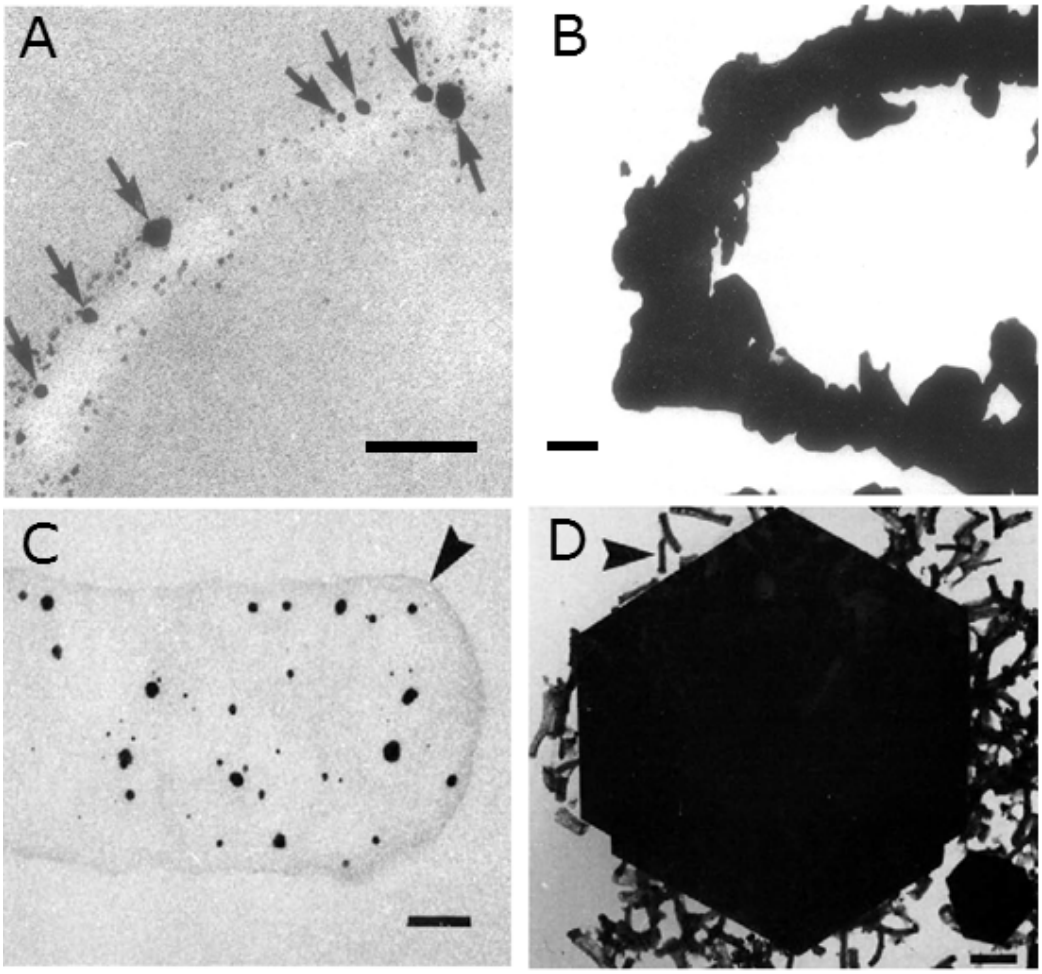

Figure 1.1. Thin sections of B. s*ubtilis* wall fragments (modified from Beveridge and Murray, 1976) with very dense, growing crystals of gold (A; arrows) and the result of growth of the same granules (B). Unstained thin-section electron micrographs (modified from Southam and Beveridge, 1994) of part of a *B. subtilis* cell (arrowhead) with gold colloids (A) and post diagenesis pellet analysis revealing octahedral gold dominating bacterial cells in which they began (D; arrowhead). Scale bars are 100 nm, 100 nm, 200 nm 2 μm respectively.

Cyanobacteria are an ancient group of prokaryotic microorganisms, one of the largest and most important groups of bacteria on earth, commonly found in natural environments and exhibit the characteristics of gram-negative bacteria (Rasmussen and Svenning, 1998). As such cyanobacterium, *Plectonema boryanum*, was exposed to Au(III)-chloride resulting in the formation of metallic gold (Lengke *et al.*, 2006a,b). Both

intracellular and extracellular precipitation of gold was observed with nanoparticles found within cells (< 10 nm) and gold platelets (1-100 μm) with octahedral habit, similar to that observed by Southam and Beveridge (1994, 1996), in solution (Lengke *et al*., 2006a,b; Figure 1.1D). The reduction mechanism of Au(III)-chloride by *P. boryanum* was studied using real time synchrotron radiation XAS and the formation of an intermediate Au(I)-species, similar to Au(I)-sulfide, was demonstrated.

Fe(III)-reducing microorganisms are capable of transferring electrons to metals and can thus influence the fate of metals in aquatic sediments, submerged soils and the subsurface (Lovley, 1995). Kashefi *et al*. (2001) studied the reductive precipitation of gold by Fe(III)-reducing bacteria (and archaea) and found gold was precipitated extracellularly by the Fe(III)-reducing bacteria, suggesting a different microbial mechanism for the accumulation of gold than other Au(III) reducers. The reductive precipitation of gold by Fe(III) microorganisms appears to be an active enzymatically catalyzed reaction that depends on H_2 as an electron donor that may involve a specific membrane bound hydrogenase (Kashefi *et al*., 2001). Reduction of Au(III)-chloride by the Fe(III)-reducing bacterium *Shewanella algae* was seen to result in intracellular gold nanoparticles (in the presence of H_2 as the electron donor; Konishi *et al*., 2006). Nanoparticulate gold 10-20 nm was seen to form in the periplasmic space and it was found that at pH 2.8, gold nanoparticles precipitated by *S. algae* were 15-200nm in size with some larger (350nm) gold particles being deposited extracellularly at pH 2 (Konishi *et al.*, 2007).

The growth of extracellular and intracellular gold nanoparticles by bacteria has been demonstrated with a range of microorganisms with Au(III)-chloride; however, thiosulfate is considered to be one of the most likely, or important, gold complexing agents in natural systems (Saunders, 1989; Vlassopoulos *et al*., 1990a). As such, it is important to investigate uptake of gold from Au(I)-complexes by microbes, specifically bacteria. Lengke *et al.* (2006a), recognized that work on bacterial synthesis of gold nanoparticles from Au(I)-thiosulfate had not been investigated and studied the interaction of gram-negative cyanobacterium, *P. boryanum*, with Au(I)-thiosulfate. Cyanobacteria were seen to release membrane vesicles that coated the cells (Figure 1.2A; presumably to prevent cellular uptake of Au(I)-thiosulfate), thus protecting sensitive cellular components (Lengke *et al*., 2006a). Gold nanoparticles (< 10-25 nm) were deposited on the surface of membrane vesicles (Figure 1.2B) and were not observed within cells. When incubated at temperatures of 60 and 200 ^{o}C the cyanobacteria were seen to be encrusted with nanoparticles of gold, mixed with gold sulfide (as determined by the results of transmission electron microscopy energy dispersive spectroscopy; Lengke *et al.*, 2006a). Similarly, the deposition of elemental gold by thiosulfate oxidizing, *A. thiooxidans* spp. (Lengke and Southam, 2005, 2006, 2007) resulted in gold precipitated inside the bacterial cells as fine grained colloids (5-10 nm) and as crystalline micrometer scale gold in the bulk fluid phase in experiments. Seven months after the population growth had stopped, wire gold had formed (Figure 1.2C). Intracellular precipitation and formation of gold nanoparticles (< 10 nm) from gold(I)-thiosulfate was also

observed in SRB (Lengke and Southam, 2006, 2007) with extracellular precipitation of octahedral gold (Figure 1.2D) forming due to the presence of localized reducing conditions, produced by bacterial energy-generating reactions (Lengke and Southam, 2006, 2007).

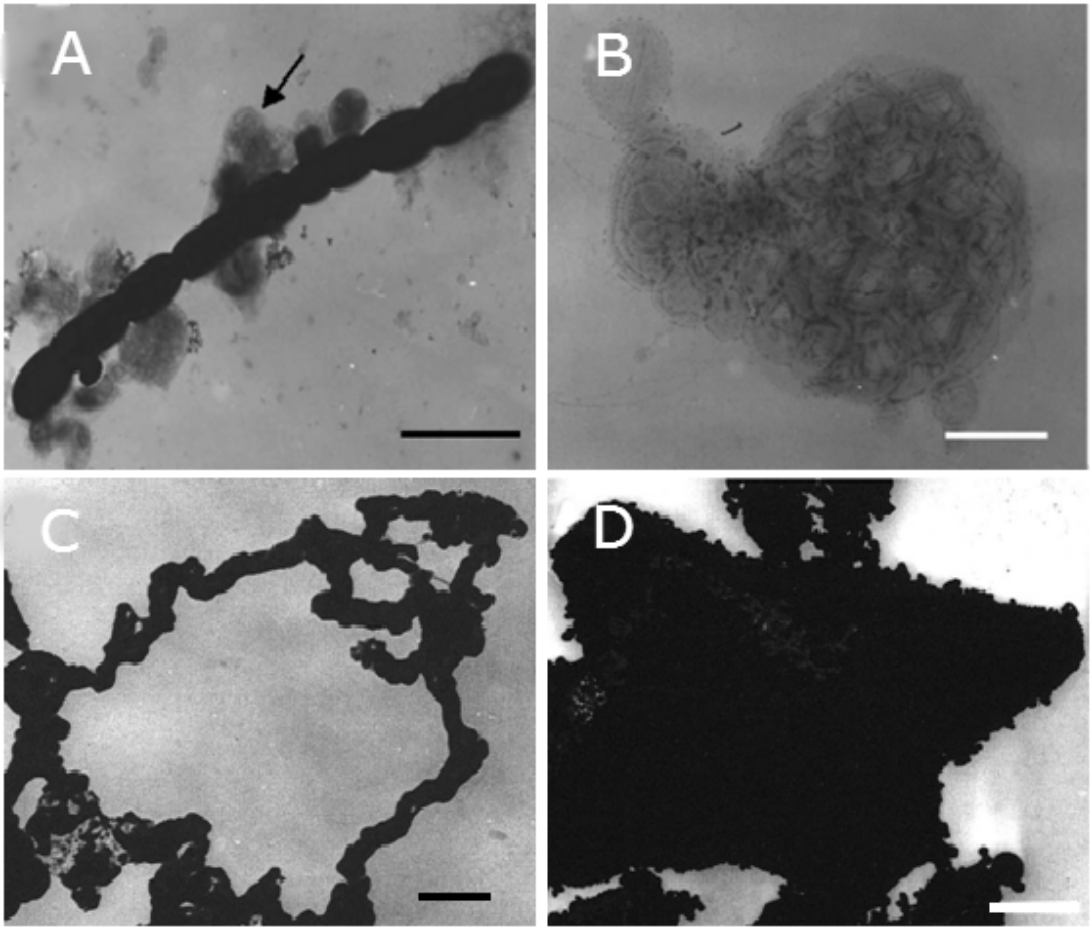

Figure 1.2. TEM of whole mounts of *P. boryanum* cultured in the presence of Au(III)-thiosulfate (modified from Lengke *et al*., 2006a), with membrane vesicles present on the exterior wall (A; arrow) and gold nanoparticles precipitated on membrane vesicles (B). TEM micrographs (modified from Lengke and Southam, 2005) of a formation of wire gold resulting from exposure of Au(I)-thiosulfate to *A. thiooxidans* (C) and octahedral gold resulting from bacterial exposure to Au(I)-thiosulfate (D). Scale bars are 5, 0.5, 0.1, 1 μm respectively.

Passive gold accumulation occurs via sulfur- and phosphorus-containing molecules (such as the carboxylates and phosphates) present in the lipopolysaccharides in the cell walls of common soil bacterial cells.

Passive uptake is thought to be the process that leads to gold accumulation along cell walls. Batch Au(III) removal experiments, conducted using inactive cells of *B. subtilis* and *P. putida* demonstrated that both species passively remove more than 85 % of the gold from Au(III)-chloride solution after 2 hours of exposure below pH 5 (Kenney *et al.*, 2012; Song *et al* 2012). However, the studies presented in this section (1.3.) point to different active, bioaccumulation mechanisms depending on whether the gold is extracellularly or intracellularly precipitated, or accumulated in minerals or exopolymeric substances (Higham *et al*., 1986; Southam *et al*., 2000; Ahmad *et al*., 2003; Konishi *et al*., 2006; Lengke and Southam, 2006, 2007; Lengke *et al*. 2006a,b; Reith *et al*., 2006). An example of this is the specific regulation of transcription by Au-complexes demonstrated by Stoyanov and Brown (2003) via metal induction experiments conducted on cultures of *Escherichia coli*. Standard enzyme assay showed that CueR, an MerR-like transcriptional activator that usually responds to Cu^{+}, is also activated by Au-complexes and that this activation is promoted by specific binding of gold (Stoyanov and Brown, 2003).

1.4. *Cupriavidus metallidurans*; gold resistance and inherent advantages

Cupriavidus metallidurans is a gram-negative chemolithoautotrophic β-proteobacterium that harbors the ability to withstand high concentrations of heavy metal ions (such as, Cu, Pb, Zn, Cd, Ag and Au; Mergeay *et al.*, 2003; Reith *et al.*, 2006) and accumulates gold (Reith *et al*., 2006, 2009b; Wiesseman *et al*., 2013).

Standard molecular genetic techniques, such as minimal inhibitory concentration (MIC), dose-response growth curves determined by optical density (OD), ribonucleic acid (RNA) isolation, polymerase chain reaction (PCR) amplification, microarrays, and deletion mutants (Nies *et al*., 1987; Sambrook *et al*., 1989; Wiesemann *et al*., 2013), have allowed the identification of gene clusters that enable cell detoxification via a number of mechanisms such as cation efflux, cation reduction, cytoplasmic accumulation, organic compound formation and complexation (Mergeay *et al*., 2003; Ledrich *et. al*., 2005). Planktonic cells of *C. metallidurans* have been shown to biomineralize gold in the form of nanoparticles from Au(III)-chloride complexes (Reith *et al.*, 2006). As a result of this reductive precipitation, cellular gold accumulation occurs via the formation of a Au(I)-S complex (Reith *et al*., 2009b), which may bind more strongly as demonstrated by Kenney *et al.*, (2012). Energy dependant reductive precipitation of toxic Au(III)-complexes, coupled to formation of Au(I)-S

promotes gold toxicity by inducing oxidative stress and metal resistance gene clusters to promote cellular defense. Gold detoxification is mediated by combination of efflux, reduction (possible methylation of Au-complexes) leading to the formation of Au(I)-C compound and nanoparticulate Au(0). Wiesemann *et al*., (2013) demonstrated the systems involved in gold transformation in *C. metallidurans* via the systematic investigation of the up-regulation of genes involved in the detoxification of reactive oxygen species and metal ions. *C. metallidurans* cells were exposed to Au(I)-complexes, which occur in this organism's natural environment, and led to the upregulation of genes similar to those observed for treatment with Au(III) complexes. A determinant (copABCD on chromosome 2) that encodes periplasmic proteins involved in copper resistance, was found to be required for full gold resistance in *C. metallidurans* (Wiesemann *et al*., 2013). The reduction of Au(I/III)-complexes appears to occur in the periplasmic space via these copper-handling systems (Wiesemann *et al.*, 2013). This ability of *C. metallidurans* to actively accumulate gold is suggestive that it actively contributes to the formation of secondary gold grains via biomineralization (Reith *et al.*, 2006, 2010; Wiesemann *et al*., 2013).

1.4.1. *Cupriavidus metallidurans* biofilms on gold grains

Active bacterial biofilms on untreated supergene gold grains from two Australian field sites, bore a 99 % similarity to *C. metallidurans* on all DNA-

positive gold grains and was not detected in soils surrounding mineralization (Reith *et al.*, 2006).

Recent research has shown that biofilms are less susceptible to metal toxicity compared to planktonic cells (Workentine *et al*., 2008; Kuimova and Pavlova, 2011) *i.e.*, single-species biofilms of *Burkholderia cepacia* and *E. coli* have shown resistance to five times higher concentrations of silver nano-particles and Ga^{3+}, respectively, compared to planktonic cells (Geslin *et al*., 2001; Harrison *et al*., 2007). The increased resistance to metal toxicity in biofilm communities is the result of the interaction of chemical, physical, physiological and biochemical factors that govern biofilm activities (Harrison *et al*., 2007). The presence of extensive extracellular polymeric layers, observed in biofilms, leads to the temporary or permanent immobilization of metal ions and complexes (Harrison *et al*., 2006, 2007). Thus the amount of toxic metal-ions, *i.e.*, gold, reaching viable cells is reduced through the reactivity of dead cells contained in the biofilms, which have been shown to rapidly accumulate transition metals (Peeters *et al*., 2008). Planktonic cells however, predominately rely on their inherent or accumulated genetic resistance mechanisms, as expressed through the number of specific and unspecific metal-resistance gene clusters, to counteract the toxic effects of metals (Nies, 2003; Harrison *et al*., 2007). *Cupriavidus metallidurans*, growing in a biofilm, drastically increases the organism's ability to sustain viable populations and thus survive toxic Au-complexes (Harrison *et al*., 2007; Wiesemann *et al*., 2013).

1.4.2. *Cupriavidus metallidurans* and the formation of secondary gold structures

Biogeochemical processes transform gold grains (via biofilms promoting the dispersion of gold by continuously recycling coarse gold and releasing nano-particulate gold (Reith *et al.*, 2007, 2010; Southam *et al.*, 2009). The rates of gold cycling in the environment is likely to be controlled by periods of biofilm growth and desiccation, which is in turn controlled by water availability (Costerton *et al.*, 1995) leading to the release of mobile nano-particulate gold in the environment. As biofilms have a limited lifespan (interrupted by episodic drying out events), formation of nano-particles and secondary (bacterioform) structures on gold grains within the biofilms occurs periodically (Reith *et al.*, 2010). Biofilms are hotspots of microbial activity and accelerate the weathering of minerals as well as the corrosion of metals (Tebo and Obraztsova, 1998; Stolz and Oremland, 1999; Ehrlich, 2002; Lloyd, 2003; Tebo *et al*., 2005; Madigan and Martinko, 2006; Nguyen *et al*., 2008). Often supergene gold grains are covered by lacelike structures that have been described as bacterial 'pseudomorphs' or 'bacterioform' secondary gold (Watterson, 1992; Keeling, 1993; Bischoff, 1997; McCready *et al*., 2003; Reith *et al*., 2006, 2010). The formation of these 'bacterioform' structures is poorly understood and has been attributed to both dissolution and (bio)-geochemical aggregation (e.g., Southam & Beveridge 1996; Lengke & Southam, 2005; Reith *et al*., 2005, 2006). In a number of studies with gold-silver alloys as well as pure gold similar 'bacterioform' structures were

produced using concentrated, hot nitric acid, suggesting that dissolution processes may be responsible for the formation of these structures (Watterson, 1994); but such extreme acidic conditions do not occur in soil or placer environments (Reith *et al*., 2007).

Recently gold grains from tropical Australia found microbial supergene processes occurring within polymorphic (*i.e.*, having many forms or shapes) layers of microbial biofilms, dominated by *C. metallidurans* (Reith *et al*., 2006, 2010). Secondary nanoparticulate gold, bacterioform gold and silicate minerals were found to be dispersed throughout the polymorphic layer that covered the surfaces of these gold grains (Reith *et al*., 2006, 2010). Such morphologies are termed secondary as they are thought to form authigenically and are up to 99 wt.% gold (Reith *et al*., 2007). Aggregates of nanoparticulate gold lined open spaces beneath the active biofilm layer and were found to be the result of precipitation of gold as internal growth structures provided direct evidence for coarsening. Between the polymorphic layer and the primary gold grain, bacterioform gold was found consisting of solid rounded forms with crystal boundaries extending from the underlying gold. Based on observations of grains from Australia, New Zealand, Africa and the Americas, secondary gold occurs in a wide variety of morphotypes, including nano- and μ-particles, triangular plate gold, sheet-like gold, bacterioform gold, wire gold as well as purely secondary gold grains (Bischoff, 1994, 1997; Reith *et al*., 2007; Falconer and Craw, 2009; Hough *et al*., 2011). These morphologies are the result of silver dealloying and gold precipitation acting simultaneously (Reith *et al*., 2007; Southam *et al*., 2009).

1.5. Formation theories of secondary structures on primary grains

The most abundant source of alluvial and elluvial gold are gold grains or nuggets between 0.1 and 4.0 mm (Mossman, 1999) the origin of which has long been the subject of discussion among those studying placers (Giusti and Smith, 1984; Groen *et al.*, 1990; Watterson, 1992, 1994; Craw and Youngson 1993; Southam and Beveridge, 1994; Youngson and Craw, 1995; Knight *et al.*, 1999; McCready *et al.*, 2003; Hough *et al.*, 2007; Reith *et al*., 2007, 2010; Falconer and Craw, 2009). Different theories of supergene gold grain formation exist; however, some formations cannot be explained by any one theory entirely. Gold grains in supergene environments are commonly coarser grained, *i.e.*, larger, than those observed in potential source rocks (Wilson, 1984; Watterson, 1992; Mossman *et al*., 1999; Reith *et al*., 2009a). A wide range of gold grain morphologies are associated with authigenic supergene gold formations, which are not commonly observed in source ore deposits. These morphologies include wire, dendritic, octahedral, porous and sponge gold (Kampf and Keller, 1982; Leicht, 1982; Lieber, 1982; Wilson, 1984; Watterson, 1992; Ma´rquez-Zavalı´a *et al*., 2004). The origin of these supergene gold grains (and nuggets) has long been the subject of study and speculation and presently several models have been established to explain their formation. These models include the detrital theory and the theory of

chemical accretion, which have recently expanded to include bacterial involvement in the biogeochemical cycling of gold.

The detrital theory involves the physical movement of primary gold through the environment via weathering of source rocks and a dealloying process (Boyle, 1979). Detrital gold grains are generally large and have an alloyed gold-silver core but are typically identifiable in that, when sectioned and measured with electron microprobe analysis (EMPA), they exhibit a rim depleted in silver (Hough *et al*., 2007). These detrital grains also have indicators of physical movement through the environment present on their surfaces, e.g. striations and rounding (Knight *et al*., 1999; Hough *et al*., 2007).

The theories of chemical accretion and bacterial involvement both involve the solubilization of primary gold, transport through the environment as aqueous complexes and eventual precipitation. The difference between the chemical and bacterial accretion theories is how suitable ligands for the complexation of gold become present in the environment; whether this is by purely abiotic mechanisms or via excretion of microbial metabolites and exudates. Precipitated gold is identified as being pulverulent, dendritic, arborescent, filiform, and aggregates, masses and more rarely foils and crystals (Boyle, 1987). Gold forming via these pathways has little silver (or other metal content) and exhibits little if any mechanical abrasion (Boyle, 1987).

These theories of supergene gold grain genesis rely on the mobility and transport of gold through the environment. In order for gold to become

mobile in the environment, from reefs or from placer gold, weathering and solubilization has to occur. Although abiotic solubilization and precipitation has been shown, a biogeochemical cycling of gold has been observed in which solubilization and precipitation occurs via microorganisms (as discussed in sections 1.2. and 1.3., respectively), and plants which occurs in conjunction with abiotic processes (Figure 1.3.; Aspandiar *et al*., 2004; Reith *et*. *al*., 2005, 2007).

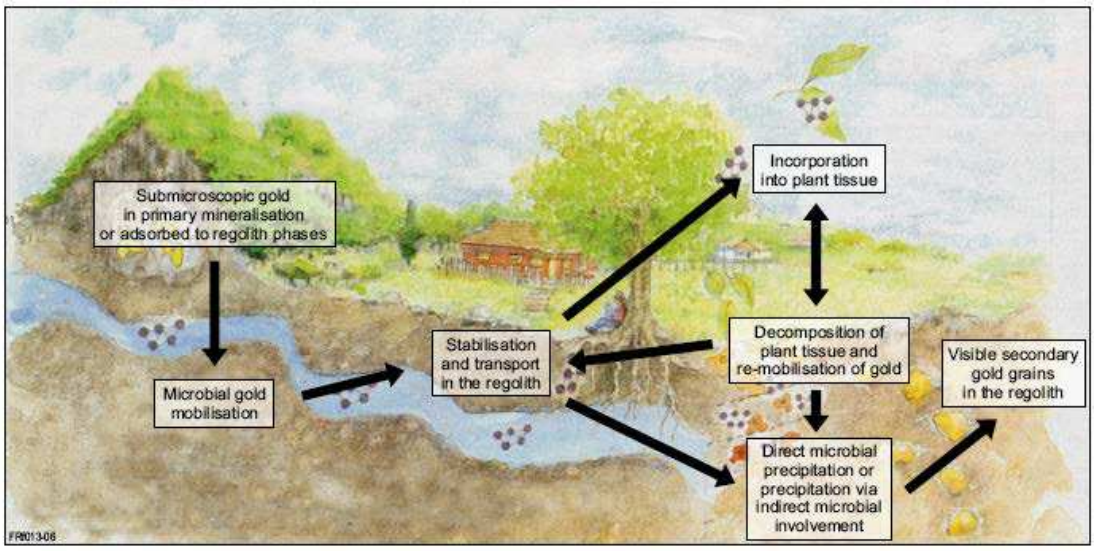

Figure 1.3. A biogeochemical model of gold solubilization and precipitation involving the formation of secondary gold in the regolith (modified from Reith *et al*., 2005).

Plants are able to take up gold (Girling and Peterson, 1980; Bali *et al*., 2010) and even reduce Au(III)-complexes to metallic gold (Armendariz *et al*., 2004; Kumar and Yadav, 2009; Raju *et al*., 2012). Plant uptake is suggested to be dependent on secretions (e.g., cyanide; Lungwitz, 1900); however, the ability of plants to accumulate gold is improved if complexing agents such as thiocyanate, cyanide, thiourea or thiosulfate solutions are present in

auriferous soils (Kulkarni, *et al*., 2009; Ebbs *et al*., 2010; Wilson-Corral *et al*., 2013).

The processes of solubilization and reprecipitation on the scale of supergene environments can also occur on the scale of individual gold grains with the grains being solubilized and gold being deposited authigenically on their surfaces (Reith *et al*., 2010). A detailed understanding of microbial activity and its effects on gold solubilization, precipitation and surfaces is important for linking the observed biogeochemical solubilization and precipitation of gold. By directly linking microbial functions of gold uptake and precipitation to existing supergene grains the understanding of the genesis and transformations of supergene gold grains in the regolith can be improved and thus an updated model proposed.

1.6. Aims, hypotheses and objectives

The evidence summarized in Sections 1.1. - 1.5. (and further elaborated at the start of each chapter) strongly suggests that metal resistant bacteria, particularly *C. metallidurans*, are involved in the formation of secondary gold on grains found in supergene settings. It is believed that this biomineralization occurs, via precipitation and solubilization of gold and Au-complexes, within biofilms surrounding mineralization.

As such, a unified model for the formation of nano-particulate and secondary gold has been proposed (Reith *et al*., 2010; Hough *et al.*, 2011). However the role of gold biomineralization and the biogenic formation of gold in this process must be demonstrated. Thus the aim of this research is to obtain direct evidence of the ability of *C. metallidurans* to take-up and precipitate Au-complexes (specifically the less studied, environmentally relevant Au(I)-complexes) and to then study and compare the morphology and composition of resultant precipitates and compare these to secondary gold features on supergene grains collected from Australian sites. To address this general aim the specific hypotheses and objectives of this research are as follows.

1. ***Cupriavidus metallidurans*** **is capable of accumulating a range of Au(I)-complexes likely to be found in the supergene environment.**

2. **Parameters such as the metabolic activity and structural integrity of *C. metallidurans* cells, as well as pH and length of exposure affects gold uptake from Au(I)-complexes in solution.**

3. ***C. metallidurans*** **biofilms precipitate metallic gold-particles to a greater extent than metabolically active planktonic cells or inactive or abiotic controls.**

4. **Secondary gold morphologies, resultant from precipitation, are comparable to those observed on natural gold grains.**

5. **Microbial biofilms, polymorphic layers or remnants thereof, are present on gold grains from arid sites and their morphology and chemical composition along with the occurrence of gold nano-particles and µ-crystals on them are indicative of biogeochemical transformations.**

6. **Surface transformations, of gold grain morphology and chemical composition, are accumulative and correspond to geobiological supergene transformations.**

To test these hypotheses the following objectives were set:

1. To measure gold concentrations in solutions before and after exposure to metabolically active, inactive and sterile cells as well as abiotic conditions across a range of pH, Au(I)-complex concentration and exposure times to determine the optimal parameters and extent of gold uptake by *C. metallidurans;*
2. To develop column experiments, based on optimal uptake conditions as determined via adsorption experiments, that will provide highly suitable conditions for gold precipitation by *C. metallidurans* from aqueous Au(I)-complexes;
3. To determine via measured gold concentration in solutions before and after exposure if uptake of Au(I)-complexes is more efficient in the presence of viable *C. metallidurans* biofilms compared to sterile and abiotic controls;
4. To use electron microscopy and spectroscopy to study the results of *C. metallidurans* (planktonic and biofilm) uptake of Au(I)-complexes and thus determine its capability to fulfill the central role of bacterial biomineralization in a model of secondary gold formation in surface environments;
5. To collect gold grains at increasing distances from primary mineralization, and characterize their composition and morphology, associated with primary, elluvial, colluvial and alluvial deposit styles from arid Australia;

6. To use microscopy techniques to assess if the morphologies of biofilms and gold biominerals formed in the laboratory are comparable to those observed on natural gold grains;
7. To evaluate the influences of (bio)geochemical processes on the transformation of gold grains in semi-arid and arid environments;
8. To assess if microbial biofilms, polymorphic layers or remnants thereof, are present on gold grains from semi-arid and arid sites;
9. To determine the occurrence of gold nano-particles and micro-crystals on gold grains from Australian supergene environments and if their presence is indicative of biogeochemical transformations;
10. To compare the effect and development of biogeochemical transformations on contrasting deposit styles, *i.e.*, primary underground and epithermal deposits as well as secondary elluvial-, colluvial- and alluvial placers; and
11. To develop an updated model of secondary gold formation in the Australian regolith.

Chapter 2: Uptake of gold from Au-complexes by *Cupriavidus metallidurans*

Abstract

Bacteria have many pathways to deal with metal-toxicity, particularly gold. Adsorption, subsequent reduction and precipitation of gold are the main mechanisms with which bacterial cells deal with toxic Au-complexes in their surroundings. This leads to creation and sorption of intermediates, such as Au(I)-S to cell walls, and the formation of nanoparticles and neo-formed gold structures, commonly observable on grains in the regolith. Although the phenomena have been researched qualitatively there is comparatively little quantitative study of uptake by metal-resistant bacteria of Au(I)-complexes. Thus, *C. metallidurans*, found to exist in biofilms on gold mineralization, was exposed to three environmentally relevant Au(I)-complexes. This was to investigate the effect of parameters such as cell metabolism, pH, exposure times and available nutrients on active uptake and passive retention by *C. metallidurans*. An observable effect of viable cells on gold uptake was greatest with exposure of Au(I)-thiosulfate occurring between 6 and 144 hours. After 144 hours, uptake by viable cells is observed at pH 7, reaching 60-70 % uptake of the gold in solution, approximately 60 times greater than the retention observed in controls. By demonstrating the ability of viable *C. metallidurans* cells to take up Au-complexes, common to ground waters

surrounding mineralization, further evidence is provided of the role that *C. metallidurans* plays in gold biomineralization. Furthermore this provides a basis for work into the determination of the role *C. metallidurans* plays in the biomineralization of secondary gold grain formations similar to those found in the supergene.

2.1. Introduction

Mobilization of gold via dissolution, complexation by microbial metabolites and/or abiotic pathways, coupled with the precipitation of said complexes results in the formation of neo-formed gold as well as the distribution of gold anomalies and halos throughout the environment (Southam *et al.*, 2009; Reith *et al.*, 2010). Bacteria play a pivotal role in this gold neo-formation on both existing supergene grains and in the regolith at large, via metal binding capabilities such as adsorption (Fein *et al.*, 1997, Pagnanelli *et al.*, 2000; Yee and Fein 2001; Borrok *et al.*, 2004a,b) and precipitation (e.g., Kashefi *et al.*, 2001; Karthikeyan and Beveridge, 2002), resulting in the passive retention, and active uptake, of Au-complexes respectively. A wide range of bacterial consortia and monoculture experiments demonstrate metal binding as a function of pH (Fein *et al.*, 1997; Yee and Fein, 2001; Borrok *et al.,* 2004b; Reith *et al*., 2009b; Kenney *et al*., 2012). Bacterial cell walls contain functional groups such as carboxyl, phosphoryl, hydroxyl, amino and

sulfhydryl groups (Beveridge and Murray, 1976; Mishra *et al.*, 2010; Kenney *et al.*, 2012), which above pH 2, have the ability to adsorb metal cations from solution (Beveridge and Murray, 1976; Fein *et al.*, 1997; Boyanov *et al.*, 2003). The simple presence of bacteria, even inactive common soil bacteria, can cause significant gold removal (Kenney *et al.*, 2012); however, this decreases dramatically with increasing pH (Reith *et al*., 2009b; Kenney *et al.*, 2012).

Metabolizing bacterial cells can also precipitate gold from Au-complexes in solution, as cell bound nanoparticles (Beveridge and Murray 1976; Southam and Beveridge 1994; Kashefi *et al.*, 2001; Karthikeyan and Beveridge 2002; Lengke and Southam 2006, 2007; He *et al*., 2006; Lengke *et al.,* 2006a,b; Reith *et al.*, 2006). *Cupriavidus metallidurans* actively reduces Au-complexes and accumulates native gold, and may provide a critical link between the precipitation of gold observed in the laboratory and the bacterioform gold observed in natural systems (Nies, 2000; Reith *et al.*, 2006, 2010). *Cupriavidus metallidurans* relies on many redundant and unspecific secondary metal uptake systems, which are transition metal transport systems with broad substrate specificity (Kirsten *et al*., 2011). An uptake system for Au-complexes is not clearly identified (Wiesemann *et al*., 2013). Gold formations resembling bacteria (pseudomorphs) and active bacterial biofilms bearing a 99 % similarity to *C. metallidurans* were found on all DNA-positive gold grains from two Australian field sites, where the organism was not detected in the surrounding soils (Reith *et al.*, 2006). *Cupriavidus metallidurans* has been shown to biomineralize gold in the form

of nanoparticles, from Au(III)-chloride complexes, which may be present in arid and semi-arid zones due to oxidizing groundwaters with high levels of dissolved chloride (Gray, 1998; Reith *et al.*, 2007). As a result of this reductive precipitation, cellular gold accumulation occurs via the formation of a Au(I)-S complex intermediate, which may bind to cells more strongly than Au(III)-complexes, as demonstrated by Kenney *et al.* (2012). This ability of *C. metallidurans* to actively accumulate gold from Au(III)-complexes is suggestive that it may actively contribute to the formation of secondary gold grains (Reith *et al.*, 2006, 2009b, 2010; Southam *et al*., 2009). Bacterial interaction with Au(III)-complexes is well documented and microorganisms can accumulate similar amounts of gold from solutions containing either Au(I)-complexes or Au(III)-complexes (e.g., Nakajima, 2003). Wiesemann *et al*. (2013) showed that biomineralization of gold particles via the reduction of Au(I)- and Au(III)-complexes appears to primarily occur in the periplasmic space in *C. metallidurans*, via copper handling systems.

A clearer understanding of the reductive uptake of Au-complexes and possible precipitation of secondary gold structures (such as nanoparticles) can be obtained through further sorption experiments. These experiments will also help to determine a passive or active uptake of gold by *C. metallidurans*. Thus, investigation must focus on microbial interaction with other complexes, specifically Au(I)-complexes that are likely to dominate in groundwaters surrounding gold deposits (Reith *et al*., 2007).

Thiosulfate has been shown to readily solubilize gold, and the resulting Au(I)-thiosulfate complex is stable from mildly acid to highly alkaline

pH, and moderately oxidizing to reducing conditions (Mineyev, 1976; Webster, 1986; Aylmore and Muir, 2001). Produced during the (bio)-oxidation of sulfide minerals, thiosulfate and thus Au(I)-thiosulfate is likely to dominate in groundwaters surrounding gold-bearing sulfide deposits (Stoffregen, 1986). The intracellular precipitation and formation of gold nanoparticles (< 10 nm) from Au(I)-thiosulfate has been observed in SRB (Lengke and Southam, 2006, 2007).

An injectable anti-arthritic drug (Brown and Smith, 1980; Berners-Price and Sadler, 1998), Au(I)-thiomalate has XANES spectra that are nearly identical to those of Au(I)-sulfide and Au(I)-thiosulfate suggestive of a similar Au-S atomic environment in these compounds (Song *et al*., 2012). Gold(I)-thiomalate has also been shown to be accumulated by *P. cepacia* when grown in a defined medium in the presence of mM concentrations of Au(I)-thiolates including Au(I)-thiomalate (Higham *et al*., 1986).

Cyanide can dissolve oxidized gold grains, forming dicyanaurate (Au(I)-cyanide) and providing a source of soluble Au-complexes for biomineralization in an environment where organisms, such as *C. metallidurans,* reside. A range of microorganisms also produce cyanide (Michaels and Corpe, 1964; Knowles, 1976; Blummer and Haas, 2000; Campbell *et al*., 2001; Faramarzi and Brandl, 2006) and contribute to transformations on gold via dissolution of gold (Fairbrother *et al.*, 2009) and accumulation (Niu and Volesky, 1999).

Although work has been conducted on qualitatively identifying uptake of Au(I)-complexes by *C. metallidurans* via speciation and genetic studies

(Jian *et al*., 2009; Reith *et al*., 2009b; Wiesemann *et al*., 2013), the quantitative uptake of gold complexes needs further study. A clearer understanding of microbial gold uptake, the first step in processes such as nanoparticle formation, is critical in understanding the genesis of biogenic deposits in the regolith. By investigating the effect of parameters, while roughly approximating regolith conditions, on % gold uptake from Au(I)-complexes in solutions, the aims of this study are to determine; 1) The effect of cell state (*i.e.*, metabolizing, inactive, or sterile) and growth medium composition (pH and length of exposure) on the amount of gold taken up; 2) If uptake of Au(I)-complexes by *C. metallidurans* is primarily an active mechanism or a function of adsorption to components of the cell wall; and 3) The most responsive Au(I)-complex and media (in terms of an observable biotic effect) for further gold-bacteria interaction experiments.

2.2. Materials and methods

2.2.1. Bacterial growth

Cupriavidus metallidurans glycerol stocks were grown up on agar plates (PCA, Oxoid Ltd., USA). A colony was then selected and placed into 500 mL of 1:1 peptone meat extract (PME, Dicfo^{TM}, USA) at pH 6.5, 25 ^{o}C, 100 rpm on a shaker plate for 24 hours, or tris-buffered minimal medium (MME) at pH 6.5, 30 ^{o}C, 200 rpm for 48 hours. The MME was prepared by the methods

described by Mergeay *et al.*, (1985). To provide a carbon source 2 $g.L^{-1}$ of sodium gluconate was added. Cells were harvested by centrifugation at 3,000 x g for 20 minutes, discarding the supernatant and washing the cells by vortex in sterile filtered 0.9 wt. % saline (9 $g.L^{-1}$ NaCl) solution. Cells were then spun down again and the supernatant discarded once more. Fresh 0.9 wt. % saline solution was added and the cells stored at 4 ^{o}C. This solution served as the stock solution for the inoculation of uptake experiments.

The next stage of the experiments was conducted in 2 mL tubes. Uptake experiments were conducted in three growth mediums (PME, MME and ultrapure milliQ water (dH_2O)) in order to further understand the degree of both passive and active mechanisms on gold uptake in *C. metallidurans*. As both MME and PME contain organics with which gold sorption and/or complexation may occur, uptake experiments in dH_2O allows investigation in the absence of any organics or carbon source for the organism. For uptake experiments with full media, 2 mL of PME was inoculated with 10 μL of the *C. metallidurans* inoculation stock at neutral pH and incubated for 24 hours at 100 x rpm and 25 ^{o}C. In experiments with minimal media, 2 mL of MME was inoculated with 10 μL of the MME *C. metallidurans* inoculation stock at neutral pH, incubated for 48 hours at 200 x rpm and 30 ^{o}C as per Reith *et al.* (2009b). These differing incubations were to ensure the stationary growth phase was reached before uptake experiments began. Experiments without nutrients were run in dH_2O and prepared by inoculating 2 mL of dH_2O with 10 μL of *C. metallidurans* stock at neutral pH for 24 hours at 100 rpm and 25 ^{o}C.

Cells were spun down at 10,000 x g for 5 minutes, the supernatant discarded, and the cells washed. The cells were then spun down again, the supernatant discarded and placed in fresh 0.9 wt. % saline, following which bacterial cells were prepped for conditions of the absorption experiments. Cells that were to be viable and fully functioning during experimentation were simply stored in the dark at 4 ^{o}C. Live full functioning *C. metallidurans* cells will be termed “viable” cells throughout the thesis. Most bacteria live in areas of nutrient-poor conditions (Erlich, 1996; Kenney *et al*., 2012) and are not actively metabolizing and, as such, passive cell wall adsorption becomes an important factor and it is important to understand the role such bacterial cells play in the geomicrobiological cycling of gold. Thus, cells that were intact but non-functioning (termed “inactive” throughout the thesis) were also studied. Cells were prepared by treatment with 1 mL of 0.1 % formaline for six hours, washed and stored at 4 ^{o}C as per Reith *et al.*, (2009b). A control consisting of presumably lysed and non-functioning cells (termed “sterile” throughout the thesis) were prepared via autoclaving under standard conditions (121 ^{o}C for 20 minutes) then stored at 4 ^{o}C. The cells of all conditions were stored at 4 ^{o}C for a maximum of 24 hours before gold uptake experimentation began. Controls containing no cells were prepared by autoclaving 2 mL tubes in the absence of any inoculation (these are termed “abiotic” controls throughout the thesis).

To ensure purity of cultures, DNA was extracted using UltraClean Microbial DNA kit (MoBio, CA, USA). Community structures were analyzed using PCR-denaturing gradient gel electrophoresis (DGGE) profiling of a

variable region of the 16S rRNA gene. Bacteria-specific PCR primers F968-GC and R1401 were used and a 16S rRNA PCR-DGGE analysis was conducted against a *C. metallidurans* control using an Ingeny PhorU system (Ingeny International, The Netherlands).

2.2.2. Gold retention experiments

Stock gold solutions were prepared for each of the complexes in sterile, syringe filtered dH_2O. The three complexes studied here; Au(I)-thiosulfate (sodium aurothiosulfate; $AuNa_3O_6S_4$, 490.19 M), Au(I)-thiomalate (Sodium aurothiomalate; $C_4H_3AuNa_2O_4S$, 390.08 M) and Au(I)-cyanide (Potassium dicyanoaurate; C_2AuKN_2, 288.10 M) were prepared from analytical reagents obtained from Alfa Aesar (CAS 15283-45-1) Sigma-Aldrich (CAS 12244-57-4) and Aldrich (CAS 13967-50-5) respectively. Growth media (PME, MME or dH_2O) were adjusted to pH 4-10 (via NaOH or HCl) allowing both the passive retention of gold at low pH and the effects of maximal cell numbers on gold uptake to be observed. The pH of solutions was measured before exposure to cells using a Hanna Instruments H11134 pH-electrode with a CyberScan pH 310 meter. The meter was calibrated using Colourkey buffer solutions at pH-values of 3.98-4.02, 6.98-7.02 and 9.95-10.05 (at 20^{o}C; VWR International Ltd., Poole, England). Aliquots from the stock solutions were added in order to obtain the desired concentrations of Au-complexes. Two mL of the pH-adjusted and gold-amended solutions were then syringe filtered

(0.22 μL, GM sterile syringe filters) and distributed to the viable cells and controls (inactive, sterile and abiotic). Immediately following the inoculation process, 100 μL was collected, from replicates run in parallel, to establish starting cell forming units ($CFU.mL^{-1}$) via classic plate counting techniques (Miles *et al.*, 1938). The cells (and abiotic vials) were incubated for 6 and 144 hours in the dark in order to simulate the regolith environment. The PME and dH_2O experiments were incubated at 25 ^{o}C at 100 x RPM, whereas the experiments in MME were incubated at 30 ^{o}C at 200 x RPM. Experimentation was carried out in triplicate, with data collected averaged and standard deviation calculated (presented in parentheses or represented as error bars). It is important to understand that the addition of a solid Au-complex to media may not result in the formation of the same Au-complex in solution. Wiesemann *et al*., (2013) modeled the speciation of sodium Au-thiosulfate hydrate and potassium dicyanaurate in MME using Geochemist's Workbench (GWB). Due to the undefined nature of PME its modeling was not conducted. Wiesemann *et al*., (2013) found that in MME titrated with Au(I)-thiosulfate, > 99.9 % of gold exists as a Au(I)-thiosulfate complex and in MME amended with $AU(CN)_2^-$ > 99 % exists as the dicyanaurate(I)-complex (Au(I)-cyanide; Wiesemann *et al*., 2013).

2.2.3. Analysis of solutions

Following incubation, samples were vortexed to obtain a homogenous solution and 100 µL collected for the determination of final CFU.mL^{-1} numbers. The samples were spun down (10,000 x g for 5 minutes), the supernatant collected and analyzed for gold content along with the stock gold solutions. This was done in order to achieve gold concentrations before and after incubation. Gold concentrations were determined using an Agilent 7500cs ICP-MS (Agilent Technologies, Japan) and detection limit (0.4 µg.L^{-1} gold) was determined via the use of an internal indium standard and calibration curves prepared from stock gold solutions. The concentration of gold that was removed in each system was calculated by subtracting the concentration of gold remaining in solution at the end of the experiment from the original gold concentration at the beginning of the experiment. By subtracting the abiotic uptake from that observed in the viable, inactive and sterile conditions the biotic effect was determined.

Cell counts were conducted following the technique of Miles *et al.* (1938). This technique involves eight 1:10 serial dilutions in 0.9 wt. % NaCl to x 10^{-8}. These solutions were pipetted onto plate count agar and CFUs counted manually.

2.3. Results and discussion

The following sections are presented with uptake of gold from Au(I)-thiosulfate first (Section 2.3.1.), as this was seen to have the most variation, with the affects of both full and minimal media discussed therein (Sections 2.3.1.1. And 2.3.1.2., respectively). Uptake of gold from Au(I)-thiomalate and Au(I)-cyanide follows (Sections 2.3.2. and 2.3.3.) with the exception that uptake investigations at lower gold concentrations are included in the case of Au(I)-thiomalate (Section 2.3.2.3.). Uptake from the three complexes in the absence of a growth media is presented last (Section 2.3.4.).

2.3.1. Gold uptake from Au(I)-thiosulfate by *Cupriavidus metallidurans*

Of the three complexes studied Au(I)-thiosulfate displayed the largest contrast in uptake by viable cells compared to the retention of gold in controls (Table 2.2.). Uptake by the viable cells is shown to be easily definable over passive retention observed in controls (Figure 2.1.) and this may suggest an active mechanism. The Au(I)-thiosulfate complex was the least affected by organics within the growth media used (Table 2.1.), with a biotic effect on uptake of Au(I)-complexes only observable in MME. Thus Au(I)-thiosulfate serves as a good complex for further investigation for Au-cell interactions in the study of gold grain formation in the regolith.

2.3.1.1. Retention of gold from 500 μM Au(I)-thiosulfate in full medium

After six hours exposure to 500 μM Au(I)-thiosulfate in PME, accounting for standard deviation, the uptake by the viable cells at pH 4-10 is comparable to that of the sterile and abiotic controls (Table 2.1). The *C. metallidurans* cells survive in pH 4-9 with cell numbers reaching an expected maximum at pH 7 (1.4×10^5 CFU.mL^{-1}) and no growth observed at pH 10. While the conditions at pH 7 are optimum for the growth of viable *C. metallidurans*, the growth of cells is inhibited above pH 9 and this is likely due to the lysis of the cells due to the alkaline conditions on the cell surface (Bimboim and Doly, 1979).

Table 2.1. Summary of gold retention from 500 μM Au(I) thiosulfate, by *Cupriavidus Metallidurans* in different metabolic states, in PME media for 6 hours at pH 7.

pH	Gold retention by viable cells [%]	Gold retention by sterile cells [%]	Abiotic retention of gold [%]
4	24.8 (± 9.2)[a]	20.6 (± 15.7)	30.2 (± 3.0)
5	25.1 (± 2.5)	21.0 (± 7.3)	29.8 (± 3.3)
6	13.9 (± 11.5)	26.0 (± 10.7)	34.9 (± 1.0)
7	13.1 (± 13.7)	24.7 (± 17.9)	36.3 (± 3.5)
8	11.2 (± 8.3)	29.0 (± 7.3)	32.6 (± 2.3)
9	21.4 (± 4.2)	12.4 (± 7.8)	31.8 (± 2.6)
10	13.2 (± 10.1)	22.6 (± 8.6)	31.7 (± 6.3)

[a]Gold uptake % as averages and standard deviation from three replicates.

Although *C. metallidurans* is known to be able to take up Au-complexes (Nies, 2000; Meargay *et al*., 2003; Monchy *et al*., 2006; Reith *et al*., 2006, 2007, 2009b; Jian *et al*., 2009) it appears that the organics within PME mask any noticeable effect of an active or passive mechanism after six

hours exposure to Au(I)-thiosulfate. Similarly, batch experiments with PME alone and sterile *C. metallidurans* cells incubated in PME, resulted in the retention of Au(III)-complexes (Reith *et al*, 2009b).

At pH 7, after 6 hours exposure, the optimal concentration range for growth of *C. metallidurans* cells in PME extends from 50-500 μM Au(I)-thiosulfate (Table 2.2). Toxic effects began at concentrations of approximately 700 μM, above which growth became erratic for the remainder of the concentration range investigated.

Table 2.2. Cell numbers [CFU.mL^{-1}] of viable planktonic cells of *C. metallidurans* exposed to 50-5000 μM Au(I)-thiosulfate in PME for 6 hours at pH 7.

Au(I)-thiosulfate [μM]	Cell numbers [CFU.mL^{-1}]
50	7.7×10^7 ($\pm 1.5 \times 10^7$)[a]
100	5.9×10^7 ($\pm 2.1 \times 10^7$)
150	3.4×10^7 ($\pm 6.7 \times 10^5$)
200	4.2×10^7 ($\pm 3.7 \times 10^7$)
250	4.5×10^7 ($\pm 1.3 \times 10^7$)
300	3.7×10^7 ($\pm 5.6 \times 10^6$)
500	2.9×10^7 ($\pm 1.2 \times 10^7$)
700-5000	$1.4 \times 10^4 - 1.5 \times 10^8$

[a] Cell numbers given as averages and standard deviation of three replicates.

In order to gain a thorough understanding of this interaction it is imperative to study the effects on gold uptake and cell survivability in a media that supports the *C. metallidurans* cells without masking the microbial effect on gold uptake. Experiments in MME will result in less interactions due to

fewer organics than in the full media and as *C. metallidurans* is found to predictably survive exposure of up to 500 μM Au(I)-thiosulfate in full media, gold uptake measurements in MME will begin at this concentration.

2.3.1.2. Uptake of gold from 500 μM Au(I)-thiosulfate in minimal medium

C. metallidurans growth curves in MME without Au(I)-complexes over 6 hours to 144 hours found changes in pH had no effect on cell numbers and that after 144 hours cell numbers were an order of magnitude higher than at 6 hours. Thus exposure times were extended. Experimentation suggests that uptake of Au(I)-thiosulfate may be an active mechanism that begins after 6 hours but before 144 hours. A small effect is seen at low pH (where no cell growth was recorded; Table 2.3.) with gold uptake approximating 30 %. It is worth mentioning here that the abiotic data may contain localized errors as some values in Table 2.3. are only representative of a single data point and thus have no associated standard error for comparison. After 144 hours active uptake is observed at pH 7, where the cells survive, reaching 60-70 % uptake of the gold in solution (Table 2.3.), approximately 60 times greater than the retention observed in controls. In contrast to the experiments in PME, here the abiotic uptake provides a baseline above which the effect of *C. metallidurans* cells can be seen (*i.e.*, Figure 2.1., biotic effect).

Table 2.3. Summary of gold uptake and cell numbers from exposing *C. metallidurans* cells and controls to 500 µM Au(I)-thiosulfate in MME at pH 4 to 8. Cells not exposed to Au-complexes after 6 and 144 hours were measured as 1.6×10^6 (2.1×10^5) and 1.6×10^7 (3.5×10^6) CFU.mL^{-1} respectively.

		6 hours		144 hours	
pH	**Condition**	**Gold uptake [%]**	**Cell numbers [CFU.mL^{-1}]**	**Gold uptake [%]**	**Cell numbers [CFU.mL^{-1}]**
4	**Viable**	28.7 (± 5.3)[a]	*[b]	27.7 (± 7.7)	*
	Inactive	30.0 (± 1.4)	*	14.1 (± 5.7)	*
	Sterile	29.3 (± 6.2)	*	9.2 (± 4.1)	*
	Abiotic	22.3	*	11.7	*
5	**Viable**	35.9 (± 3.4)	*	24.3 (± 4.4)	*
	Inactive	23.1 (± 3.6)	*	16.1 (± 2.3)	*
	Sterile	27.1 (± 3.5)	*	7.9	*
	Abiotic	20.3	*	6.8	*
6	**Viable**	23.0 (± 4.4)	2.7×10^5 ($\pm 3.5 \times 10^4$)	39.8 (± 22.7)	*
	Inactive	0.8 (± 1.6)	*	7.6 (± 7.0)	*
	Sterile	13.6(± 16.5)	*	0.2 (± 1.5)	*
	Abiotic	0.0	*	10.7	*
7	**Viable**	4.4 (± 10.5)	1.1×10^6 ($\pm 2.9 \times 10^5$)	68.9 (± 17.2)	1.1×10^5 ($\pm 3.0 \times 10^4$)
	Inactive	4.8 (± 2.3)	*	17.5	*
	Sterile	7.7 (± 3.3)	*	7.9	*
	Abiotic	2.4	*	3.6	*
8	**Viable**	13.9 (± 2.3)	6.0×10^5 ($\pm 1.0 \times 10^5$)	62.1 (± 18.0)	2.1×10^6 ($\pm 2.0 \times 10^5$)
	Inactive	2.6 (± 4.6)	*	10.0 (± 1.4)	*
	Sterile	4.5 (± 2.9)	*	14.1	*
	Abiotic	0.5	*	0	*

[a] Gold uptake and retention given as averages and standard deviation of three replicates.
[b] No observed growth.

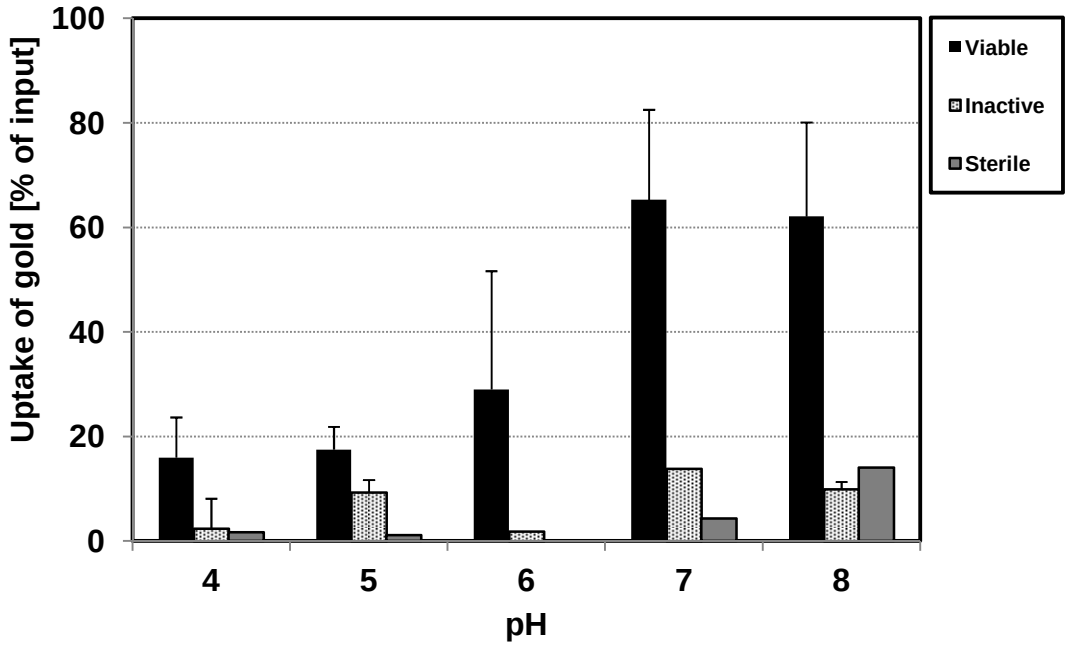

Figure 2.1. The biotic effect of viable, inactive and sterile planktonic *C. metallidurans* cells on uptake of gold from Au(I)-thiosulfate in MME over 144 hours. The average and standard deviations of triplicate experiments are given.

After 6 hours, *C. metallidurans* cells in MME exposed to 500 μM Au(I)-thiosulfate, were only viable at pH 7 with 2.7 x 10^5 (± 3.5 x 10^4) CFU.mL^{-1} at pH 6, 1.1 x 10^6 (± 2.9 x 10^5) CFU.mL^{-1} at pH 7 and 6.0 x 10^5 (± 1.0 x 10^5) CFU.mL^{-1} at pH 8 (Table 2.3.), corresponding to the highest cell counts in the PME experiments. A slightly elevated uptake above that of controls was observable after 6 hours of exposure above pH 4 (uptake at pH 5 may be the result of growth, uptake and then cell death). At pH 6 the viable cells result in maximal uptake of 23.0 (± 4.4) % while uptake by the inactive and abiotic condition is practically negligible. Several groups have measured Au(I) and Au(III) removal from solution by bacterial adsorption reactions, finding that gold removal from solution is most extensive at low pH conditions (Niu and

Volesky, 1999; Ran *et al*., 2002; Nakajima, 2003; Tsuruta, 2004; Kenney *et al*., 2012). Independent of bacterial cell species cell wall ligands are protonated to a higher degree at lower pH conditions, which results in an overall more positive surface charge increasing electrostatically driven passive sorption of negatively charged Au(III)-complexes onto cells (Nakajima, 2003; Mack *et al*., 2007). Electrostatic repulsion is low enough below ~pH 5-6 to enable extensive binding of the Au(III) onto sulfhydryl sites and/or onto positively charged amine sites (Kenney *et al*., 2012). Similarly a strong correlation to pH has been observed for uptake of with Au(III)-complex by *C. metallidurans* (Reith *et al*., 2009b).

After 144 hours of exposure viable bacteria result in a maxima in uptake at pH 7 and 8 (68.9 (± 17.2) % and 62.1 (± 18.0) % respectively) however the measured uptake at pH 6 is 39.8 (± 22.70) % (Table 2.3.). This uptake coincides with the only instance of viable cells after 6 days (1.1×10^5 ($\pm 3.0 \times 10^4$) $CFU.mL^{-1}$ at pH 7 and 2.1×10^6 ($\pm 2.0 \times 10^5$) $CFU.mL^{-1}$ at pH8; Table 2.3.). The net biotic effect on gold uptake is determined by deducting uptake in the abiotic condition (*i.e.*, the baseline) and is presented in Figure 2.1. Thus the maximum biotic effect on uptake for *C. metallidurans* cells exposed to Au(I)-thiosulfate in MME over 144 hours is 65.3 % at pH 7 (Figure 2.1.). The marked increase of biotic gold uptake after 6 hours occurs at pH 7 and 8 where cells are healthier, more prolific resulting in the more cells in solution and in the presence of toxic Au-complexes (Table 2.3.). Where cells failed to grow following the initial gold spiking there has been no significant

changes to gold uptake (Table 2.3.). Gold uptake due to a biotic effect at pH 4-6 after 144 hours exposure is comparable to that after 6 hours. It appears that there is an initial passive uptake occurring within the first 6 hours followed by an active uptake before 144 hours in healthy cells. *Cupriavidus metallidurans* has been observed to take up aqueous Au-complexes, forming nanoparticles over a few days, and although an uptake system for gold is undefined (Wiesemann *et al*., 2013) it is thought to be the result of active detoxification via efflux and reductive precipitation mediated by gold specific operons (*i.e.*, Rmet_4682–86 and Cop; Jian *et al.*, 2009; Reith *et al.*, 2009b). The amendment of *C. metallidurans* with Au(III)-complexes leads to the concentration of gold in discrete areas in some cells but is homogenously distributed throughout others (Reith *et al*., 2009b). Group IB metals, gold and silver share many similar properties. As such, a study concerning the bioremediation of silver in wastewater found that in the same MME used in these studies, *C. metallidurans* removed 75 % of the silver from silver(I)-thiosulfate (5×10^4 cells.mL^{-1} exposed to 1.2 mM) and precipitated metallic silver after 144 hours. These precipitates were observed to form in the outer membrane and not in the cytoplasm with no precipitates forming in the controls (Ledrich *et al.*, 2005). Wiesemann *et al*., (2013) showed *C. metallidurans* precipitated gold nanoparticles from Au(III)-complexes located in the periplasm (Wiesemann *et al*., 2013). In contrast, Reith *et al*. (2009b) found that no metallic gold formed during this process by measuring micro X-

ray absorption near edge spectroscopy (XANES) spectra from a single *C. metallidurans* cell incubated in 100 μM Au(I)-thiosulfate over 6 hours.

The retention of gold in the abiotic conditions, presented here, is higher at lower pH (Table 2.3.). Uptake in the cell control experiments (inactive and sterile) in excess of this abiotic baseline is presumably due to the passive uptake of gold to cell wall material, more of which would be dispersed following the lysation of the cells at death (Madigan and Martinko, 2006). The passive sorption observed (Table 2.3.) is assumedly electostatically driven and may explain the strong similarities at low pH between the inactive and sterile conditions above the uptake in the abiotic condition (Table 2.3.; Figure 2.1.).

2.3.2. Gold uptake from Au(I)-thiomalate by *Cupriavidus metallidurans*

2.3.2.1. Retention of gold from 500 μM Au(I)-thiomalate in full medium

Cupriavidus metallidurans took up similar amounts of gold from 500 μM of Au(I)-thiomalate and Au(I)-thiosulfate under the same conditions (Table 2.4.). Although there is a small discernible difference between the viable, sterile and abiotic conditions there are no apparent trends in the data. A slight drop in gold retention is observed from pH 4 to the rest of the pH range; however, uptake from one condition to another, across the pH range, are comparable (within standard deviation).

Table 2.4. Summary of uptake of gold from 500 μM Au(I)-thiomalate by different cell metabolism states of *C. metallidurans* for 6 hours in PME at pH 7.

pH	Gold retention by viable cells [%]	Gold retention by sterile cells [%]	Abiotic retention of gold [%]
4	63.0 (± 7.2)[a]	75.3 (± 3.0)	71.5 (± 7.8)
5	42.7 (± 4.0)	58.0 (± 6.2)	55.5 (± 4.3)
6	38.2 (± 5.7)	53.7 (± 2.3)	62.7 (± 6.4)
7	45.1 (± 2.7)	46.4 (± 7.6)	57.3 (± 3.7)
8	39.1 (± 6.2)	50.0 (± 8.8)	62.7 (± 6.7)
9	41.4 (± 8.2)	49.8 (± 1.4)	57.2 (± 0.9)
10	38.3 (± 7.1)	45.6 (± 8.8)	57.9 (± 0.9)

[a] Gold retention given as averages and standard deviation of three replicates.

The retention of gold from Au(I)-thiomalate approximates 40-60 % uptake and when compared to the 20-40 % gold retention for Au(I)-thiosulfate, this would suggest that the thiomalate complex is less stable in the full media

than the thiosulfate complex. Modeling of the resultant complex from the addition of Au(I)-thiosulfate to MME indicated that 99.9 % of gold in solutions was present as Au(I)-thiosulfate (Wiesemann *et al*., 2013). Gold(I)-thiosulfate is a stable complex with a stability constant ($\log K_{stab}$) of 26.0 (Hiskey and Atluri, 1988), making it one of the stronger Au-complexes (*i.e.*, $AuCl2^-$ has a $\log K_{stab}$ of 9.0; Smith and Martell, 1976). Due to a lack of geochemical information for Au(I)-thiomalate this complex could not be modeled in a similar fashion; however, it seems unlikely that it would match the calculated stability for Au(I)-thiosulfate.

Cupriavidus metallidurans survives 6 hours of exposure to 500 µM Au(I)-thiomalate in PME (at pH 7) and is viable from 50 µM with essentially the same amount of growth across the concentration range (Table 2.5.).

Table 2.5. Cell numbers [$CFU.mL^{-1}$] of viable *C. metallidurans* cells exposed to 50-500 µM Au(I)-thiomalate in PME for 6 hours at pH 7.

Au(I)-thiomalate [µM]	**Cell numbers [$CFU.mL^{-1}$]**
50	2.2×10^8 ($\pm 1.0 \times 10^7$)[a]
100	2.2×10^8 ($\pm 4.6 \times 10^7$)
150	2.3×10^8 ($\pm 1.9 \times 10^7$)
200	2.6×10^8 ($\pm 2.9 \times 10^7$)
250	3.1×10^8 ($\pm 2.2 \times 10^7$)
300	3.1×10^8 ($\pm 5.6 \times 10^7$)
500	3.2×10^8 ($\pm 7.6 \times 10^7$)

[a] Cell numbers given as averages and standard deviation of three replicates.

As was the case for the Au(I)-thiosulfate complex, investigation in MME must be used to minimize the impact of organics in the media to illuminate any biotic effects on uptake.

2.3.2.2. Retention of gold from 500 μM Au(I)-thiomalate in minimal medium

After 6 hours exposure there was comparatively less growth at 500 μM in MME than in PME, as was the case with thiosulfate (Table 2.2.). This is to be expected due to the presence of fewer nutrients in MME. Even so, there was no observable biotic effect and uptake was found to be erratic across all conditions despite healthy $CFU.mL^{-1}$ numbers that increased with prolonged exposure to the complex.

Table 2.6. Retention and cell counts from exposing 500 μM Au(I)-thiomalate to viable *C. metallidurans* cells and controls in MME at pH 4-8. After 6 and 144 hours, cells not exposed to Au(I)-thiomalate measured 1.3×10^4 ($\pm 6.6 \times 10^3$) and 1.3×10^7 ($\pm 1.7 \times 10^6$) CFU.mL^{-1} respectively.

		6 hours		144 hours	
pH	**Condition**	**Gold uptake [%]**	**Cell numbers [CFU.mL^{-1}]**	**Gold uptake [%]**	**Cell numbers [CFU.mL^{-1}]**
4	**Viable**	6.5 (± 5.6)[a]	2.8×10^3 ($\pm 6.8 \times 10^2$)	10.6 (± 7.6)	1.4×10^6 ($\pm 2.7 \times 10^5$)
	Inactive	10.5 (± 2.4)	*[b]	25.8 (± 1.3)	*
	Sterile	17.9 (± 1.3)	*	27.5 (± 3.4)	*
	Abiotic	3.9 (± 2.5)	*	1.2 (± 1.7)	*
5	**Viable**	0.9	2.2×10^5 ($\pm 1.6 \times 10^5$)	4.2 (± 6.1)	2.1×10^6 ($\pm 5.5 \times 10^5$)
	Inactive	4.9 (± 2.2)	*	21.9 (± 6.7)	*
	Sterile	5.2 (± 2.0)	*	22.8 (± 4.0)	*
	Abiotic	0.6 (± 0.5)	*	10.9 (± 8.7)	*
6	**Viable**	8.5 (± 2.6)	2.1×10^5 ($\pm 1.7 \times 10^4$)	4.8 (± 2.0)	1.9×10^6 ($\pm 1.2 \times 10^5$)
	Inactive	13.7 (± 1.8)	*	7.9 (± 6.2)	*
	Sterile	7.5 (± 4.3)	*	19.0 (± 7.3)	*
	Abiotic	0.1 (± 0.2)	*	10.9 (± 9.8)	*
7	**Viable**	4.4 (± 2.8)	3.9×10^4 ($\pm 4.0 \times 10^4$)	4.1 (± 4.6)	2.4×10^6 ($\pm 4.1 \times 10^5$)
	Inactive	7.3 (± 2.5)	*	7.9 (± 2.8)	*
	Sterile	9.4 (± 1.5)	*	19.8 (± 1.1)	*
	Abiotic	3.5 (± 1.1)	*	11.0 (± 2.3)	*
8	**Viable**	6.5 (± 5.6)[a]	2.8×10^3 ($\pm 6.8 \times 10^2$)	10.6 (± 7.6)	1.4×10^6 ($\pm 2.7 \times 10^5$)
	Inactive	10.5 (± 2.4)	*	25.8 (± 1.3)	*
	Sterile	17.9 (± 1.3)	*	27.5 (± 3.4)	*
	Abiotic	3.9 (± 2.5)	*	1.2 (± 1.7)	*

[a] Gold uptake and retention given as averages and standard deviation of three replicates.
[b] No observed growth.

Cupriavidus metallidurans when exposed to Au(I)-thiomalate in MME results in only a few genes changing their expression significantly (Wiesemann *et al*., 2013). Even though there is little genomic response by *C. metallidurans* to the Au(I)-thiomalate complex and little observable gold retention was observed at 500 μM, investigation turned to lower concentrations of the Au(I)-complex due to the similar CFU.mL^{-1} numbers across concentrations in PME (Table 2.5.).

2.3.2.3. Uptake of gold from 50 μM Au(I)-thiomalate in minimal medium

In order to see if the cell numbers were comparable to 500 μM at the full pH range at 50 μM growth curves were first investigated in PME. Viable *C. metallidurans* cells, when exposed to 50 μM Au(I)-thiomalate at a range of pH, were found to be viable over pH 4-9 ranging from x 10^5 CFU.mL^{-1} at pH 4, and x 10^8 CFU.mL^{-1} at pH 5-9. No cell growth was observed at pH 10 (Table 2.7.).

Table 2.7. Cell numbers [CFU.mL^{-1}] of viable *C. metallidurans* cells exposed to 50 μM Au(I)-thiomalate for 6 hours in MME at pH 4-10.

pH	Cell numbers [CFU.mL^{-1}]
4	5.7 x 10^5 (± 8.1 x 10^5)[a]
5	2.4 x 10^8 (± 2.1 x 10^7)
6	3.1 x 10^8 (± 1.5 x 10^7)
7	2.9 x 10^8 (± 4.4 x 10^7)
8	2.9 x 10^8 (± 4.4 x 10^7)
9	2.4 x 10^8 (± 6.2 x 10^7)
10	*[b]

[a] Cell counts given as averages and standard deviation of three replicates.
[b] No observed growth.

Further investigation of uptake of gold from Au(I)-thiomalate in MME was found to show an initial passive sorption to cell components at low pH, with an active mechanism that occurs after 6 hours and before 144 hours, resulting in almost complete uptake of gold from the solutions (Table 2.8.).

Table 2.8. Summary of gold uptake, retention and cell counts from exposing *C. metallidurans* cells and controls to 50 μM Au(I)-thiomalate in MME at pH 4-8. Cells not exposed to gold were measured as 1.6×10^6 ($\pm 2.1 \times 10^5$) and 1.6×10^7 (3.5×10^6) CFU.mL^{-1} after 6 and 144 hours respectively.

		6 hours		144 hours	
pH	**Condition**	**Gold uptake [%]**	**Cell numbers [CFU.ml^{-1}]**	**Gold uptake [%]**	**Cell numbers [CFU.ml^{-1}]**
4	**Viable**	24.8(± 3.1)[a]	1.0×10^4 ($\pm 3.1 \times 10^3$)	57.0 (± 7.6)	8.0×10^3 ($\pm 2.7 \times 10^3$)
	Inactive	30.8 (± 7.2)	*[b]	64.6 (± 9.5)	*
	Sterile	92.5 (± 6.0)	*	87.3 (± 1.2)	*
	Abiotic	12.7	*	40.0	*
5	**Viable**	10.9 (± 2.8)	3.0×10^6 ($\pm 1.0 \times 10^6$)	76.8 (± 4.0)	1.3×10^7 ($\pm 3.8 \times 10^6$)
	Inactive	18.3 (± 7.4)	*	43.1 (± 21.9)	*
	Sterile	44.3 (± 4.7)	*	45.0 (± 7.5)	*
	Abiotic	10.1	*	36.1	*
6	**Viable**	25.5 (± 8.9)	2.6×10^6 ($\pm 4.0 \times 10^5$)	83.5 (± 7.6)	1.1×10^7 ($\pm 4.5 \times 10^6$)
	Inactive	12.5 (± 7.8)	*	10.8 (± 5.8)	*
	Sterile	11.0 (± 4.5)	*	32.9 (± 23.2)	*
	Abiotic	0.0	*	20.6	*
7	**Viable**	22.1 (± 3.0)	2.3×10^6 ($\pm 5.1 \times 10^5$)	86.9 (± 8.2)	1.8×10^7 ($\pm 1.5 \times 10^6$)
	Inactive	2.8 (± 5.2)	*	13.7 (± 7.7)	*
	Sterile	6.1 (± 1.8)	*	7.3 (± 0.4)	*
	Abiotic	19.4	*	0.0	*
8	**Viable**	49.6 (± 11.3)	1.8×10^6 ($\pm 6.0 \times 10^5$)	96.5 (± 2.3)	1.4×10^6 ($\pm 3.8 \times 10^5$)
	Inactive	18.5 (± 0.2)	*	5.8 (± 6.0)	*
	Sterile	21.3 (± 5.8)	*	3.7 (± 4.9)	*
	Abiotic	17.9	*	2.0	*

[a] Gold uptake and retention given as averages and standard deviation of three replicates.
[b] No observed growth.

After 6 hours measurable uptake was observed over the abiotic condition with an increase in uptake with pH and viable cell numbers. The viable and inactive conditions cause comparable gold uptake up until neutrality, above which the viable cells are driving active uptake of gold. At pH 4 nearly 100 % of the gold is retained by the sterile cells, with this falling to 44.3 [± 4.7] % and then half again to 11.0 [± 4.5] % by pH 6 before essentially remaining at this level of uptake through pH 7 and pH 8. If the vast majority of the cells in the sterile conditions have lysed during the process of autoclaving, components (ligands such as S, N and O moieties; Niu and Volesky 1999; Lengke *et al.*, 2006a; Kenney *et al.*, 2012) of the cell walls become available to electrostatically bind gold which corresponds to the high uptake seen in the more acidic solutions (Table 2.8.). This is evident by the marked uptake in the viable, inactive and sterile conditions over that of the abiotic condition (baseline) up until neutrality (Figure 2.2.) where they become comparable due to the lack of electronegative passive uptake. At neutrality the uptake of the abiotic conditions is generally comparable to that of the viable conditions, however this, again, may be due to representation of single data points (Table 2.8.).

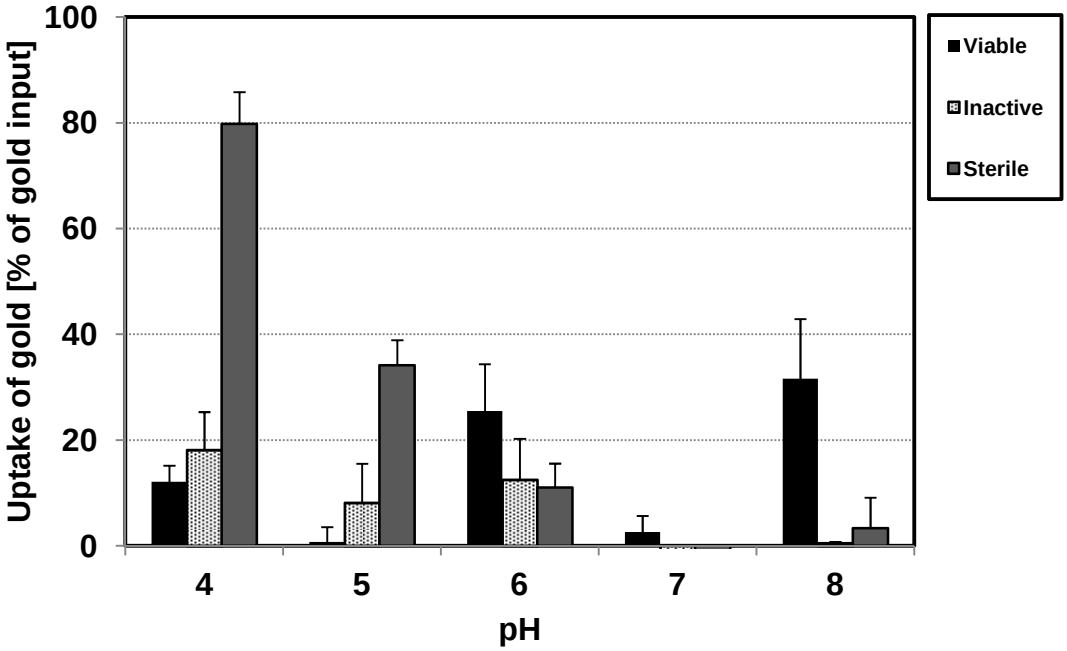

Figure 2.2. The biotic effect of viable, inactive and sterile planktonic *C. metallidurans* cells on uptake of gold from 50 μM Au(I)-thiomalate over 6 hours in MME at pH 4-8. The average and standard deviations of the triplicate experiments are given.

Cell counts of the viable condition in the Au(I)-thiomalate experiments after 6 hours were lowest at pH 4 with 1.0×10^4 ($\pm 3.1 \times 10^3$) CFU.mL^{-1} and ~ $\times 10^6$ CFU.mL^{-1} above that (Table 2.8.). These cell numbers are an order of magnitude higher than the growth observed in MME at 500 μM Au(I)-thiomalate and is likely due to the lower toxicity of the complex at this concentration. The concentration (as well as the speciation of gold *i.e.* oxidation state, complexing ligand, and stability of the aqueous complex) determines the toxicity and consequently the genetic and biogeochemical responses of cells (Wiesemann *et al*., 2013). The highest gold uptake by viable cells occurs after 6 hours at the highest pH, with 49.6 [± 11.3] % (Table 2.8.; 31.6 %, net biotic effect Figure 2.2.). It appears that the viable cells, at high pH, are taking up gold to an extent that is observable over

controls after 6 hours (1.8×10^6 ($\pm$ 6.0×10^5) $CFU.mL^{-1}$ Table 2.8.). The reason for the greater degree of active uptake above pH 7 is unknown.

After 144 hours exposed to 50 μM Au(I)-thiomalate in MME, active uptake of gold by Viable *C. metallidurans* cells increased dramatically across the pH range (Table 2.8.). Passive uptake by the sterile cells has not increased from 6 hours however retention in the inactive and abiotic conditions increased at low pH, likely due to extended exposure. The 500 μM Au(I)-thiomalate experiment had a greater concentration of gold ions compared to the 50 μM solution and this may have resulted in all the available sites for gold uptake being immediately occupied in the higher concentration experiment. An active mechanism in the viable cells is seen after 144 hours that was not observed after 6 hours. The viable cells are taking up gold in conjunction with both active and passive mechanisms. At lowest pH values the uptake is driven by passive mechanisms, as seen by comparison to the inactive condition (57.0 (± 7.6) % and 64.6 (± 9.5) % respectively; Table 2.8.). At pH 5 and pH 6 both mechanisms are acting to bring on uptake until pH 7 where the passive sorption no longer has an effect on gold uptake and the active mechanism begins to take up effectively 100 % of the gold in solution at pH 8 (Table 2.8.; Figure 2.3.).

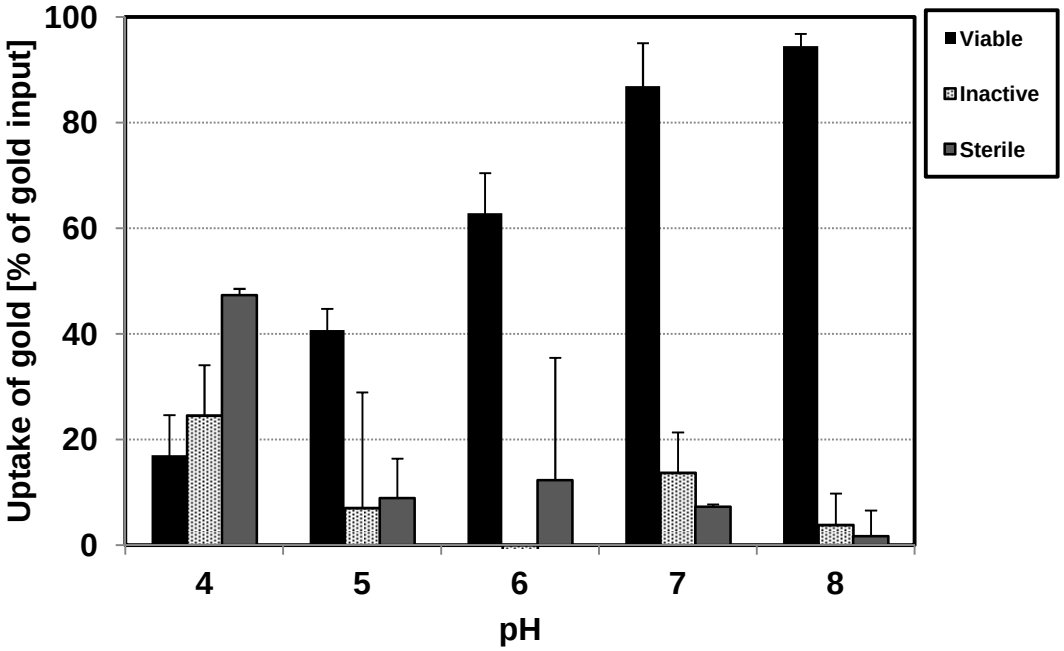

Figure 2.3. The biotic effect of viable, inactive and sterile planktonic *C. metallidurans* cells on uptake of gold from 50 μM Au(I)-thiomalate over 144 hours in MME at pH 4-8. The average and standard deviations of the triplicate experiments are given.

At pH 4, viable cell counts were at 8.0 x 10^3 (± 2.7 x 10^3) CFU.mL^{-1}, before rising to 1.3 x 10^7 (± 3.8 x 10^6) CFU.mL^{-1} and remaining at this order of magnitude before falling to 1.4 x 10^6 (± 3.8 x 10^5) CFU.mL^{-1} at pH 8. A general trend of more gold taken up with an increase in pH is seen for the viable cell uptake of gold from Au(I)-thiomalate after 144 hours in MME. At pH 4, 17.0 (± 7.6) % of gold in solution is adsorbed with 40.7 % being taken up at pH 5 and 62.9 % at pH 7. This trend of increasing uptake with increasing pH continues with uptake of gold from solution reaching 94.5 % at pH 8 (Figure 2.3.) and is the highest recorded value for gold uptake at any condition in these studies. The viable cells are taking up gold as a function of cell wall components at low pH; however, at neutral pH and above the

passive mechanism is superseded and the effects of H^+ on gold uptake falls away (as observed in the sterile and inactive conditions, and to a lesser extent the gold in the abiotic condition).

Jian *et al*. (2009) and Reith *et al*. (2009b) have also observed the coupled passive and active accumulation of gold by *C. metallidurans*. In those studies, the organism was found to reduce Au(III)-complexes to metallic gold via a rapid passive accumulation and the formation of Au(I)-S intermediate on the cell wall followed by a slow biogeochemically-driven reduction and intra and extracellular deposition of metallic gold particles (potentially occurring here). In a similar study Song *et al*. (2012) found that > 90 % of passively adsorbed gold was reduced to Au(I) from Au(III)-complexes by inactive bacteria, from both gram positive and negative species.

Pseudomonas cepacia, Corynebacterium equi and *P. maltophilia* also demonstrated the ability to take up gold from Au(I)-thiomalate (Higham *et al.*, 1986; Nakajima, 2003). *Pseudomonas cepacia*, in a defined media with 2.5 mM Au(I)-thiomalate, after 16 hours of growth, took up 95 % of the initial gold present in the medium. This is reflected here, with *C. metallidurans* able to take up ~90 % of gold from Au(I)-thiomalate, admittedly at much lower concentrations. Of the gold taken up by *P. cepacia*, 35 % was strongly bound to the cells and may have been intracellular in nature (Higham *et al.*, 1986).

Adsorption after 144 hours for the sterile condition is practically identical to the 6 hour experiment with a gradual decrease across the pH

range investigated. Overall the uptake of gold is the same for the sterile cells for 6 and 144 hours due to lyses and dispersion of cell material present throughout solutions from the very start of the experiment. The similar effects of uptake in the sterile condition over 6 hours to 144 hours shows that the passive sorption is a rapid mechanism that reaches its full potential after 6 hours and is most effective at low pH. Retention by cells in the inactive condition closely follows the trends of the sterile condition. The amount of gold that is taken up by the inactive cells falls with increasing pH with the amount of gold taken up falling from 64.6 (± 9.5) % at pH 4 and falling with increasing pH and ending up at 5.8 (± 6.0) % uptake at pH 8, (*i.e.*, as pH increases, less gold is taken up). The cells in this condition are not taking up as much gold as they have not undergone lyses and thus do not have the same amount of cell wall material exposed to the gold in solution with which passive gold sorption can occur. The uptake of gold by inactive cells is seen to be almost identical with the 6 hour experiment with the exception that the uptake at the most acidic condition has increased due to the increased time period with which the gold-cell wall interaction can take place. At lowest pH the similar uptake between the viable and inactive condition reinforces the fact that the passive sorption is the dominant mechanism at low pH.

.

2.3.3. Retention of gold from Au(I)-cyanide by *Cupriavidus metallidurans*

The interaction of Au(I)-cyanide with *C. metallidurans* was investigated due to the possibility of the presence of both of these around primary gold mineralization (Gray, 1988; Reith *et al.*, 2007, 2010). The cells were initially provided a full array of minerals to insure maximal cell growth in the form of PME and then due to a lack of an observable biotic effect, MME was used. However, even in the presence of minimal nutrients no biotic gold uptake, passive or active, was observed.

2.3.3.1. Retention of gold from 500 μM Au(I)-cyanide in full medium

Due to the tendency of cyanide to gas out of solution at low pH (Fairbrother *et al*., 2009; Blummer and Haas, 2000), uptake experiments were carried out at neutral pH conditions and above to ensure that this did not happen. No observable trends in measurements of gold uptake were found. The conditions investigated, (viable, dead and abiotic) were indefinable from one another across the pH range (Table 2.9.).

Table 2.9. Summary of gold uptake from 500 μM Au(I)-cyanide after exposure to viable *C. metallidurans* and controls for 6 hours in PME at pH 7-9.

pH	Gold uptake by viable cells [%]	Gold uptake by sterile cells [%]	Abiotic retention of gold [%]
7	53.6 (± 5.2)[a]	63.4 (± 11.0)	60.9 (± 2.9)
8	52.7 (± 6.5)	57.9 (± 1.9)	63.8 (± 3.7)
9	53.0 (± 3.2)	66.7 (± 10.6)	62.5 (± 1.8)

[a] Gold uptake and retention given as averages and standard deviation of three replicates.

Similarly to gold uptake from Au(I)-thiosulfate and Au(I)-thiomalate in full media, uptake from Au(I)-cyanide had no observable trends and so MME was used to elucidate passive and/or active uptake.

2.3.3.2. Retention of gold from 500 μM Au(I)-cyanide in minimal medium

Little difference was observable between the four (viable, inactive, sterile and abiotic) conditions for gold uptake experimentation in MME.

Gold retention is seen to be fairly constant across the conditions. However, it would appear that there is some gold uptake due to an active mechanism at pH 8 with 22.8 (± 10.8) % measured (Table 2.10). The difference in retention compared to the controls is negligible when standard deviations are compared. The uptake that is occurring in these conditions is likely due to sorption to the few organics within the minimal media. This is apparent by the similarity of uptake between inactive and sterile cells where the sterile cells have lysed and spilt more components into the solutions. This is further bolstered by the amount of uptake seen at this gold concentration in the PME (Table 2.9.) which was ~50-60 % compared to 10-30 % in MME

(Table 2.10.). There is no passive electronegative uptake as the pH is too high. The Au(I)-cyanide complex being such a stable complex anion, is hardly dissociated which previously resulted in very small amounts (typically $1/5^{th}$ that observed in solutions containing Au(III)-chloride across a range of microorganisms) of Au(I) accumulation in other studies involving Au(I)-cyanide, defined media and a range of organisms (Nakajima, 2003). Wiesemann *et al*., (2013) showed, via titration modeling that MME amended with potassium dicyanaurate will exist as dicyanaurate(I) with an occurrence of > 99 %. Exposure of *C. metallidurans* to Au(I)-cyanide results in strong transcriptomic response with 359 genes and the transcription of 223 intergenic regions upregulated by 50 μM $KAu(I)CN_2$ compared to KCN (Wiesemann *et al*., 2013).

When compared to Au(I)-thiosulfate and Au(I)-thiomalate, the effective pH range for working with Au(I)-cyanide is comparatively small as Au(I)-cyanide solutions below pH 7 are likely to release HCN gas (Fairbrother *et al*., 2009). A small pH range, coupled with the prospect of having to use a lower Au-complex concentration, make the restrictions on parameters of further investigation too narrow to successfully determine the role of this complex in biomineralization within the laboratory.

Table 2.10. Summary of gold retention and viable cell counts from exposing viable *C. metallidurans* cells and controls to 500 µM Au(I)-cyanide in MME at pH 7-9. There are no clear trends of uptake, passive or active in this data. Cells not exposed to gold measured 2.3 x 10^8 (± 2.6 x 10^7) and 8.5 x 10^8 (± 3.1 x 10^8) CFU.mL^{-1} after 6 and 144 hours respectively.

		6 hours		144 hours	
pH	**Condition**	**Gold uptake [%]**	**Cell numbers [CFU.ml^{-1}]**	**Gold uptake [%]**	**Cell numbers [CFU.ml^{-1}]**
7	**Viable**	15.2 (± 2.2)[a]	5.4 x 10^8 (± 2.2 x 10^8)	7.8 (± 3.0)	5.5 x 10^7 (± 5.4 x 10^7)
	Inactive	15.1 (± 3.0)	*[b]	10.3 (± 4.5)	*
	Sterile	15.7 (± 3.3)	*	*	*
	Abiotic	11.1 (± 1.7)	*	4.6 (± 1.9)	*
8	**Viable**	7.3 (± 3.2)	1.8 x 10^8 (± 6.1 x 10^7)	22.8 (± 10.8)	1.1 x 10^7 (± 10.0 x 10^6)
	Inactive	6.4 (± 5.0)	*	9.9 (± 3.8)	*
	Sterile	8.7 (± 4.3)	*	13.2 (± 1.4)	*
	Abiotic	9.0 (± 1.5)	*	2.0 (± 2.0)	*
9	**Viable**	8.0 (± 1.2)	1.6 x 10^7 (± 4.7 x 10^6)	9.2 (± 1.7)	*
	Inactive	9.8 (± 4.8)	*	10.4 (± 3.5)	*
	Sterile	6.5 (± 3.0)	*	9.0 (± 0.8)	*
	Abiotic	5.8 (± 6.5)	*	8.4 (± 1.7)	*

[a] Gold uptake and retention given as averages and standard deviation of three replicates.
[b] No observed growth.

2.3.4. Gold uptake from 0.5 μM Au(I)-complexes by *Cupriavidus metallidurans* in the absence of nutrients

As both the MME and PME media retained gold to some extent, experiments were undertaken to determine if an observable biotic effect could be seen under subtoxic (*i.e.,* below MIC) conditions in the absence of any organics or carbon source for the organism. As no carbon source or nutrients were provided cell counts were not carried out and this was done at low Au-complex concentration to avoid toxic death of *C. metallidurans* at 0.5 μM in dH_2O at pH 7.

Viable and sterile *C. metallidurans* cells exposed to 0.5 μM in dH_2O at pH 7 exhibit clear trends in gold uptake (Figure 2.4.). The viable cells are seen to take up approximately 40 % of the gold for all complexes (Figure 2.4.). The sterile condition, takes up approximately 15 % of the gold from Au(I)-cyanide, 20 % from the Au(I)-thiosulfate and approximately 30 % from the Au(I)-thiomalate complex (Figure 2.4.). The trends seen here, are also seen at higher concentrations in MME, with the thiosulfate complex having the most noticeable viable-cell effect on uptake over the other conditions (Figure 2.1.) and the thiomalate complex having high levels of sterile cell retention with regard to the other conditions (Figure 2.2.). Interestingly the cyanide complex shows promising results, with a measurable active mechanism in viable cells above that of the sterile and abiotic conditions

(Figure 2.4.). This concurs with the results of Wiesemann *et al*. (2013). The abiotic condition is seen to take up almost no gold from the solutions. The absence of organics is the probable cause for the almost complete lack of uptake in the abiotic condition. After 6 hours exposure, the viable cells were likely still metabolizing as evident by the marked uptake in this condition over the controls.

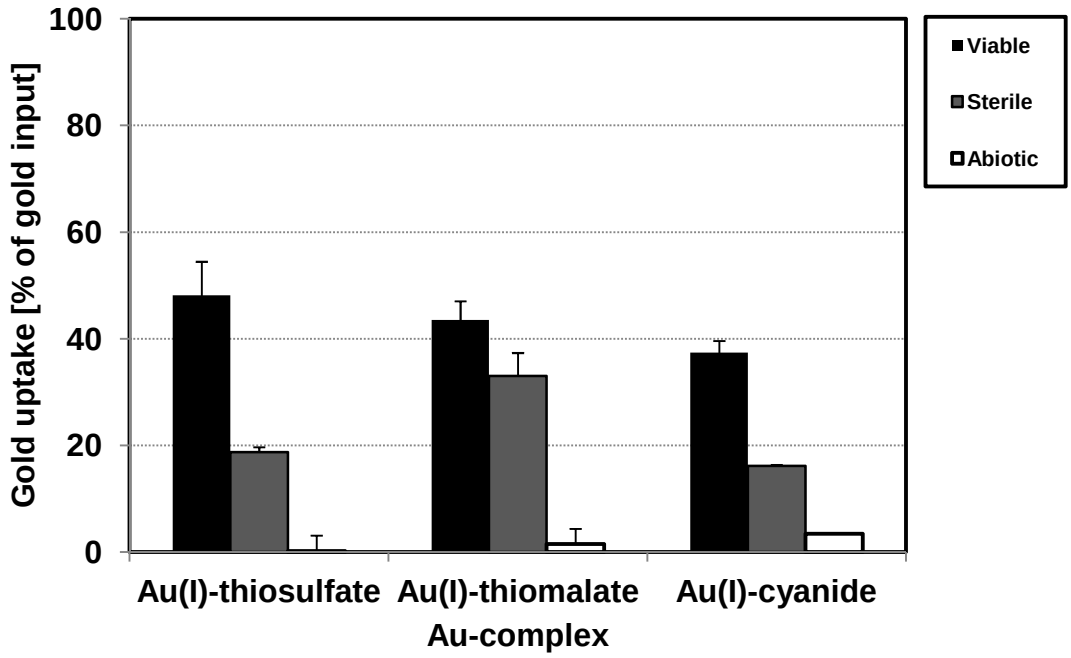

Figure 2.4. Gold uptake from 0.5 μM Au(I)-complexes by planktonic *C. metallidurans cells* over 6 hours in dH_2O at pH 7. A clear biotic effect is seen, with viable cells taking up more gold than that retained in the sterile condition. Abiotic conditions were seen to retain almost no gold.

2.4. *Cupriavidus metallidurans*; active and passive adsorption and the biomineralization of supergene gold

Across the pH conditions investigated in the uptake of Au(I)-complexes, gold uptake was found to be taking place in viable and cell controls, which has been described as active and passive mechanisms respectively, by authors working with Au(III)-complexes (Reith *et al.*, 2006, 2009b, 2010; Kenney *et al.* 2012; Wiesemann *et al*. 2013). Gold uptake by viable planktonic cells *of C. metallidurans* is found to be strongest around pH 7 and may represent an active mechanism, while at low pH conditions, particularly in the sterile cell experiments, a presumably passive, electrostatic, adsorption of gold to components of the cell walls was observed. The biotic effects of gold uptake are most obvious in MME due to lower instances of Au-complex interaction with organics than that observed in PME. Interestingly, Au(I)-cyanide and Au(I)-thiomalate leads to the upregulation of *C. metallidurans* genes that are also upregulated in the presence of Au(III)-complexes (Wiesemann *et al.*, 2013). Although the intensity of responses is highest in Au(III) and Au(I)-cyanide, CN^- also causes transcriptome response due to toxicity (Wiesemann *et al.*, 2013) and no observable biotic uptake was observed here.

Increasing the duration of *C. metallidurans* exposure to Au(I)-complexes results in an increased amount of gold uptake and, as expected due to nutrient availability, cell growth is more prolific in PME. This work

further supports the possibility that *C. metallidurans* is one of the drivers of gold biomineralization by demonstrating the ability to actively take up Au-complexes that are common to ground waters surrounding mineralization.

Although it is unclear whether such studies of relatively high gold concentrations apply to gold:cell ratios more typical of natural systems, defining optimal conditions for maximal growth and uptake of Au-complexes will allow for the design of experiments to investigate if *C. metallidurans* will form gold structures similar to those found in nature. Thus future experiments investigating biomineralization of gold and Au(I)-complex uptake should be run at, or near, pH 7 over longer exposure periods than used here, in full media to insure that possible active mechanisms of gold uptake for *C. metallidurans* are observable over the presumed electrostatic sorption seen at low pH. Additionally, as bacteria exposed to metal solutions are seen to have less toxic effects in subsequent exposures, experiments with periodic and incremental concentrations of Au(I)-complexes in PME media over an extended time scale may allow the capacity of an active uptake of Au-complexes by *C. metallidurans* to be measured and possibly qualified via the use of microscopy techniques. Ideally if this were to occur in a setting that approximates the environmental regolith settings then great inroads may be made into the determination of the role *C. metallidurans* plays in the biomineralization of secondary gold in the supergene.

Chapter 3: Biomineralization of gold in biofilms of Cupriavidus metallidurans

Abstract

Cupriavidus metallidurans, a bacterium capable of reductively precipitating toxic, aqueous gold(I/III)-complexes, dominates biofilm communities on gold grains from Australia. This suggests that this bacterium plays a fundamental role in the formation of highly pure (secondary) gold in Earth surface environments. As experimental verification of this hypothesis was lacking, we assessed the biomineralization of gold in *C. metallidurans* biofilms grown in quartz-sand-packed columns. Formation of metallic gold-particles was only observed in the presence of viable biofilms. In these experiments > 99 wt.% of gold, introduced to the columns through periodic amendment with Au(I)-thiosulfate, was taken up compared to < 30 wt.% in sterilized and abiotic controls. Biomineralization of gold within columns occurred via the formation of intra- and extracellular spherical nano-particles, which aggregated into spheroidal and framboidal micro-particles of up to 2 µm in diameter. Aggregates of gold formed around cells, eventually encapsulating and ultimately replacing them. These particles were morphologically analogous to gold-particles commonly observed on natural gold grains. Bacterial cells were connected via exopolymer or nanowires to µm-sized, extracellular gold-aggregates, which would intuitively improve the flow of electrons through the

biofilm. This study demonstrates the importance of *C. metallidurans* biofilms for the detoxification of Au-complexes and demonstrates a central role for bacterial biomineralization in the formation of highly pure gold in surface environments.

3.1. Introduction

The biosphere catalyses a variety of biogeochemical reactions that transform gold (Southam *et al*., 2009). Microbial weathering and bioleaching contribute to the mobilization of gold by liberating gold from associated minerals, e.g., pyrite or arsenopyrite (e.g., Rawlings and Johnson, 2007). Excretion of Au-complexing ligands, e.g., thiosulfate, amino acids and cyanide, can lead to the solubilization of gold via oxidation-promoting complexation (Reith *et al*, 2007). The resulting aqueous Au-complexes are highly toxic to bacteria, because they generate oxidative stress and inhibit enzyme function inside cells (Nies, 1999; Reith *et al*., 2009b). Subsequent decomposition of the complexing ligands coupled with biochemical reduction of Au(I/III) leading to bio-precipitation can immobilize gold (Kenney *et al*., 2012). However, the relative contributions of biogenic versus abiogenic processes in the formation of the highly pure (secondary) gold that is common in Earth surface environments, is an ongoing subject of controversy (Bischoff, 1994, 1997;

Falconer *et al*., 2006; Falconer and Craw, 2009; Reith *et al*., 2010; Hough *et al*., 2011; Kenney *et al*., 2012). Secondary gold commonly consists of > 99 wt.% gold, compared to primary gold that forms from hydrothermal fluids in the deep subsurface and contains 5-30 wt.% silver (Wilson, 1984). Secondary gold is finely crystalline (0.01 to < 5 µm), and occurs in a variety of morphotypes, including nano- and µ-particles, triangular-plate (pseudo-trigonal octahedral) gold, sheet-like gold, secondary grains as well as bacteriomorphic and spheroidal gold, which is widespread on surfaces of transforming gold grains (Falconer *et al*., 2005; Reith *et al*., 2006, 2010; Falconer and Craw, 2009; Hough *et al*., 2011).

It is now widely accepted that most bacteria live in biofilms that adhere to surfaces (e.g., Harrison *et al*., 2007). Biofilm communities can withstand a diverse range of environmental stresses, because they commonly contain multiple species co-existing in symbiotic relationships (Hansen *et al*., 2007). An important component of biofilms are the self-produced extracellular polymeric substances (EPS), which are critical to biofilm development by facilitating adhesion to surfaces, enabling cell aggregation, providing protection from desiccation and increasing resistance to toxic heavy metals (Mittelman and Geesey, 1985).

Recently, polymorphic layers consisting of sheet-like biofilms intermingled with bacteriomorphic-, nano- and µ-particulate gold as well as iron and silicate minerals were detected on gold grains from temperate and tropical Australian sites (Reith *et al*., 2010). Spheroidal gold nano- and micro-

particles were associated with bacteria cells and exopolymeric substances, constituting the active layer of the biofilm (Reith *et al*., 2010). In that study, sectioning through the entire polymorphic layer, which was up to 40 µm wide, using a focused ion beam (FIB) revealed that larger aggregates of nano-crystalline gold line open spaces underneath the active biofilm layer. Other studies have described similar polymorphic layers on gold grains from arid Australian and temperate New Zealand sites (Reith *et al*., 2010).

Biofilm communities on the Australian grains have been found to be dominated by a rod-shaped, metallophilic bacterium, *C. metallidurans* (Reith *et al*., 2006, 2010). This gram-negative *Beta-proteobacterium* harbors numerous metal-resistance gene clusters enabling detoxification of transition metal ions and –complexes (Nies, 1999, 2003). Planktonic *C. metallidurans* cells rapidly accumulate gold from Au(III)-complexes in solution, promoting the biomineralization of gold nano-particles via energy-dependent reductive precipitation (Nies, 1999). Studies with biofilms of cyano-, sulfide-oxidizing- and sulfate-reducing bacteria have demonstrated their ability to mediate gold biomineralization and form secondary gold (Lengke and Southam, 2005, 2006, 2007; Lengke *et al*., 2006a, b). For example, the formation of µm-sized octahedral gold crystals and mm-sized gold foils was observed in column experiments inoculated with a consortium of SRB amended with Au(I)-complexes (Lengke and Southam, 2007). However, the ability of viable *C. metallidurans* biofilms to biomineralize gold, and hence drive gold-cycling in near-surface environments has not been experimentally verified. The aims of

this study are to assess if: (i) viable biofilms of *C. metallidurans* amended with aqueous Au(I)-complexes are capable of precipitating metallic gold-particles; (ii) uptake and transformation of gold-complexes are more efficient in the presence of viable biofilms compared to sterile and abiotic controls; and (iii) the morphologies of biofilms and gold biominerals are comparable to those observed on natural gold grains.

3.2. Materials and methods

3.2.1. Column experiments

The main objective of this study was to assess the formation and morphologies of gold biominerals in *C. metallidurans* biofilms, hence experimental conditions were chosen to reflect this. Gold(I)-thiosulfate was used for amendments, because it is considered to be an important gold-complex in near surface systems, especially in zones surrounding sulfide-bearing gold-mineralization (Vlassopoulos *et al*., 1990a). Preliminary investigations have shown that planktonic *C. metallidurans* cells were able to maintain viability at concentrations of 100 µM of Au(I)-thiosulfate (Table 2.2.). Data from preliminary column experiments have shown that increasing the concentration of gold over time did not lead to a significant loss of viable cells in the outlet solution, as bacteria are able to adapt to increasing

concentrations of toxic metals by increasing metal sorption- and/or detoxification capabilities (Borrok *et al*., 2004a). Therefore, the concentrations of Au-complexes in amended solutions were increased to provide enough gold for detectable gold biominerals and a widespread distribution of gold in the biofilms to occur within a feasible timeframe.

Experimental procedures followed the methodology published by Lengke and Southam (2007), and were conducted in pre-sterilized glass columns (10 mm in diameter and 500 mm in length) filled via wet packing of 24 g of autoclaved sterile, acid-washed, quartz sand (Lenkge and Southam, 2007). For experiments with viable and sterile biofilms, columns were inoculated with 10 µL of washed cell concentrate harvested from a pre-culture in 10 mL PME (8 $g.L^{-1}$, Difco^{TM}, USA). Cell numbers were monitored in outlet solutions from columns run in parallel to those that would be used for ongoing experimentation and once they had stabilized at 3.4×10^{7} cells mL^{-1} after 14 days, amendment with gold-containing media commenced (Table 3.1.). Control experiments, *i.e.*, columns without biofilms and with dead biofilms, were sterilized by autoclaving under standard conditions. To maintain sterility, columns were amended with 0.15 mL of sodium azide (1 % wt:vol) with each amendment of PME. All experiments were conducted in triplicate and incubated at 25 ºC in the dark.

Table 3.1. Summary of experimental schedule, pHs and viable cells in outlet solutions.

			Columns with viable biofilms		Sterile columns	Abiotic columns
Time [days]	**Gold amendment [µM]**	**Solutions collected[b]**	**Viable planktonic cells [CFU.mL^{-1}][c]**	**pH[c]**	**pH[c]**	**pH[c]**
0	100	n.a.	3.4 x 10^7(± 3.5 x 10^7)[c]	7.0 (± 0.1)	7.0 (± 0.1)	7.0 (± 0.1)
7	180	•	1.4 x 10^7 (± 2.4 x 10^6)	8.0 (± 0.6)	7.3 (± 0.1)	7.3 (± 0.1)
14	320	•	3.3 x 10^9 (± 1.0 x 10^9)	8.1 (± 0.7)	7.3 (± 0.1)	7.4 (± 0.1)
28	420	•	4.2 x 10^9 (± 1.2 x 10^9)	8.2 (± 0.5)	7.4 (± 0.1)	7.4 (± 0.2)
56	520	•	1.6 x 10^9 (± 8.2 x 10^8)	8.4 (± 0.1)	7.3 (± 0.1)	7.5 (± 0.1)
70	615	•	1.7 x 10^9 (± 5.9 x 10^8)	8.6 (± 0.1)	7.3 (± 0.1)	7.4 (± 0.1)
84	n.a.[a]	•	2.8 x 10^9 (± 1.2 x 10^9)	8.5 (± 0.1)	7.6 (± 0.1)	7.8 (± 0.1)

[a] non applicable
[b] solutions collected following the previous spiking period.
[c] cell numbers and pHs are given as averages ± standard deviations of three replicates.

All columns were amended successively with 5 mL PME containing 100, 180, 320, 420, 520 and 615 µM Au(I)-thiosulfate at days, 0, 7, 14, 28, 56, and 70, respectively. These spiking solutions completely immersed the sand grains for the length of the exposure. Sampling and amendment times were chosen to ensure that gold distribution in the columns, *i.e.*, gold taken up in biofilms, adsorbed to minerals and remaining in solution, could reach steady-state enabling the formation of metallic gold in biogenic and abiogenic experiments. At each sampling time columns were completely drained by gravity, prior to the immediate amendment with the next spiking solution. While the formation of Au-organic complexes upon contact of Au(I)-thiosulfate with a medium rich in complex organic compounds cannot be

excluded, X-ray adsorption near edge spectroscopy did not show changes in speciation of Au(I)-thiosulfate in PME (*i.e.*, reduced to Au(0) or oxidized to Au(III), data not shown). On sand grains from control experiments a layer of organic matter was detected by EDX analysis. This layer was most likely derived from biofilm remnants (sterilized controls) and/or from sorption of organic molecules from the medium to mineral surfaces (abiotic controls).

3.2.2. Analyses of outlet solutions

Cell counts were conducted in outlet solutions to assess the viability of cells in columns and check the sterility of the controls throughout the incubation (Lengke and Southam, 2007). Cell counts were conducted using plate count agar (Oxoid Ltd., USA) following the method of Miles *et al.,* (1938). pH was measured using a Hanna Instruments H11134 pH-electrode with a CyberScan pH 310 meter. The meter was calibrated using Colourkey buffer solutions at pH-values of 3.98-4.02, 6.98-7.02 and 9.95-10.05 (at 20 ^{o}C; VWR International Ltd., Poole, England). Gold concentrations in outlet solutions were determined, after centrifugation (20 min at 3000 x g), filtration (0.22 µm sterile syringe filters) and acidification to 10 wt.% HCl, using an Agilent 7500cs ICP-MS, (Agilent Technologies, Japan; detection limit: 0.4 $\mu g.L^{-1}$ for gold). ICP-MS detection limit was determined via the use of an internal indium standard and calibration curves prepared from stock gold solutions. The pellet resulting from centrifugation was fixed in 1.25 wt.%

glutaraldehyde for TEM. Whole mounts of *C. metallidurans* cells, adsorbed to Formvar-carbon coated 200 mesh copper grids, were imaged using a Phillips CM-200 TEM equipped with a light element EDX-detector and operating at 200 kV.

3.2.3. Analyses of solid phases

At the end of the incubation period, columns were destructively sampled by dividing into 20 mm segments, of which 0.1 g of sand per segment was digested in *aqua regia*, and gold concentrations in the digest were measured by ICPMS. Cell counts were conducted to determine cell numbers in biofilms associated with the sand grains, hence 0.1 g of the sand per segment was vigorously vortexed for three minutes in 100 µL of 0.9 wt.% NaCl solution to extract biofilms (Miles *et al.*, 1938). Sand grains from all experiments were fixed using 1.25 wt.% glutaraldehyde. Fixed materials were dehydrated using a series of 25, 50, 75 and 100 % ethanol solutions, and critical point dried (CPD). For high resolution imaging, CPD grains were carbon-coated and analyzed using FIB-SEM (Helios NanoLab, FEI, The Netherlands). Secondary electron and BSE images were obtained at 3 kV to 15 kV, respectively, with sectioning and cleaning carried out at 30 kV / 21 nA and 20 kV / 0.34 nA. Unprocessed sand grains were also analyzed using a Philips XL30 field emission gun (FEG) SEM at an acceleration voltage of 10 to 20 kV. Both SEM instruments are equipped with a 10 mm^2 Sapphire Si(Li)

energy dispersive spectrometer; EDX analyses were conducted using acceleration voltages of 15 keV.

One column containing viable biofilms was set in epoxy resin, cut in half using a diamond saw and polished with 1 µm diamond paste. Micro-synchrotron X-ray fluorescence (SXRF) imaging was used to map the distribution of gold in the column. SXRF data were collected at the XFM beamline (Australian Synchrotron, Melbourne). The XFM beamline is an undulator beamline with a Si(111) monochromator and an energy resolution of ($\Delta E/E$) of 2×10^{-4} at 10 keV (Paterson *et al*., 2011). Kirkpatrick-Baez mirrors were used to focus the beam to a spot size of ~1.5 μm^2, and the 384-element Maia detector system was used for analyses (Ryan *et al*., 2010). The detector was placed in front of the sample at a distance of 2 mm, resulting in a 1.8 steradian solid angle (Ryan *et al*., 2010). The incident X-rays travel through a central hole in the detector. The elastic scatter peak was used as a proxy for Si, since the Si-Kα line is below the energy range of the Maia X-ray detector.

Molecular microbial techniques were used to confirm the integrity of the one-species biofilms at the end of the incubation, and consequently throughout the experiment. DNA was extracted in triplicate from 0.25 g of sand grains with viable cells using UltraClean Microbial DNA kit (MoBio, CA, USA). Community structures of bacteria in the columns were analyzed using PCR-DGGE of the V6-V8 hypervariable regions of the 16S rRNA gene. Bacteria-specific PCR primers F968-GC and R1401 were used (Duineveld *et*

al., 1998). 16S rRNA PCR-DGGE analysis was conducted against a *C. metallidurans* CH34 DNA control using an Ingeny PhorU system (Ingeny International, The Netherlands; Wakelin *et al*., 2008).

3.3. Results and discussion

3.3.1. Uptake of Au(I)-thiosulfate in columns

Each column was amended with 10.775 µmol of Au(I)-thiosulfate. Overall, > 99 wt.% of gold was taken up in columns containing viable biofilms compared to < 30 wt.% in sterile and abiotic columns after a month (Figure 3.1.). Uptake of gold was initially high in all experiments, *e.g.*, after seven days of exposure to a solution containing 0.5 µmol Au(I)-thiosulfate, approximately 99 wt.% of the gold was retained (Figure 3.1.). While uptake rates remained high in experiments with viable biofilms, significantly smaller percentages were retained in controls after 14 and especially 30 days of incubation. Significant differences between sterile and abiotic experiments were not detected (Figure 3.1.). The pH of outlet solutions was approximately 7 in all columns after 14 days (inlet solution pH was 6.8), and increased gradually during the experiment (Table 3.1.).

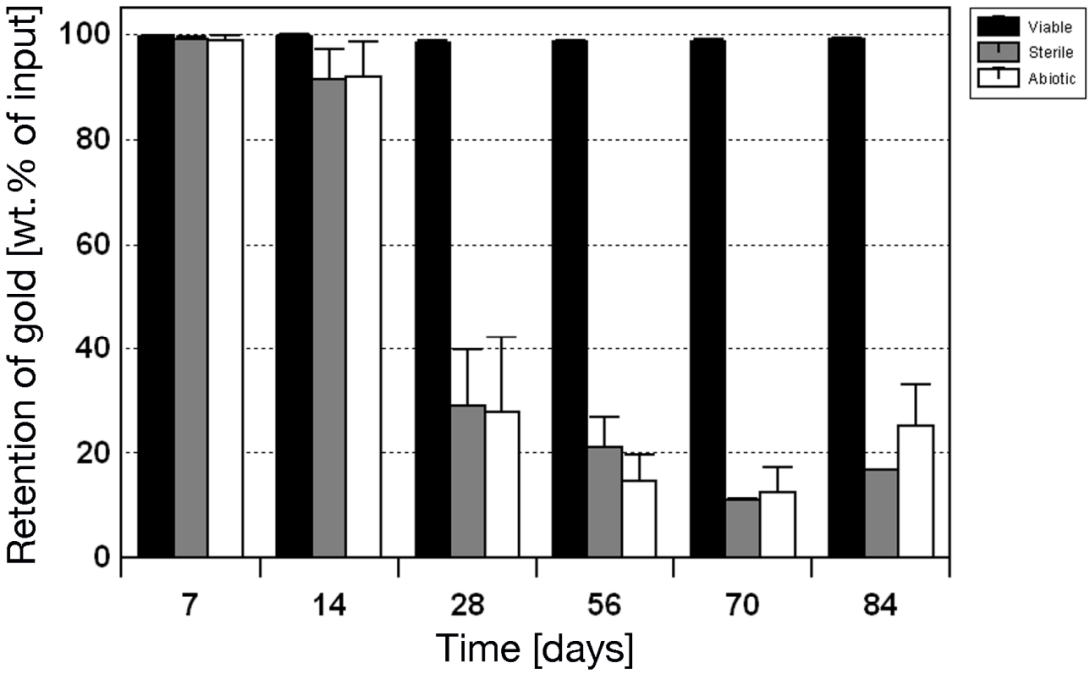

Figure 3.1. Gold uptake and retention in columns with viable biofilms and in the controls; given are averages and standard deviations of the triplicate experiments.

While the near-complete uptake of gold in experiments containing viable biofilms was largely a result of gold bio-precipitation and the formation of gold biominerals associated with the biofilms, considerable quantities of gold were also retained in the columns of the controls. However, no metallic gold particles were observed in the controls and gold distribution was uniform throughout the columns (Figure 3.2). This suggests sorption of Au-complexes to quartz grains and to an organic layer derived from remnant biofilms and/or organics derived from the medium, as a carbon-rich layer was detected on sand grain surfaces from control experiments after 84 days of incubation.

The surface of quartz grains exposed to aqueous solutions becomes covered with a layer of silanol groups (-SiOH) that are responsible for chemisorptive interactions (Parfitt and Rochester, 1983). In a recent study,

Mohammadnejad *et al*. (2011) assessed the sorption of Au(III)-complexes by silicates. Their results showed that depending on solution-pH values and mineral surface areas between 20 and 97 wt.% of aqueous Au-complexes were adsorbed to the quartz grain surface, yet metallic gold was not observed. Using batch-experiments with PME alone and dead cells incubated in PME, retention of 30 and 20 wt.% Au(III)-complexes was observed (Reith *et al*., 2009b). This shows that dead cells can passively sorb Au(III)-complexes; however, metallic gold particles did not form (Reith *et al*., 2009b). These results suggest that active metabolic processes mediated by viable cells are required to form metallic gold biominerals which is further supported here (Figure 3.2.). It is noted that the introduction of new PME may have led to the formation of additional organic coatings harboring additional sorption capabilities, thus explaining the capability of sterile controls to retain some gold throughout the experiments.

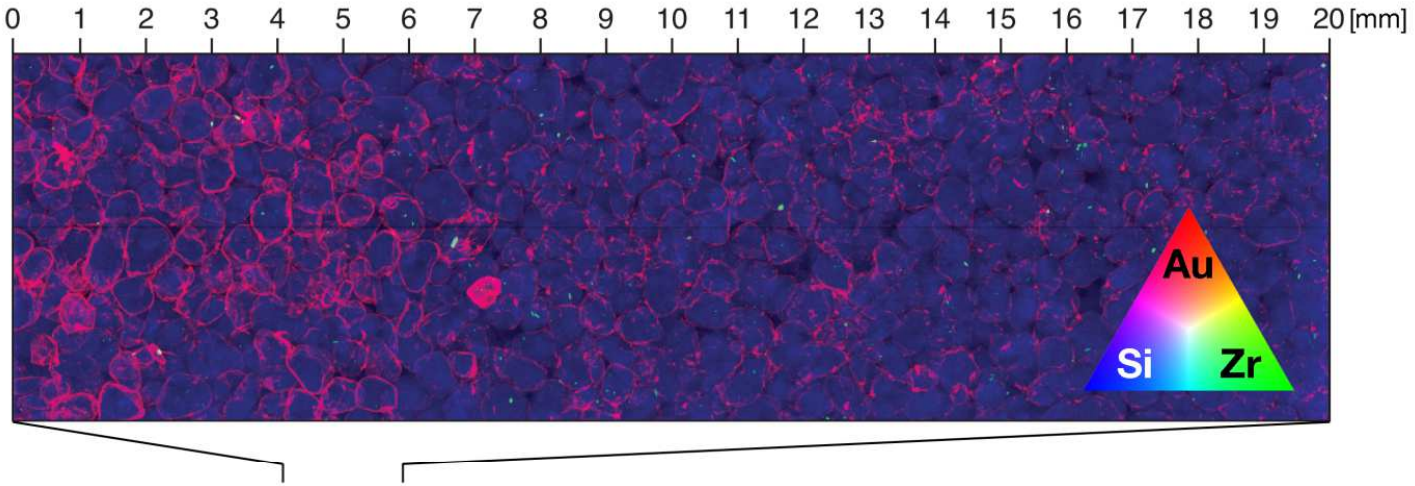

	Depth [mm]	20	40	60	80	100	120	140	160	180
Viable Biofilms	Au segment^{-1} [µmol]	10.82 (± 1.88)	0.29 (± 0.07)	0.08 (± 0.02)	0.05 (± 0.01)	0.05 (± 0.01)	0.05 (± 0.01)	0.06 (± 0.01)	0.07 (± 0.01)	0.04 (± 0.01)
	Biofilm cells segment^{-1}	2.50×10^6	2.58×10^5	2.58×10^5	2.85×10^5	1.35×10^5	1.35×10^5	1.51×10^5	7.00×10^4	2.15×10^2
Sterile Control	Au segment^{-1} [µmol]	0.33 (± 0.04)	0.21 (± 0.03)	0.19 (± 0.01)	0.22 (± 0.02)	0.24 (± 0.04)	0.23 (± 0.01)	0.26 (± 0.03)	0.28 (± 0.05)	0.25 (± 0.04)
Abiotic Control	Au segment^{-1} [µmol]	0.17 (± 0.09)	0.18 (± 0.04)	0.13 (± 0.03)	0.14 (± 0.01)	0.12 (± 0.02)				

Figure 3.2. Micro-SXRF map showing the distribution of gold (Au), zirconium (Zr) and silicon (Si) (Red-Green-Blue, respectively) in the first 20 mm segment of a destructively sampled column containing viable biofilms, and concentrations of gold and viable cells associated with sand grains throughout an entire column (n=3).

3.3.2. Assessment of bacteria and associated gold biominerals in outlet solutions

Prior to gold amendment, the number of viable planktonic cells in the outlet solutions was 3.4 x 10^7 (± 3.5 x 10^7) CFU.mL^{-1} (Table 3.1.). After the first amendment, cell numbers in the effluent was 1.4 x 10^7 (± 2.4 x 10^6) CFU.mL^{-1} (Table 3.1.). In the following sampling periods bacterial counts increased by two orders of magnitude to > 10^9 CFU.mL^{-1}, and remained constant for the duration of the experiment. The increasing concentrations of cells in outlet solutions may represent a transition from a biofilm to planktonic growth strategy, to avoid the toxic effect of the gold, or could be an effect of extending the periods between sampling from one to two weeks, *i.e.*, cells were more starved so shifted to a planktonic form, or perhaps, the biofilm may have reached its maximum thickness producing more planktonic cells.

PCR-DGGE of 16 rRNA (as per section 2.2.1.) extracted from cells on sand grains and outlet solutions showed that the biofilm consisted of a single species and remained uncontaminated by other species throughout the experiment (data not shown). TEM-analyses of cell whole mount supports this, as all cells were uniformly rod-shaped (Figure 3.3A and 3.3B). Interestingly, every bacterial cell that washed out of the column possessed abundant, apparently cell-envelope associated, spherical gold nano-particles (Figure 3.3B). The localization of individual and conglomerates of two to five particles appear to be on cell envelopes and in association with membrane

vesicles (arrows) which suggests that the reduction of Au(I)-complexes may be associated with electron transfer reactions. Larger extracellular conglomerates of 10s to 100s of gold nano-particles also occurred (Figure 3.3C). In contrast, outlet solutions from controls did not contain identifiable particulate gold.

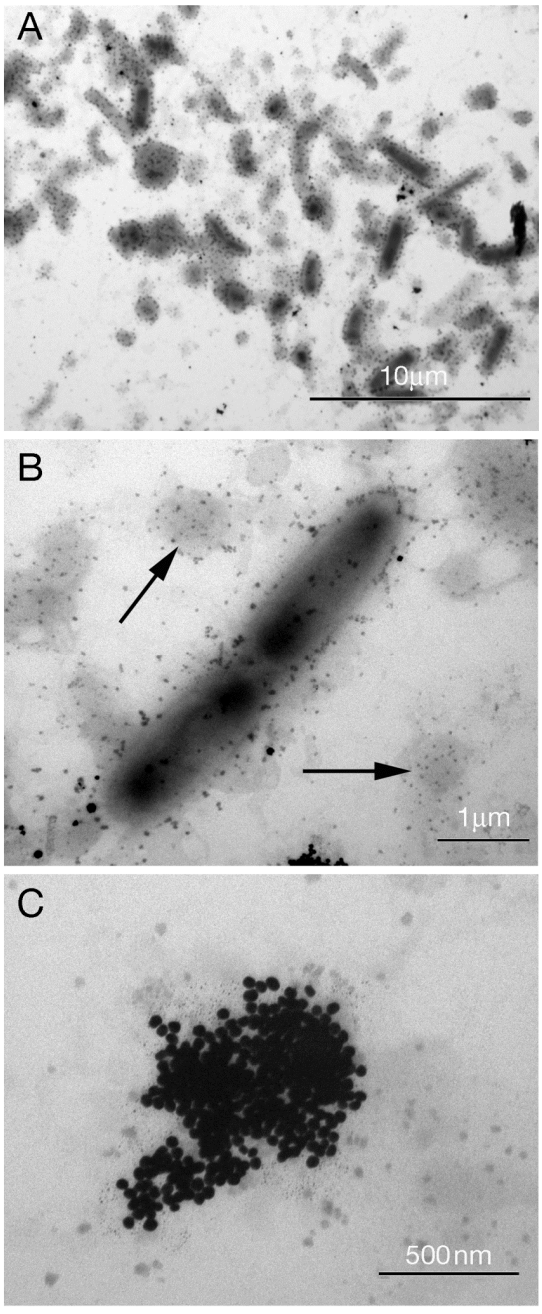

Figure 3.3. Transmission electron micrographs of cells in whole mounts from solutions collected after 84 days of incubation, showing widespread precipitation of gold nano-particles (seen as dark black spots) by cells (A), that were localized primarily in association with the cell envelope (arrows; B) as individual gold nano-particles and conglomerates of two to five particles, and as larger, extracellular conglomerates of 50-100 gold nano-particles (C).

3.3.3. Distribution of gold in biofilms

While gold was uniformly distributed throughout abiotic and sterile columns, with total amounts of gold associated with column materials ranging from 0.1 to 0.3 µmol 20 mm segment^{-1}, gold content in the upper 20 mm of columns with viable biofilms was 10.82 µmol (Figure 3.2.). Here more than 95 % of gold present in the column was concentrated and viable cell numbers were 2.5 x 10^6 CFU segment^{-1}, one order of magnitude higher compared to the following segments (Figure 3.2.). Micro SXRF mapping of the top section provided additional information. Where gold coatings on quartz grains were detected throughout the section, and higher concentrations of gold were observed in the top 10 mm (Figure 3.2.). The correlation between high cell counts and high gold concentrations indicates a link between microbial activity, biofilm formation as well as gold detoxification and biomineralization. As an aerobic, facultative chemolithoautothrophic bacterium, *C. metallidurans* grows best with organic carbon- and energy sources under oxic conditions (Mergeay *et al*., 2003). Because the amendment of PME was added to the top, the abundant carbon- and energy- sources as well as oxygen in the top section were expected to produce higher metabolic rates and form denser biofilms. Viable, metabolically active cells are required for gold detoxification and biomineralization (Reith *et al*., 2009b), hence the zone with the highest biofilm metabolic rates and the densest biofilms was also expected to display the highest rates of gold accumulation and biomineralization. High metabolic

rates in the top segment result in a lower amount of gold biominerals in the lower sections of the column. Sand grains from the top section (0-20 mm) were covered by the most extensive biofilms, in which gold particles were more abundant than in underlying sections; gold particles were not observed in controls (Figure 3.4A,B). This indicates that metabolically active cells are required for the biomineralization of metallic gold particles. An earlier study of planktonic cells showed that rapid sorption of Au(III)-complexes to metabolically active as well as dead cells led to the formation of cell-bound Au(I)-S-complexes (Reith *et al*., 2009b). This induced cell toxicity in viable cells, which reacted using efflux and reduction to produce metallic gold nano-particles demonstrating the ability of C. metallidurans to precipitate Au(I)-S complexes. In experiments with dead cells no gold particle formation was observed (Reith *et al*., 2009b).

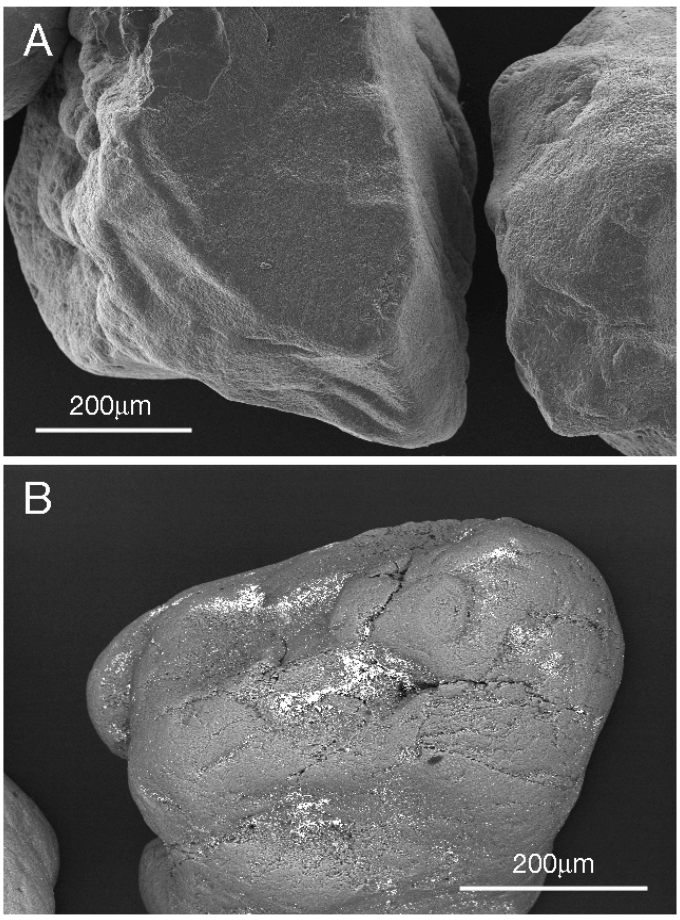

Figure 3.4. Backscatter electron micrographs of sand grains from the first 20 mm of columns incubated under sterilized conditions (A) and with viable biofilms (B), respectively, showing that metallic gold (confirmed via EDX) was only present in columns with viable biofilms.

Scanning electron microscopy showed that biofilms from the top 20 mm of the columns were made up of rod-shaped cells embedded in extensive exopolymeric substances (Figure 3.5.). Gold particles associated with cells and the exopolymeric layer ranged in sizes from approximately 10 nm to > 2 µm (Figures 3.5C-D and 3.6.). They occurred as isolated nano-particles, as conglomerates of nano-particles directly associated with cells (Figure 3.5C) and as larger (> 1 µm) extracellular spheroidal and framboidal particles (Figure 3.5D). These larger particles appeared to consist of

conglomerates of nano-particles (Figure 3.5D), and were more abundant than conglomerates directly associated with cells. Numerous, proteinaceous *pili*, *i.e.*, putative nanowires, were connected to the larger extracellular particles and cells (Figure 3.5B,C). Often clusters of up to six cells were connected to an aggregate of gold via these putative nanowires (Figure 3.5C). Recent research on mechanisms of electron transport in bacteria living in soil and biofilm communities has shown that electrically conductive nano-wires similar to those observed in this study, can be used to transfer excess electrons to remote electron acceptors (Gorby *et al*., 2006; El-Naggara *et al*., 2010; Malvankar *et al*., 2011). While we have not demonstrated that the nano-wires connected to extracellular gold particles are conductive, their presence suggests that they may contribute to the growth of *C. metallidurans* biofilms under micro-aerophilic or anaerobic conditions in the lower segments of the columns (Gorby *et al*., 2006; El-Naggara *et al*., 2010). Sectioning and analyses of the biofilm using FIB-SEM showed that gold particles were dispersed throughout the biofilms (Figure 3.6A-D). Extracellular particles displayed internal growth structures with numerous voids and channels (Figure 3.6D,E) consistent with their formation via conglomeration of nano-particles. In some instances, larger particles were rod-shaped and hollow (Figure 3.6B) supporting earlier assumptions that cellular processes led to gold nano-particle formation, eventually encapsulating cells and ultimately replacing them, yet preserving their morphology.

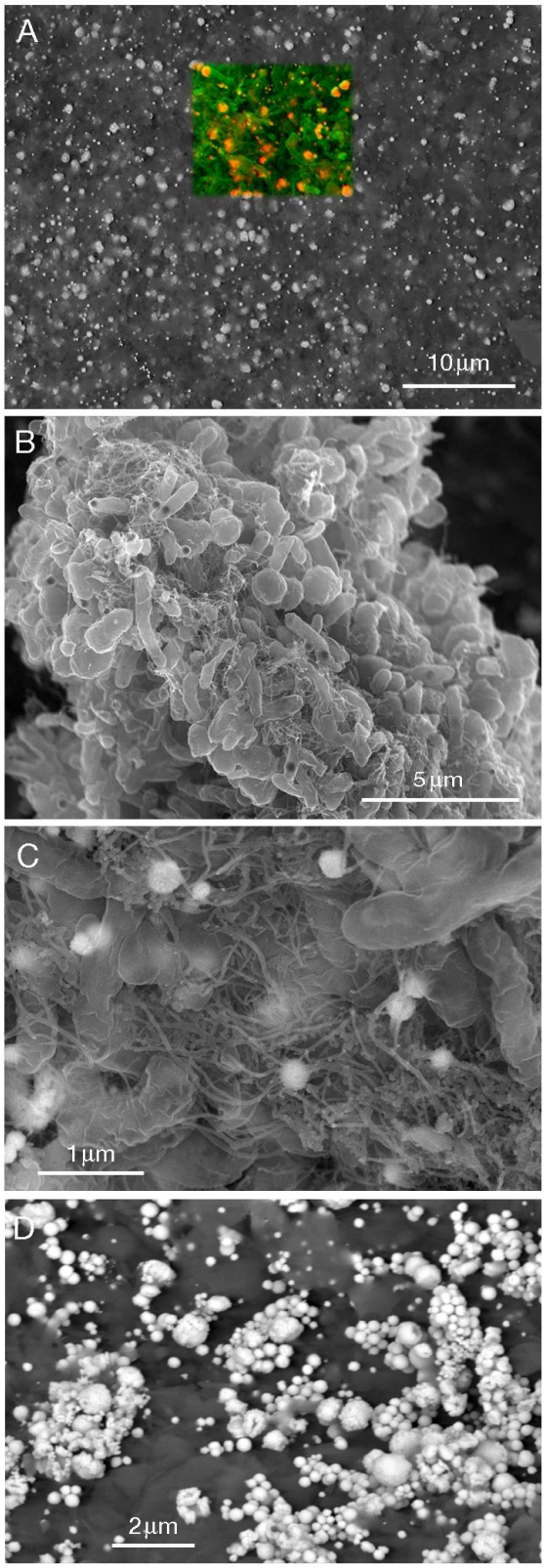

Figure 3.5. Secondary electron micrographs of grains collected from the top 20 mm of columns incubated with viable biofilms showing (A) area of the biofilm and its overall morphology, overlain is Red-Green map of gold and carbon, respectively, showing the distribution of gold in the biofilm, (B) individual cells and associated gold biominerals; (C) SE micrograph showing the connection of cells to extracellular gold aggregates via nanowires. (D) BSE micrographs showing the large abundance of metallic spheroidal gold in the biofilms.

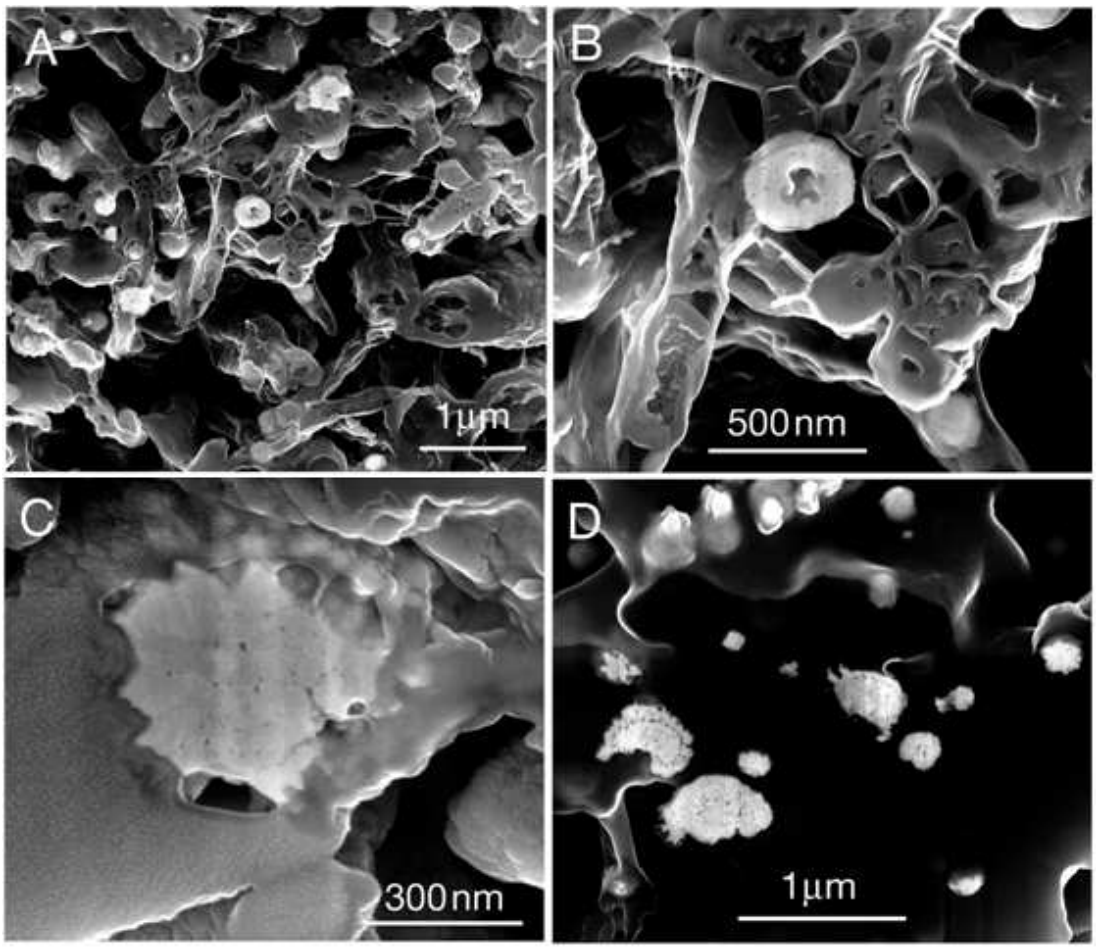

Figure 3.6. Secondary electron and BSE micrographs of FIB-milled sections of the biofilms on grains from the top 20 mm of columns incubated with viable biofilms. (A) Abundance of micro-particulate conglomerates of gold in biofilms; (B) hollow conglomerates of gold replacing bacteria cells in the biofilm; (C, D) ultrafine structure of gold conglomerates showing that these conglomerates are formed via aggregation of approx. 50 nm sized particles, displaying concentric growth structures.

3.3.4. The role of biofilms in gold biomineralization

The current study extends our understanding of the role of biofilms in gold biomineralization. Recent research has shown that biofilms are less susceptible to metal toxicity compared to planktonic cells (Workentine *et al*., 2008; Kuimova and Pavlova, 2011). For example, single-species biofilms of *B. cepacia*, a relative of *C. metallidurans*, and *E. coli* have shown resistance to five times higher concentrations of silver nano-particles and Ga^{3+}, respectively, compared to planktonic cells (Geslin *et al*., 2001; Harrison *et al*., 2007). In this study, biofilms of *C. metallidurans* displayed a similar behavior, while the minimum bactericidal concentrations (MBC) for planktonic *C. metallidurans* with aqueous Au(I)-thiosulfate approximates 100 µM, biofilm communities remained viable after amendment with solutions containing more than 6 times this concentration. The increased resistance of biofilm communities to metal toxicity is the result of the interaction of chemical, physical, physiological and biochemical factors that govern biofilm activities (Harrison *et al*., 2007). For example, extracellular signaling by quorum sensing systems improves the response of biofilms to oxidative stress caused by Au-complexes and other metals (Geslin *et al*., 2001; Choi *et al*., 2010). The presence of extensive extracellular polymeric layers, as observed on biofilms in column experiments and on natural gold grains (Figures 3.5, 3.6 and 3.7B,C respectively), leads to the temporary or permanent immobilization of metal ions and complexes, decreasing the amount of Au-

complexes reaching the cells (Harrison *et al*., 2006, 2007). The amount of toxic metal-ions reaching viable cells is reduced through the reactivity of dead cells contained in the biofilms, which have been shown to rapidly accumulate transition metals (Peeters *et al*., 2008). These processes do not apply to planktonic cells, which predominately rely on their inherent or accumulated genetic resistance mechanisms, as expressed through the number of specific and unspecific metal-resistance gene clusters, to counteract the toxic effects of metals (Nies, 2003; Harrison *et al*., 2007). Biomineralization in *C. metallidurans* biofilms resulted in gold biominerals that are morphologically analogous to those observed on natural gold grains (Figure 3.7.). For example, spherical gold nano-particles were observed in biofilms on placer gold grains from New Zealand (Orepuki Beach, South Island; Figure 3.7A, Reith *et al*., 2012); microbial biofilms containing abundant nanowires as well as gold particles were observed on gold grains from the Flinders Ranges, Australia (Arkaroola, South Australia; Figure 3.7B); and nano-particles, spheroidal and bacteriomorphic gold was observed in polymorphic layers on gold grains from Kilkivan, Australia (Queensland; Figure 3.7C,D, Reith *et al*., 2010). These sites are from regions that experience appreciable amounts of rainfall with 1300 mm and 1130 mm at Orepuki (Tait et al., 2006) and Kilkivan (Australian Bureau of Meteorology, 2011a) respectively and rainfall in excess of 300 mm in two months at Arkaroola (Australian Bureau of Meteorology, 2011b). Bacteriomorphic gold aggregates, composed of nano-particles that encapsulated void areas the

size and shape bacterial cells, were observed in the lower section of the polymorphic layer covering the grains from Kilkivan (Figure 3.7D). Aggregates common in biofilms in column experiments likely form around cells that have actively precipitated gold nano-particles. Due to the intrinsic electrochemical affinity of complexed as well as particulate gold to gold-surfaces, which is commonly known as the ‘nugget effect’, gold particles precipitated by cells may act as nuclei for further aggregation (Reith *et al.*, 2010). Gold aggregates around cells will keep growing by biomineralization and electrochemical aggregation, ultimately leading to encapsulation and replacement of cells. This effect may be even more pronounced in biofilms, in which conductive nanowires enable electron transfer from cells to gold aggregates, which promotes the reduction of aqueous Au(I)-complexes followed by precipitation, and therefore growth of existing aggregates. The data presented herein provides experimental evidence for the importance of biofilms of *C. metallidurans* for the detoxification of Au-complexes, and confirms the central role of bacterial biomineralization in the formation of highly pure gold in surface environments.

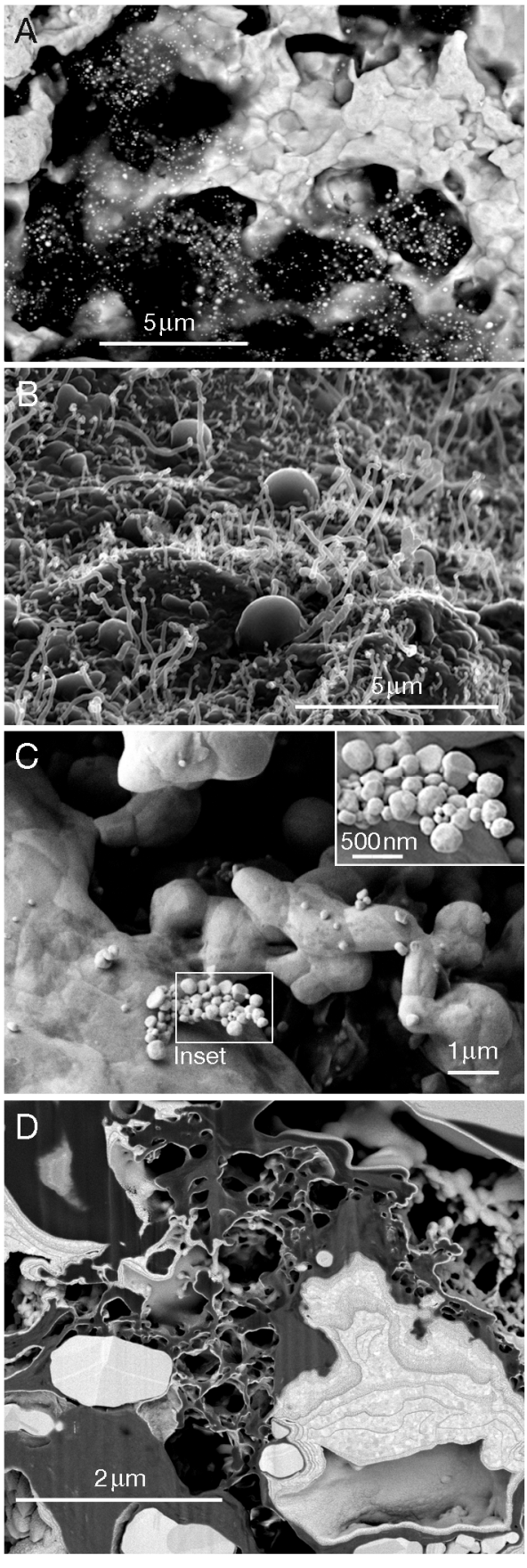

Figure 3.7. Biofilms, polymorphic layers and associated gold particles from the surfaces of natural secondary gold grains from Australian sites. (A) gold-particle containing polymorphic layer on the surface of grains from New Zealand; (B) biofilms displaying numerous nano-wires on gold grains from the Flinders Ranges in South Australia; (C) spheroidal secondary gold growing on gold grains from Kilkivan, Queensland; (D) nano-crystalline structure of neoformed gold replacing a bacterial cell from Kilkivan grains.

Chapter 4: Supergene gold transformation: biogenic secondary and nano-particulate gold from arid Australia

Abstract

Biofilms on gold grains from sub-tropical and tropical sites promote the dispersion of gold by continuously cycling coarse gold and releasing nano-particulate gold. In this study we investigated the influences of (bio)geochemical processes on the transformation of gold grains in arid environments. At these sites water and nutrient availability are limited and episodic; hence, abiogenic evaporative mechanisms were thought to control the formation of secondary, and especially nano-particulate gold. Gold grains were collected from eight arid sites in three Australian gold provinces, *i.e.*, Lawlers (Western Australia), Tanami (Northern Territory), and Flinders Ranges (South Australia). Sites were chosen based on contrasting deposit styles, *i.e.*, primary underground and epithermal deposits as well as secondary elluvial-, colluvial- and alluvial placers at increasing distances from primary mineralization. Gold grains were studied using optical microscopy, FEG-SEM, FIB-SEM-EDX, EPMA and particle induced X-ray emission (PIXE). Gold grains from all surface environments displayed supergene transformation features, *i.e.*, morphotypes indicative of gold and silver dissolution, gold aggregation and gold neoformation. The latter included spheroidal and bacteriomorphic gold, which increased in abundance with

increasing distance from source. Viable biofilms containing abundant gold nano-particles and spheroidal gold µ-crystals were detected on all grains from the Flinders Ranges. Gold grains from the Lawlers and the Tanami provinces are covered by polymorphic layers containing abundant nano-particulate, spheroidal and bacteriomorphic gold. The polymorphic layers consist of vermiform clays and organic matter, suggestive of remnant biofilms. These results indicate that biofilms capable of transforming gold grains develop episodically on gold grains in arid environments. In conclusion, this study shows that microbial processes play a critical role for the transformation of gold grains and contribute to the dispersion of gold and the formation of geochemical anomalies in arid environments.

4.1. Introduction

Although gold is rare in the Earth's crust, it is widely distributed and highly mobile in surface environments (Boyle, 1979; Reith and McPhail, 2006; Hough *et al.*, 2007; Usher *et al.* 2009). Gold grains between 0.1 and 4 mm in diameter are the most abundant sources of alluvial and elluvial gold, and constitute economically important deposits, such as the Witwatersrand deposit (Mossman *et al.*, 1999). Yet a number of fundamental questions surrounding our understanding of gold mobility and gold grain formation in supergene environments remain: (i) Which processes are responsible for the

dispersion of gold in areas surrounding primary mineralization? (ii) Do gold grains from soils and placers form by detrital or accretionary processes? (iii) What is the role of microbiota in the mobility of gold and the formation of gold grains? and (iv) How can an improved understanding of these mechanisms enhance geochemical exploration?

Until recently, debate about how gold grains develop within placer environments was dominated by proponents for formation mechanisms that were either purely detrital (*e.g*., Giusti and Smith, 1984; Knight *et al.*, 1999; Hough *et al.*, 2007) or purely accretionary (*e.g.*, Bowles, 1988; Clough and Craw, 1989; Youngson and Craw, 1993; Bischoff, 1997). The issue was recently resolved for gold grains from tropical Australia using FIB-SEM coupled with EDX analysis and electron backscatter diffraction (EBSD; Reith *et al.*, 2010). These techniques enabled the observation of processes occurring within polymorphic layers at the nm-scale. The polymorphic layer consists of microbial biofilms, secondary nano-particulate, spheroidal and bacteriomorphic gold, as well as clay and silicate minerals that cover the surfaces of gold grains (Reith *et al.*, 2010). This data (Reith *et al.*, 2010) led to the development of a model for gold grain formation that integrates a primary origin with secondary mobilization and aggregation processes, and can thus fully explain the diversity of observed textures and compositions.

In this model gold grains originate as primary gold in high temperature, *e.g.*, hydrothermal systems. Primary gold commonly occurs as silver-rich alloy, and primary grains often consist of large (10 to > 100 µm) twinned crystals (Hough *et al.*, 2007). The occurrence of such gold grains in supergene placers is due to weathering and erosion of host materials, and the subsequent physical redistribution of grains (Hough *et al.*, 2007). Secondary gold commonly occurs on the surface of primary grains or as small grains (0.05 to 4 mm), displays high purity (> 99 wt.% gold), and very small crystals (0.01 to < 5 µm; Reith *et al.*, 2010). Based on observations of grains from Australia, New Zealand, Africa and the Americas, secondary gold occurs in a wide variety of morphotypes, including nano- and µ-particles, triangular plate gold, sheet-like gold, bacterioform gold, wire gold as well as purely secondary gold grains (Bischoff 1994, 1997; Reith *et al.*, 2007; Falconer and Craw 2009; Hough *et al.*, 2011). These morphologies are the result of gold/silver dissolution and gold precipitation acting simultaneously (Reith *et al.*, 2007; Southam *et al.*, 2009). De-alloying is a process in which less noble metals (*e.g.*, silver, copper) are leached out from the gold grains, leaving behind pure nano-porous gold (Schofield *et al.*, 2008). Silver depletion, via the presence of suitable ligands, can occur at the outer surface of grains but is also known to proceed by de-alloying along defects in the crystal structure (Hough et al., 2007). In this process, the less-noble silver is dissolved, leaving behind undissolved gold atoms that diffuse together creating porosity (Ding *et al.*, 2004). The development of voids provides

further access to the interior potentially causing both the development of mineral phases within nuggets and the further depletion of external and internal crystal boundaries and silver content (Hough *et al.*, 2007; Knight *et al.*, 1999). Gold itself is also soluble in surface waters via interactions with halides, thiosulfate, organic acids and cyanide (Boyle, 1979; Korobushkina *et al*., 1983; Gray, 1998; Southam and Saunders, 2005; Reith *et al.*, 2007; Vlassopoulos *et al*., 1990b). Microorganisms capable of releasing organic acids promote de-alloying, and cyanide-producing organisms can produce the ligands for gold dissolution and transport (Reith *et al.*, 2007). Complexed gold is re-precipitated and forms secondary metallic gold via a number of biogenic and abiogenic processes. The greater part of this secondary gold precipitation occurs as nano-particles, which are then transformed to µ-crystalline gold via aggregation and re-crystallization (Lengke and Southam, 2006; Reith *et al.*, 2009b). In combination these secondary processes induce significant changes to gold grain surfaces compared to primary gold (Fairbrother *et al.*, 2009).

A recent study suggested that abiogenic processes, *e.g.*, evaporation, control the formation of nano-particles and µ-crystalline gold platelets, and therefore the dispersion of gold in arid environments (Hough *et al.*, 2008). However, the ability of microorganisms, particularly bacteria, to form gold nano-particles and secondary gold grains is well illustrated (Lengke and Southam 2005; Reith *et al.*, 2009b). For instance, reductive precipitation of dissolved gold in the metallophillic bacterium *Cupriavidus metallidurans* can

lead to the formation of spheroidal nano-particles (Reith *et al.*, 2009b). Biofilms dominated by *C. metallidurans* were observed on the surface of gold grains from moderate, sub-tropical and wet-tropical zones in Australia (Reith *et al.*, 2006, 2010; Figure 4.1.). Nano-particulate, spheroidal and bacterioform structures are common in biofilms on gold grains from these localities, demonstrating that bacteria contribute to the formation of secondary nano-particulate and spheroidal gold (Reith *et al.*, 2006, 2010). In effect, biofilms may control the rates at which gold moves in the environment by controlling the rates of gold mobilization and re-precipitation.

To date, active biofilms have only been detected on gold grains from sites where water is seasonally abundant (Figure 4.1.). In contrast, water and nutrients required to sustain microbial biofilms are much more limited in arid climates, leading some authors to favor abiogenic processes of dispersion and re-precipitation (Hough *et al.*, 2008, 2011). Hence, the aim of this study is to assess biogeochemical mechanisms leading to the transformation of gold grains in semi-arid and arid environments. Specific objectives are to assess: (i) if microbial biofilms, polymorphic layers or remnants thereof are present on gold grains from arid sites; (ii) their morphology and chemical composition; and (iii) the occurrence of gold nano-particles and µ-crystals that are indicative of biogeochemical transformations. To achieve this, three field areas were selected (Figure 4.1.; Table 4.1.) that provided access to primary gold and gold grains from related elluvial, colluvial and alluvial settings.

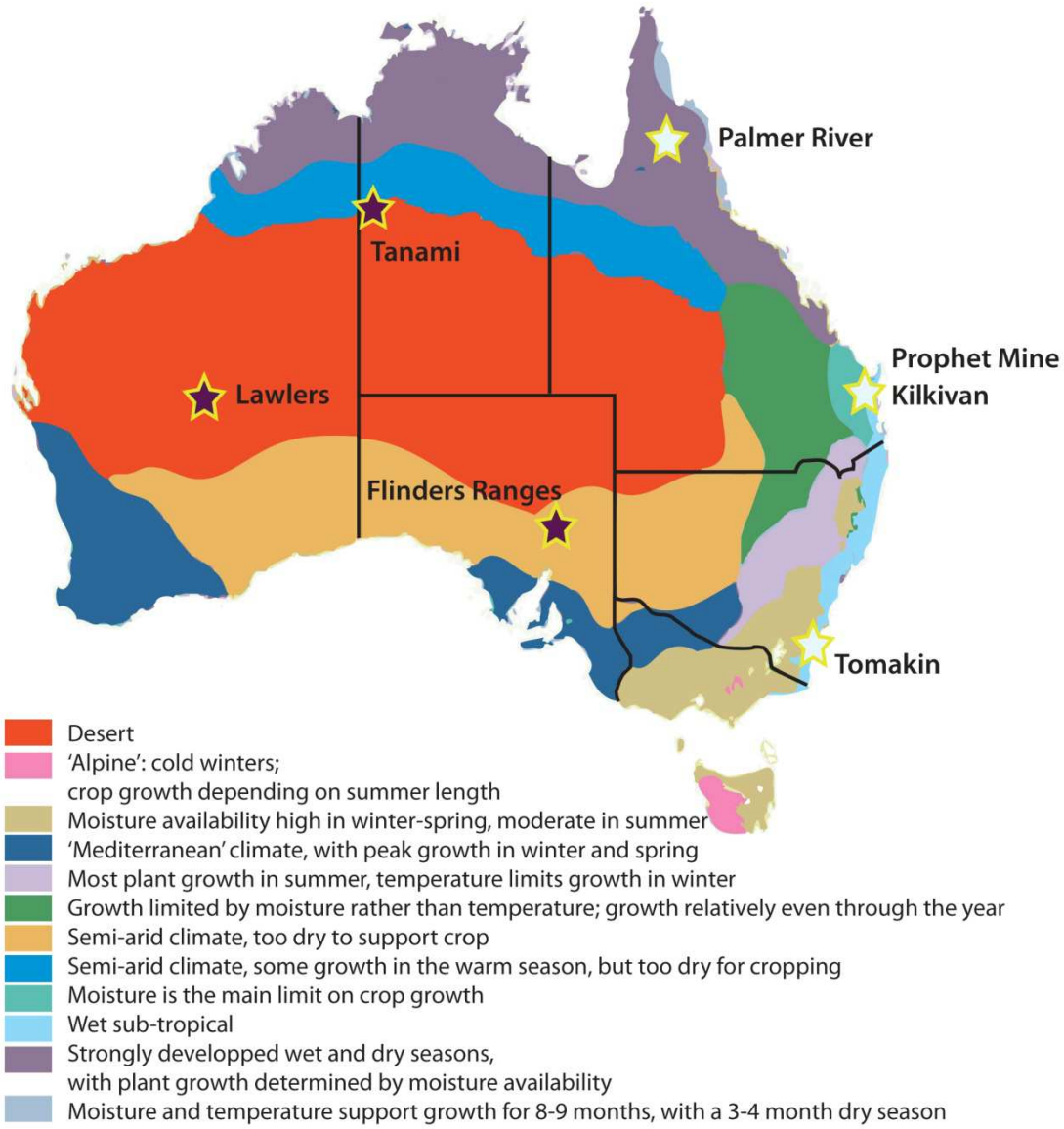

Figure 4.1. Sampling sites used in this (black stars) and previous study (light stars; Reith *et al.*, 2006, 2010), plotted on a climatic map with regions defined and categorized in terms of heat and moisture (modified from Hutchinson *et al.*, 2005).

Table 4.1. Summary of geological and environmental properties at the sampling localities.

Sample name	Climate & vegetation	Regolith setting	Geological setting	Transport distance
Lawlers, Western Australia				
New Holland Mine	600 m underground	Sandstone and pebbly sandstone, enclosed by siltstones	Siliclastic sediments	From the reef, in recent drive
Donegal Runoff	Semi-arid to arid, low acacia woodlands with dominant mulga (*Acacia aneura)*. Shrub layer dominated by rattle bush (various *Cassia* pp), poverty bush and turpentine (various *Eremophila* spp).	Elluvial on saprolith	Mafics/Basalt	< 20 m
Humpback Elluvium	*Idem*	Elluvial/placer	Granite (mainly)	< 20 m
Donegal Calcrete	*Idem*	Valley-form calcrete	Mafics	< 100 m
Coreshed Alluvium	*Idem*	Ferruginous duricrust	Mafics/Basalt	100-1000 m
Tanami, Northern Territory				
Old Pirate Reef	Savannah woodland with hummock-grass understory, the most common of which are spinifex, *Acacia* spp., *Grevillea* spp. and *Eucalyptus* or *Corymbia* spp	Sand, silt, clays and ferruginous quartzose	Monotonous sequence of turbiditic greywacke of the Killi-Killi formation	From the reef
Old Pirate Colluvium	*Idem*	Sand, silt, clays and ferruginous quartzose	Monotonous sequence of turbiditic greywacke of the Killi-Killi formation	< 20 m
Northern Flinders Ranges, South Australia				
Lively's Find Runoff	Semi-arid, low density, *Acacia aneura*	Saprolite/colluvial	Neoproterozoic siltstones and shales (Upper Callanna Beds)	5-15 m

4.2. Field Sites

4.2.1. Lawlers Tenement, Western Australia

The Lawlers gold province is located approximately 300 km north of Kalgoorlie in Western Australia, centered around S 28^{o}02‘ and E 120^{o}33’ (Figure 4.1.). The area is classified semi-arid to arid, with hot summers and cool to mild winters (Australian Bureau of Meteorology, 2011c). Annual rainfall approximates 200 mm, with drought and localized short-term flooding occurring periodically (Bunting and Williams, 1979). The vegetation cover is sparse, consisting of low acacia woodlands dominated by mulga (*Acacia aneura)*, rattle bush (*Cassia* spp.), poverty bush and turpentine bush (*Eremophila* spp.).

Geologically, the Lawlers province is located within the Agnew supracrustal belt of the Archaean Yilgarn Craton. Gold mineralization is widespread and ore bodies occur within three major rock types, *i.e*., sediments, mafic/ultramafic rocks, and felsic rocks (Figure 4.2.). The regolith was classified into three major units: i) ferruginous duricrust and gravel dominated terrains; ii) saprolite and bedrock-dominated terrains; and iii) sediment-dominated terrains (Anand, 2003). Minor valley-fill calcrete occurs on mafic/ultramafic rocks.

Gold grains were collected from five localities representative of environments where gold grains occur at Lawlers. These allowed the tracing

of detrital gold grains from placer settings back to primary mineralization (Table 4.1.). Samples were collected: i) underground within a newly developed ore body in the sediment-hosted New Holland Mine, where primary gold grains were collected at a depth of 600 m from a recently exposed quartz vein; ii) from wash materials derived from shallow historical underground workings located over mafic saprolith (Donegal Runoff); iii) from valley-form calcrete adjacent to the Donegal site (Donegal Calcrete); iv) from an elluvial deposit located in an outcropping granite intrusion (Humpback) and; v) from an alluvial channel situated within the mafic/ultramafics, collected at the base of a catchment formed by low-lying hills (Coreshed Alluvium; Table 4.1.).

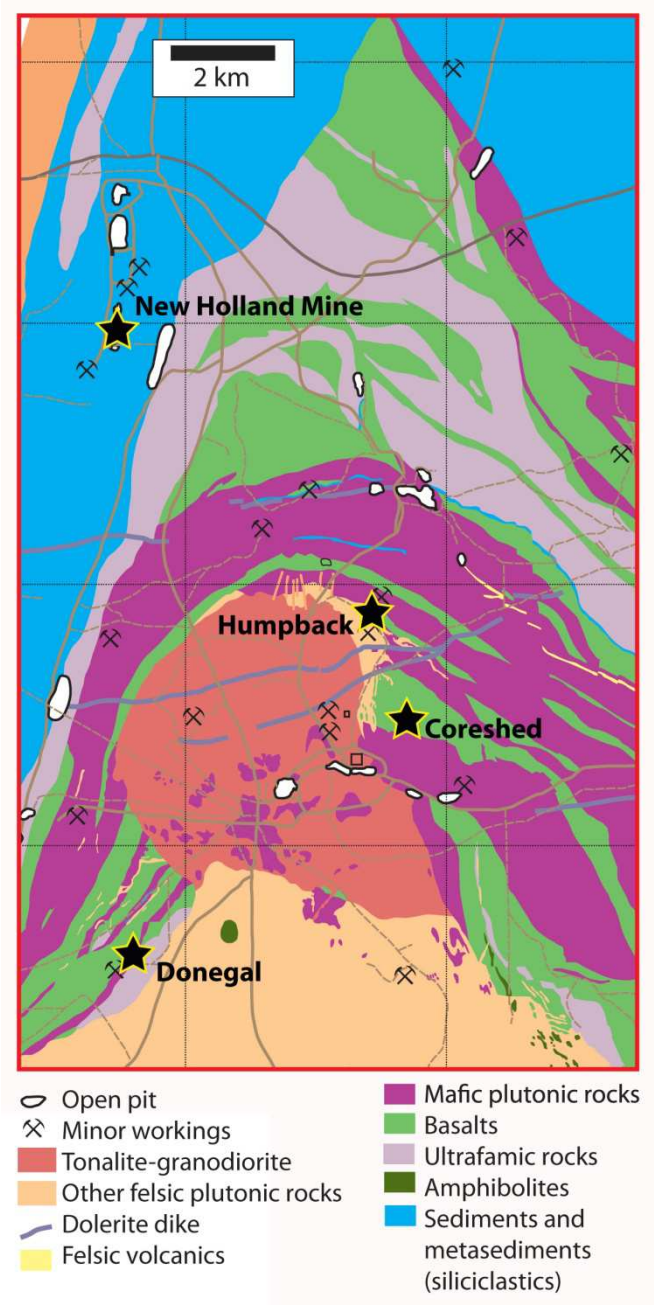

Figure 4.2. Location of the samples from the Lawlers gold field relative to mine workings and basement geology (modified after Peachey, 1999; Beardsmore and Allardyce, 2002).

4.2.2. Old Pirate prospect, Tanami Gold Province, Northern Territory

The Tanami Gold Province area is located 600 km northwest of Alice Springs in the Tanami desert (Wilford, 2003). Sampling was focused around the then mostly undisturbed Old Pirate tenement (S 20º11'29.80'' and E 129º09'35.26''), where high-grade gold veins outcrop at the surface (Figure 4.3A). The climate is semi-arid with irregular, monsoonal rainfall patterns (Figure 4.1; Gibson, 1986; Wilford, 2003), and a mean annual rainfall of 427 mm (Australian Bureau of Meteorology, 2011d). The Tanami region is vegetated by open savannah woodlands with hummock-grass understory, the most common plant species are spinifex, *Acacia* spp., *Grevillea* spp. and *Eucalyptus* or *Corymbia* spp. (Petts *et al*., 2009).

Figure 4.3. Sampling site in the Tanami (A) and Flinders Ranges (B). (A) Outcropping quartz vein with visible gold at the Old Pirate site. (B) Lively's Find workings. Samples were collected on the wash on the waste dump underneath the main trench located directly on the mineralization.

Geologically, the Tanami region consists of two major Precambrian tectonic units, the Granites-Tanami Block and the Birrindudu Basin (Blake, 1978). Outcrop in the Tanami region is sparse (less than 5 %) and gold occurrences are mostly covered by a 10 to 50 m deep regolith consisting of transported sand and laterite (Wygralak *et al*., 2001), with *in situ* weathering extending to depths of 150 m (Martin Smith, *pers. comm.*). At Old Pirate quartz veins occur within a monotonous sequence of turbiditic greywacke of the Killi-Killi formation (Granites–Tanami Block). Given the low topography of the area, the veins are likely to have been exposed since the Cretaceous. At

Old Pirate it was possible to sample gold within the outcropping quartz vein and the adjacent colluvial sheet-wash, within 50 m of the veins (Figure 4.3A).

4.2.3. Lively's Find, Northern Flinders Ranges, South Australia

The Lively's Find gold mine is located one kilometre northeast of Arkaroola Homestead in the Northern Flinders Ranges of South Australia (30'17"12.97"S 139"20'23.31"E). The climate is semi-arid with marked diurnal and seasonal temperature extremes. Rainfall is erratic, averaging 250 mm per annum, but this yearly average can be achieved over short periods (*e.g*., 306 mm in February and March 2011; Australian Bureau of Meteorology, 2011b). Vegetation is sparse, but rapid regeneration occurs within weeks after major rainfall events (Figure 4.3B). Mulga (*A. aneura*) predominates on arenaceous rock type within the ranges.

Lively's Find was discovered in 1949 and yielded 230 ounces of gold (Coats and Blissett, 1971). The mine is located on the foothill of the Eastern slope of the Mt Painter Inlier along a north-easterly striking fault plane that forms part of the Paralana Fault System. The Paralana fault is the locus of long-term fluid circulation (Mesozoic to present; Brugger *et al.*, 2005), and uplift since the Pliocene is responsible for the young topography of the Inlier (Wulser *et al*. 2011; Figure 4.3B). The mineralization is hosted by laminated siltstones and shales that form part of the Blue Mine Conglomerate member in the upper part of the Callanna Beds. Lively's Mine is interpreted to

represent an epithermal gold deposit that contains minor primary V-mica and Bi-minerals (Collier and Plimer, 2002). Vein material within the workings (< 10 m depth) is highly weathered. Gold was recovered as fine grained (<< 1 mm) gold, including wire gold, from the slope beneath the vein (Figure 4.3B).

4.3. Materials and methods

4.3.1. Sample collection and preparation

Samples were collected from Lively's Find in July 2007, the Lawlers tenement in June 2008, and Old Pirate in October 2009. Gold grains were collected using the field-sterile method aimed at keeping polymorphic layers intact (Reith *et al.*, 2010). All grains were transported refrigerated to the laboratory and kept in ~1 mL of sterile 1.25 % glutaldehyde solution. For electron microscopic studies, grains were either air dried or dried via a series of dehydration steps at the critical point of CO_2 to further insure the integrity of biofilms (Fratesi *et al*., 2004).

4.3.2. Analyses of Au grains

Optical microscopy (OM) was performed using a Nikon DXM1200 stereomicroscope with Automontage software (Nikon, Japan). Gold grains

were analyzed uncoated using a FIB-SEM (Helios NanoLab DualBeam, FEI, Netherlands). Images were obtained at 3 kV to 15 kV with sectioning and cleaning carried out at 30 kV/21 nA and 30 kV-20 kV/2.8-0.34 nA. The instrument was equipped with a 10 mm^2 Sapphire Si(Li) energy dispersive spectrometer (EDS); analyses were conducted using acceleration voltages between 15 and 20 keV. Samples for SEM-EDX analysis were carbon-coated (3 nm) prior to analysis.

Three to five grains from each site were set in epoxy resin, polished with 1 µm diamond paste, carbon-coated and subjected to EPMA using a Cameca SX51 Microprobe (Cameca, France) equipped by five wavelength dispersive spectrometers. Data collection and reduction was performed with the SAMx package. Analyses were conducted at 20 kV and 19.89 nA with a 1 µm beam diameter. The grains were analyzed for (detection limits in parenthesis as wt.%): Al (0.06), Si (0.05), S (0.05), Fe (0.08), Ni (0.09), Cu (0.11), As (0.25), Pd (0.25), Ag (0.25), Au (0.28), Hg (0.6) and Bi (0.5). Elements were calibrated on a mixture of minerals and pure metal standards from Astimex. Al, Si, and Fe were calibrated on natural garnet; S and Cu on chalcopyrite; As on arsenopyrite, Bi on Bi-telluride; Hg on HgS; and Ni, Pd, Ag, and Au on pure metal standards.

A whole mount of carbon-coated host material from Old Pirate was investigated using PIXE spectroscopy at the University of Melbourne (Ryan, 2001). All analyses were performed with a 3 MeV proton beam focused to 2 µm. During analysis, beam currents were kept to less than 10 nA to reduce

sample heating, excessive dead-time and spectral contamination due to pulse pile-up. X-rays were collected with a large area Ge(Li) detector mounted at 135º. A 300 µm Aluminum filter was positioned in front of the detector to reduce excess count rate from the iron component. The X-ray data was processed and fitted using the GeoPIXE software suite (Ryan and Jamieson, 1993).

4.4. Results and discussion

Gold grains from the New Holland Mine and the outcropping Old Pirate deposits were sampled from underground and exposed quartz veins, respectively, and their morphologies and chemical compositions were determined (Figures 4.4. and 4.5.). These were used as baseline for the assessment of supergene transformations of grains obtained from placers proximal (within 20 m) and distal (> 100 m) of their respective sources, in order to elucidate the chronosequence of transformations of supergene gold grains in arid environments.

4.4.1. Primary gold from underground and surface exposed quartz-vein systems

Gold grains from the New Holland Mine range from 0.1 to 1 mm in diameter. Gold grains are coarse, sub-angular to angular (Figure 4.4A) with no mechanical damage. The grains are comprised of a relatively homogenous gold-silver alloy (average [minimum, maximum]: 93.5 [81.0, 95.4] wt.% gold and 6.0 [5.1, 8.4] wt.% silver) with galena inclusions, as shown in the Red-Green-Blue (RGB) microprobe map (Au-Ag-Pb; Figure 4.4B); other elements were not detected. Grain boundaries between gold crystals, which are several tens of µm in diameter, showed no evidence for etching or grain boundary dissolution (Figure 4.4C). All grains contain areas that exhibit triangular shapes consistent with the {111} octahedral crystal forms common in primary gold (Hough et al., 2007, 2008, 2011; Figure 4.4D).

Primary gold grains showing similar textures and morphologies were described in earlier studies. For instance, primary gold grains from the Suzdal' deposit in Kazakhstan were shown to be crystallomorphic segregations and irregular in shape (Kalinin *et al*., 2009). These grains were 150 µm in diameter and composed of a gold-silver alloy, containing 93 to 98 wt.% gold (Kalinin *et al*., 2009). Colin and Vieillard (1991) investigated grains from unweathered quartz veins at Dondo Mobi, Gabon. Grains ranged from 63 to > 500 µm in diameter and were composed of single crystal aggregates,

which were either anhedral or euhedral, with smooth surface sides and sharp edges displaying dissolution rims (Colin and Vieillard, 1991).

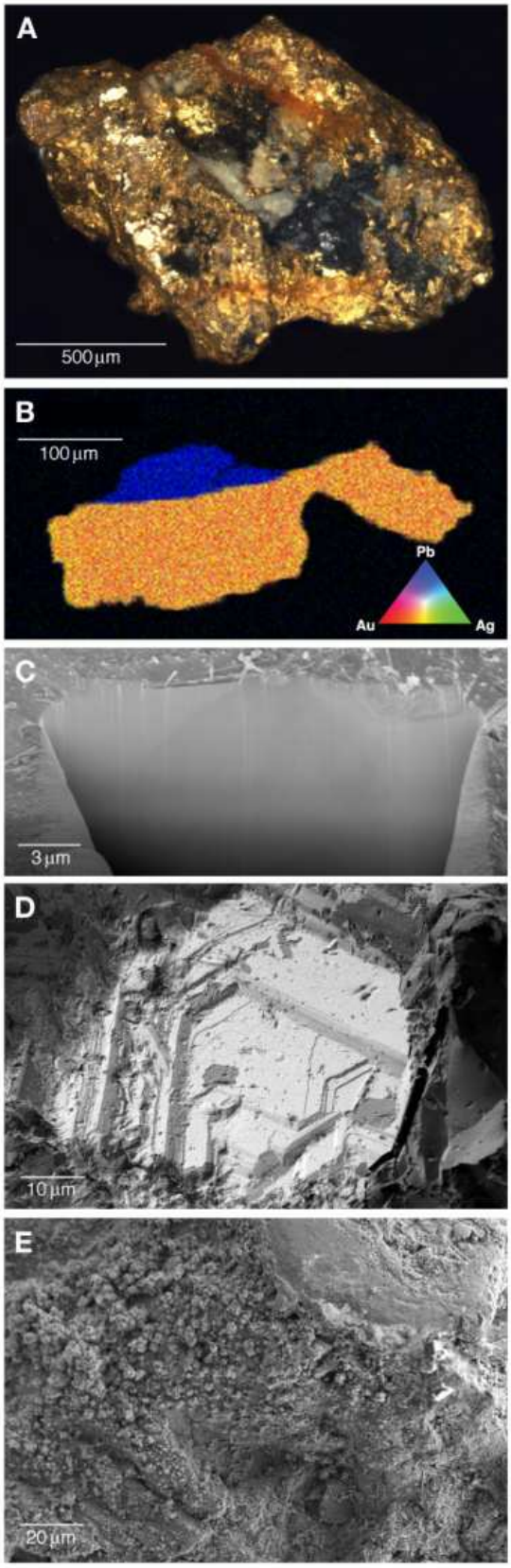

Figure 4.4. Images of grains collected from the New Holland Mine in the Lawlers tenement. (A) Optical micrograph showing that the gold grains are coarse and sub angular with no mechanical damage; quartz and galena inclusions are also visible. (B) Electron Microprobe RGB map (red = gold (Au); green = silver (Ag); blue = iron (Fe)) showing the homogenous gold-silver alloy. Note the galena inclusion. (C) FIB-SEM image showing that even at grain surface no change in crystal size and no etching or dissolution along grain boundaries is evident. (D) SEM micrograph showing the crystallographical forms with µm-high sharp terraces present on the surface of the New Holland Mine gold grains. (E) SEM micrograph of acicular iron-oxides (5-10 µm) observed on gold grains.

Grains from the New Holland Mine were collected from a recent drive (< 1 month old), where weathering was not expected, and no effect of weathering on the primary gold was observed. However, SEM revealed the presence of secondary minerals associated with the gold grains, these include acicular iron-oxides and -hydroxides (5-10 µm; Figure 4.4E), thin and spindly forms of lead-sulfate, possibly anglesite, and lead-carbonate, possibly cerussite. This suggests an influence of weathering even in these deep quartz veins, confirming the results of earlier work assessing deep weathering of ore deposits in the Yilgarn Craton (Phillips *et al*., 1998). Minerals, such as the ones observed in our study, are a result of weathering of primary sulfides (pyrite, pyrrhotite, galena; e.g., Leybourne, 2001; Moroni *et al.*, 2001). For example, the mineralogy and geochemistry of particulate matter in groundwaters associated with zinc-lead massive sulphide deposits was studied by Leybourne (2001). They noted the presence of abundant iron-oxides resulting from the weathering of the sulfide ore body. Another example is the Serra Pelada gold-platinum group element (PGE) deposit, were supergene alteration had created partial to total transformation of minerals into friable aggregates of kaolinite, iron-oxides and hydroxides, silica and secondary phosphate-sulfates, even at depths exceeding 200 m (Moroni *et al.*, 2001). While the occurrence of weathered minerals at the New Holland mine may be the result of exposure to air and water during mining activities, the observed weathering likely occurred prior to mining, and may be the result of microbial processes. Microorganisms are omnipresent in the

deeper crustal regions down to > 10 km, have been shown to drive mineral transformations under these conditions (Pedersen, 1993), and microbial mineral transformations have been observed in otherwise ‘pristine’ deep core materials (Southam and Saunders, 2005).

The exposed gold-bearing veins at Old Pirate are comprised of quartz with minor amounts of sulfides (pyrite and galena), which are heavily weathered at the surface (Figure 4.5A). Gold is abundant as fine gold usually associated with iron- and manganese-oxyhydroxides; in addition, coarse (hundreds of µm in size) gold within massive quartz occurs (Figure 4.5A). Element mapping using PIXE showed the presence of transformed primary gold, which contained a gold-silver-palladium alloy in its center as well as high purity secondary gold. The amount of gold and silver detected in the core of the grain is 86.9 [67.8, 97.3] wt.% gold and 8.6 [0.3, 19.2] wt.% silver (Figure 4.5C). High purity secondary gold particles are tens of µm in diameter and concentrated around the core of weathered pyrite (Figure 4.5B-D).

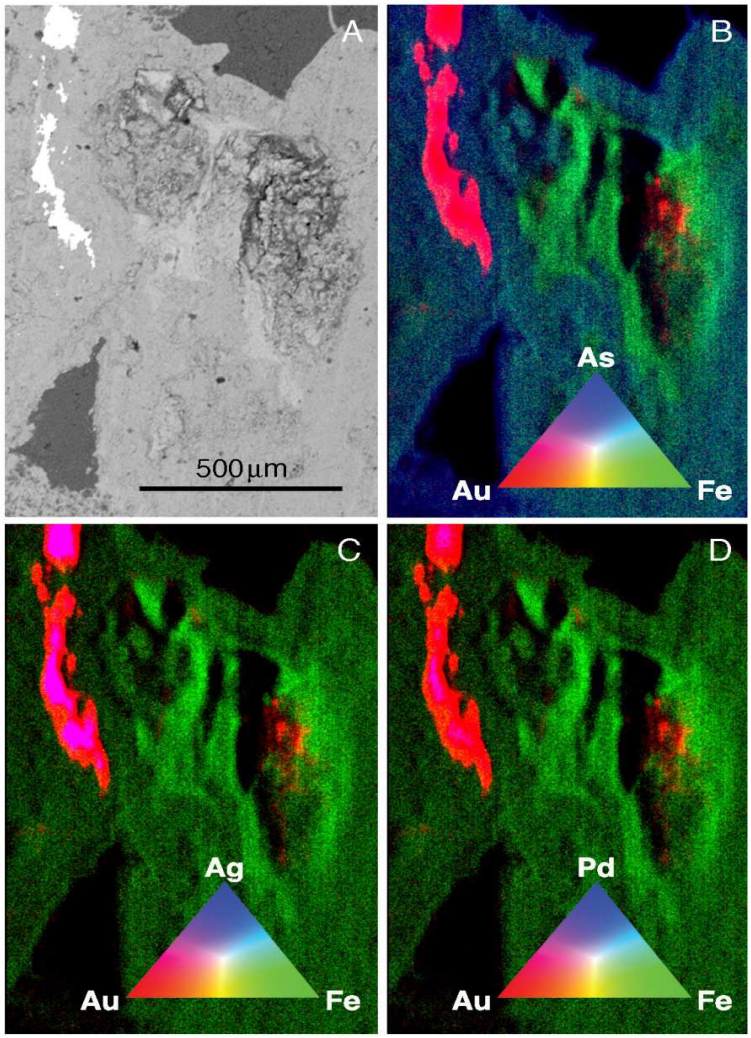

Figure 4.5. Thin section obtained from the Old Pirate Reef in the Tanami, Northern Territory. (A) SEM and elemental maps (obtained using PIXE; B-D) of a polished section of weathered gold-bearing sulfides (pyrite) in a quartz vein from the Old Pirate tenement. The RGB maps show gold-iron–arsenic (Au-Fe-Ar; B), gold-iron-silver (Au-Fe-Ag; C) and gold-iron-palladium (Au-Fe-Pd; D), and reveal the alloyed nature of the gold grain on the right.

The low topography of the Old Pirate site (Figure 4.3A) suggests that the quartz vein system has been exposed since the Cretaceous, resulting in a high abundance of weathered sulfides and gold. The association of the µ-crystalline high-purity secondary gold with iron-oxyhydroxides suggests that most of the visible gold was liberated during the oxidation of sulfides. Weathering also affected the coarse primary gold grains. While the grains from the New Holland Mine and Old Pirate Reef are both angular, only primary gold from Old Pirate contains two distinct phases: a primary core consisting of a gold-silver-palladium alloy (Figure 4.5C,D), and an outer rim of pure gold, suggesting dissolution and dispersion of silver and palladium. Depletion of silver in the rim of gold nugget is common and has also been described by Hough *et al*. (2007) and others (e.g., Giusti and Smith, 1984; Groen, 1990).

4.4.2. Gold grains from placer environments

4.4.2.1 Proximal grains

Grains collected from within 20 m of the primary mineralization (Table 4.1.) displayed angular morphologies, coarse crystal sizes and chemical compositions, *i.e.*, homogenous gold-silver-alloy, characteristic of primary gold. They showed minimal signs of physical damage. In contrast to primary grains (Table 4.1.), polymorphic layers, gold-rich rims, gold nano-particle

formation and morphologically diverse secondary gold were observed. The appearance of these secondary morphotypes appears to be a function of the length of time the grains had been exposed.

Grains collected from the Donegal Runoff (Figure 4.6.) that drains historic (pre-1922) waste dumps of underground workings, are likely the most recently exposed grains, and hence offer the opportunity to study supergene transformations occurring over historic rather than geological periods. The grains range from 0.4 to 0.8 mm in diameter, are angular (Figure 4.6A,B), and contain a core of homogenous gold-silver alloy (93.0 [91.3, 93.5] wt.% gold and 6.8 [6.1, 7.3] wt.% silver). The crystallites in the core of the gold grains are > 5 µm in size, with no evidence of damage on the rim (Figure 4.6C). Surfaces of the grains lack evidence of damage such as striations or gauges (Figure 4.6B). When compared to gold grains collected from quartz vein settings, the grains show the development of a polymorphic layer (Figure 4.6B,C; arrows) consisting of silicon, aluminum, oxygen, and sodium, similar to that described by Nakagawa *et al*., (2005; Figure 4.6B,C). Secondary gold was not detected, and no other evidence of secondary precipitation or dissolution was observed.

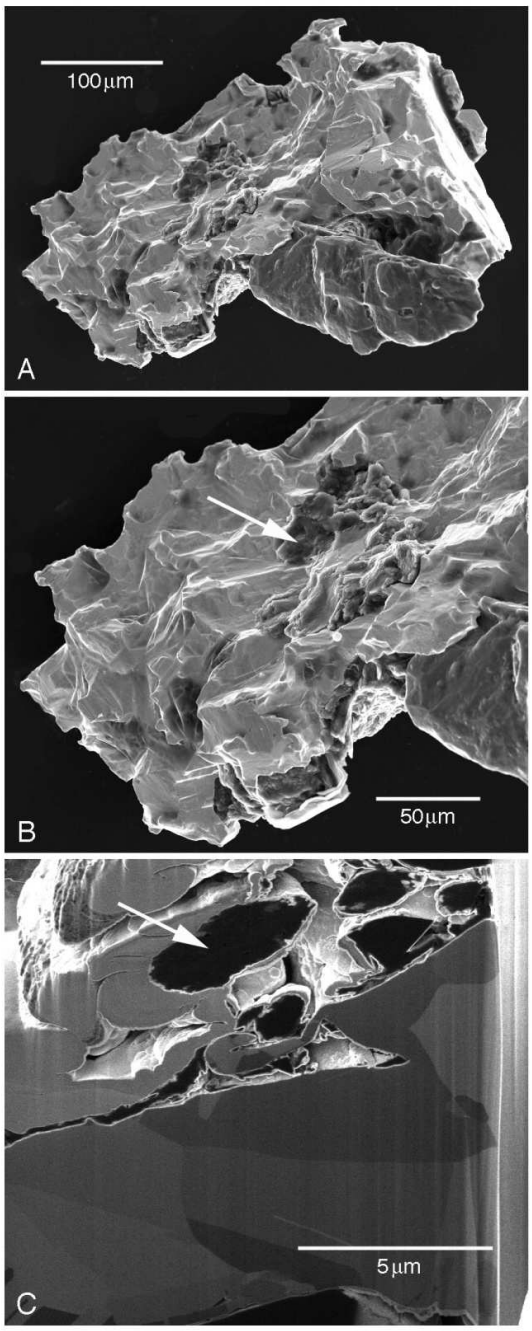

Figure 4.6. Morphology of gold grains from the Donegal Runoff within the Lawlers tenement. (A) SEM micrograph showing the angular nature of a typical grain from the Donegal Runoff with little to no striations present. (B) SEM micrograph showing the angular nature of the grains and the presence of a layer comprised of silicon, aluminum, oxygen, and sodium (arrow). (C) FIB-SEM micrograph showing a section through the layer of material shown in (B).

The grains from the Humpback Eluvium (Figure 4.7.), which are likely next in the sequence of exposure to supergene transformations, showed the development of gold-rich rims and abundant, well preserved secondary gold with morphologies ranging from flattened to framboidal µm-sized precipitates (Figure 4.7D-G). Grains range from 0.3 to 1 mm in diameter. The gold grains are angular and intergrown with quartz (Figure 4.7A). Their cores consist of a homogeneous gold-silver alloy containing 96.6 [93.8, 99.5] wt% gold and 3.3 [0.5, 4.6] wt.% silver. The rims display areas of high purity gold and iron-rich coating (Figure 4.7B). FIB-SEM sections revealed that the cores of the grains consist of large crystallites (> 10 µm), while the rims show complex, polycrystalline, flattened to framboidal, µm-sized particles (Figure 4.7C). Despite some striations (Figure 4.7A,D; arrows), the grains showed minimal rounding. A layer of material comprised of aluminum, silicon, oxygen, bismuth and iron cover their surfaces. Dissolution and pits on grain surfaces are up to several µm in diameter and also hold siliclastic material (Figure 4.7D,E,F); bridging by secondary gold was observed (Figure 4.7D). Siliclastic materials contain both nano-particulate and bacteriomorphic gold (Figure 4.7E,F); in addition framboidal bismuth minerals, likely bismuth-carbonate, were observed (Figure 4.7G). Budding gold morphotypes are made up of conglomerates of small spheroidal buds that are up to tens of nm in diameter (Figure 4.7E). These gold agglomerations were observed in protected areas within the silicate material (Figure 4.7D,E,F), but not on primary gold grains (*e.g.*, New Holland).

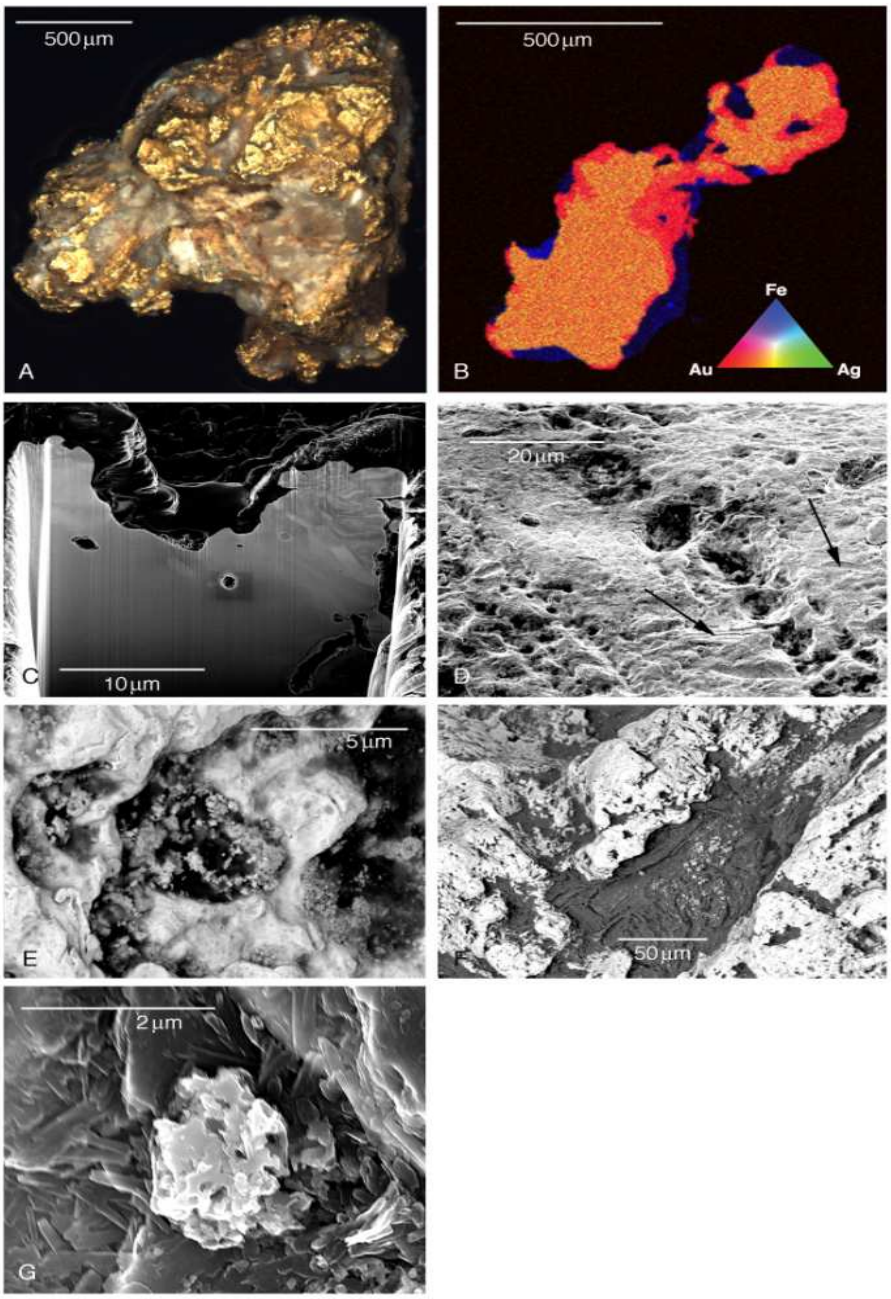

Figure 4.7. Grains collected from Humpback in the Lawlers tenement and their morphological features. (A) Optical micrograph showing typical angular and crystalline structure of the gold and the intergrowth with quartz. (B) Electron Microprobe RGB (gold-silver-iron; Au-Ag-Fe) mapping showing the alloyed nature of the bulk, silver-depletion along the rims, and a coating of iron-rich material on the grains. (C) FIB-SEM micrograph showing the larger internal grain size of the bulk compared to the polymorphic rim. (D,E) SEM micrograph displaying dissolution pits µm in diameter. The pits are filled with siliclastic material comprised of aluminum, silicon, oxygen, bismuth, iron, and containing budding gold aggregates each tens of nm across that are comprised of smaller gold nanoparticles. (F) BSE micrograph of a similar area to that of (E) showing the contrast between the bulk and budding gold and the siliciclastic material. (G) SEM micrograph of rare framboidal bismuth structures that are µm in size.

While detrital grains from many sites have a central core of primary gold (Hough *et al.*, 2007; Falconer and Craw, 2009; Reith *et al.*, 2010), grains from the Old Pirate Colluvium contain silver-rich bands, which run through the length of some grains (Figure 4.8B). Gold grains from the Old Pirate Colluvium are between 0.4 to 1 mm in diameter. Grains are angular and show a small amount of rounding (Figure 4.8A). Electron microprobe analyses revealed high silver contents with an average of 11.5 wt.%. Depletion in silver was detected on the grain rims (Figure 4.8B,E; the minimum silver concentration is 0.12 wt.%). In central areas of the grains, silver-rich bands 10's of µm in width were observed, with silver concentrations of up to 21.4 wt.% (Figure 4.8B). A band of gold depletion runs parallel to an internal gold-rich band. The silver banding in these grains may be the result of selective leaching of silver along preferential flowpaths, while the grain had been embedded in the outcropping quartz vein, or it may be the result of the fusion of multiple smaller grains in the colluvium.

Old Pirate grains show distinct gold-rich rims as well as polymorphic carbonaceous layers containing abundant gold nano-particles and µ-crystals (Figure 4.8E,F). This indicates that the length of time, not only the distance of transport, correlates to the grade of secondary transformation grains undergo, and confirms the importance of physical processes, *e.g.*, rounding through transport, for the overall shape of the grains. On the surface of the grains a layer of polymorphic material, consisting of aluminum, silicon, oxygen, iron and magnesium with vermiform structure, was observed (Figure

4.8C,E,D). This material contains sub-μm size gold aggregates and gold wires (Figure 4.8E,F). The grains also display delicate gold structures that protrude from the exterior of the grain in bulbous, and budding formations that are reminiscent of bacteriomorphic structures (Figure 4.8D). These structures appear to form via the agglomeration of 100s of individual nm-sized spheroidal particles.

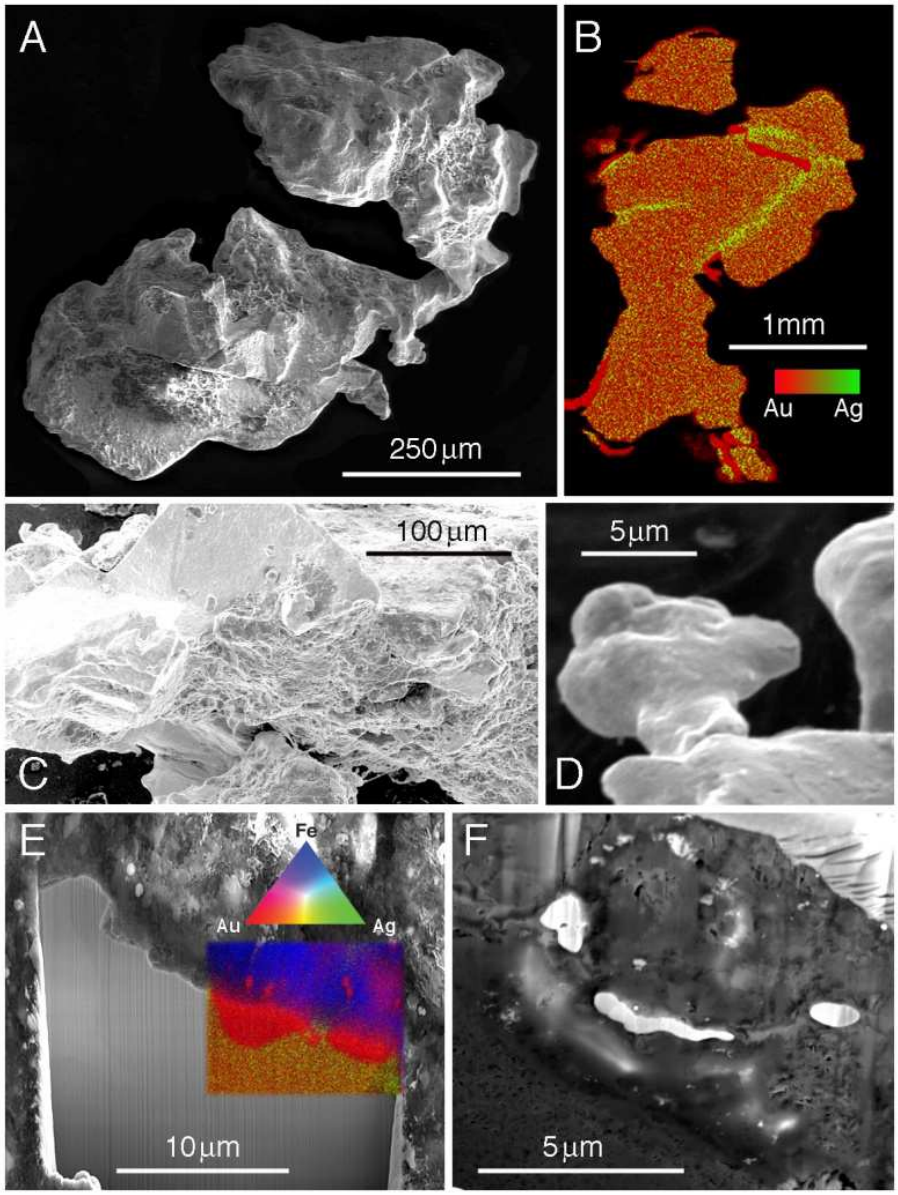

Figure 4.8. Morphology and features typical of grains collected in the Old Pirate Colluvium, Tanami. (A) SEM micrograph showing the typical size (500 µm) and the crystalline and angular nature of the grains. (B) EPMA map showing gold and silver in Red and Green respectively, highlighting areas of banding. (C) SEM micrograph of the surface of the grain showing the striations and morphology of the grain. (D) SEM micrograph of bacteriomorphic gold on the surface of grains from the Tanami alluvial wash. (E) FIB-SEM image revealing the difference in crystal structure between the bulk of the grain and the rim. Overlain in this image is an RGB map with gold (Au; red) silver (Ag; green) and iron (Fe; blue). The rim and the gold nanoparticles dispersed throughout the material are silver-poor. (F) FIB-SEM (BSE mode) micrograph of wire and nano-particulate gold structures and their inner crystal makeup.

In contrast, proximal grains from Lively's Find are highly transformed, with rounded edges, no silver-rich cores, and abundant secondary features covering surfaces (Figure 4.9.). The Lively's Find gold grains are between 0.4 and 1 mm in diameter, rounded (Figure 4.9A), and heavily striated, despite the short distance of transport. Elemental analysis showed that these grains are comprised of gold (96.0 [91.0, 99.5] wt.%) and silver (3.4 [0.3, 8.4] wt.%) with measurable amounts of bismuth (0.7 [0.54, 0.97] wt.%) (Figure 4.9B). Gold-rich rims were observed, as were regions of silver-rich banding that extend into the bulk of the grains. Silver-rich bands are widespread throughout the bulk of the grain and tens of µm thick (Figure 4.9B). The internal crystallinity of the grains is > 10 µm, while the rims show µm-sized subgrains (Figure 4.9C). Gold grains of an epithermal origin are commonly transformed even before surface exposure. For example, gold grains from the Chelopech volcanic-hosted gold-copper epithermal deposit in Bulgaria were similar in morphology and silver-content to the Lively's grains (Bonev *et al*., 2002). There, gold occurred as subhedral flakes, irregular grains, euhedral isometric crystals, elongated rods, wires and fine fibrous crystals, dendrite-like formations, spongy gold and polycrystalline grains and consists of 94.1 wt.% gold, 5.3 wt.% silver and 0.5 wt.% copper. Similar to Old Pirate Colluvium grains, Lively's Find grains show a zonation of silver and gold (Figure 4.9B), which may be the result of selective leaching of silver along preferential flowpaths, or it could be the result of extended periods of

epithermal conditions, consistent with the long history of recurrent fluid flow along the Paralana Fault Zone (Brugger *et al.*, 2005).

All Lively's grains are almost completely covered by viable biofilms, which are up to 10 µm thick. The biofilm consists of round cells that are between 1 and 5 µm in diameter and are coated with exopolymeric substances. In addition, large quantities of filaments, resembling bacterial nano-wires, were observed (Figure 4.9D,E). Gold nano-particles were dispersed throughout the biofilms, and were most abundant at its base. Here the biofilms were in direct contact with the grain surfaces, and large numbers of gold nano-particles and spheroidal µm-crystals had been released (Figure 4.9F-G). This suggests that the gold grains have undergone supergene transformations, probably driven by microbial dissolution and re-precipitation of gold, after exposure to the surface, or within the weathered vein material.

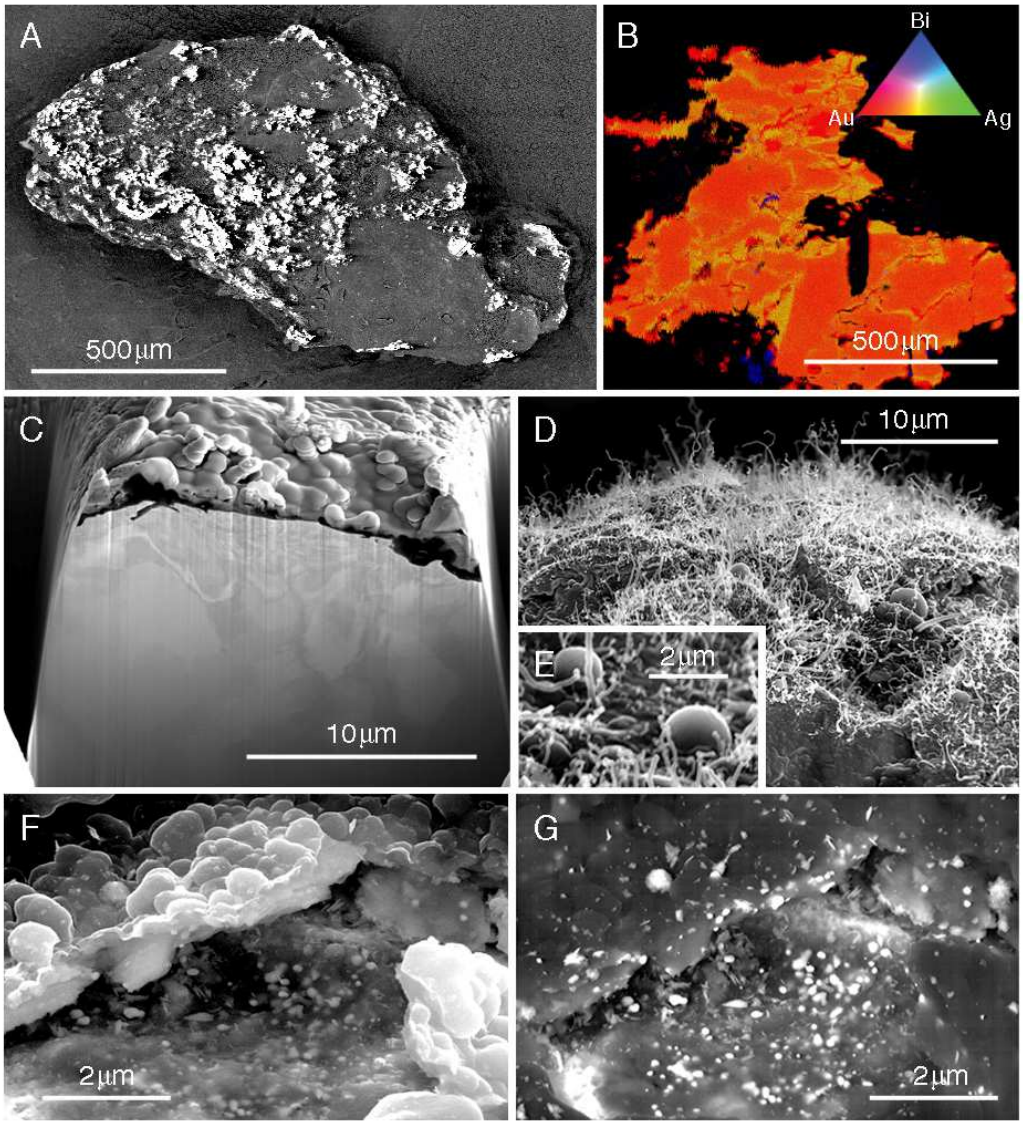

Figure 4.9. Gold grain from Lively's Find in the Flinders Ranges, South Australia. (A) SEM micrograph (BSE mode) showing the rounded morphology of the gold grains. (B) Electron Microprobe map showing gold (Au; Red) and silver (Ag; Green), highlighting the alloyed nature of the grain and areas of higher purity gold. (C) Inner crystallinity of the grains as revealed via FIB. The size of the crystal grains is smaller on the exterior rim of the grains and larger towards the bulk of the gold grain. (D) SEM micrograph of a viable biofilm on the surface of the grains with (E) showing the surface of the grains and the gold nanoparticles distributed in interstices between the nano-wires. (F,G) Micrographs displaying BSE/SEM respectively gold precipitates seen to be distributed on the surface of the Lively's gold grains.

4.4.2.2 Distal grains

Gold grains were collected further than 100 m from their source in alluvial placers to assess the degree of supergene transformation the grains have undergone. Gold grains collected from the Donegal Calcrete alluvial channel provide an opportunity to investigate transformations in the presence of calcrete. Donegal Calcrete grains are between 0.4 and 3 mm in diameter, are rounded, folded and display irregular shapes (Figure 4.10A). Striations from physical transport are common on their surfaces (Figure 4.10A,C,D). The composition of grain cores is homogenous, with average silver contents of 5.0 [4.2, 6.7] wt.%. Silver depletion (< 50 µm in width) was observed locally along the rims. Gold crystals in the core are several µm in size (Figure 4.10B). The surface of the gold grains is dominated by flattened aggregates and sheets (~10 x 10 μm^2; Figure 4.10C,D) consisting of high fineness gold (> 99 wt.%). A surface layer of vermiform, siliciclastic material comprised of aluminum, silicon, and oxygen with small amounts of magnesium, iron and calcium fills the low lying areas (Figure 4.10A-F). Dissolution pits are common, they are several hundred nm in diameter and filled with the siliclastic material (Figure 4.10E). Spheroidal µ-crystalline gold particles (~1 µm in diameter) are embedded in the siliclastic matrix. These particles did not display clear crystalline faces (Figure 4.10C,D), suggesting that the particles were in an early stage of aggregation. Nano-particulate gold of less than 50 nm is common (Figure 4.10E). Most of these particles are in direct

contact with grain surfaces, yet some are also dispersed throughout the siliclastic layer (Figure 4.10C,D).

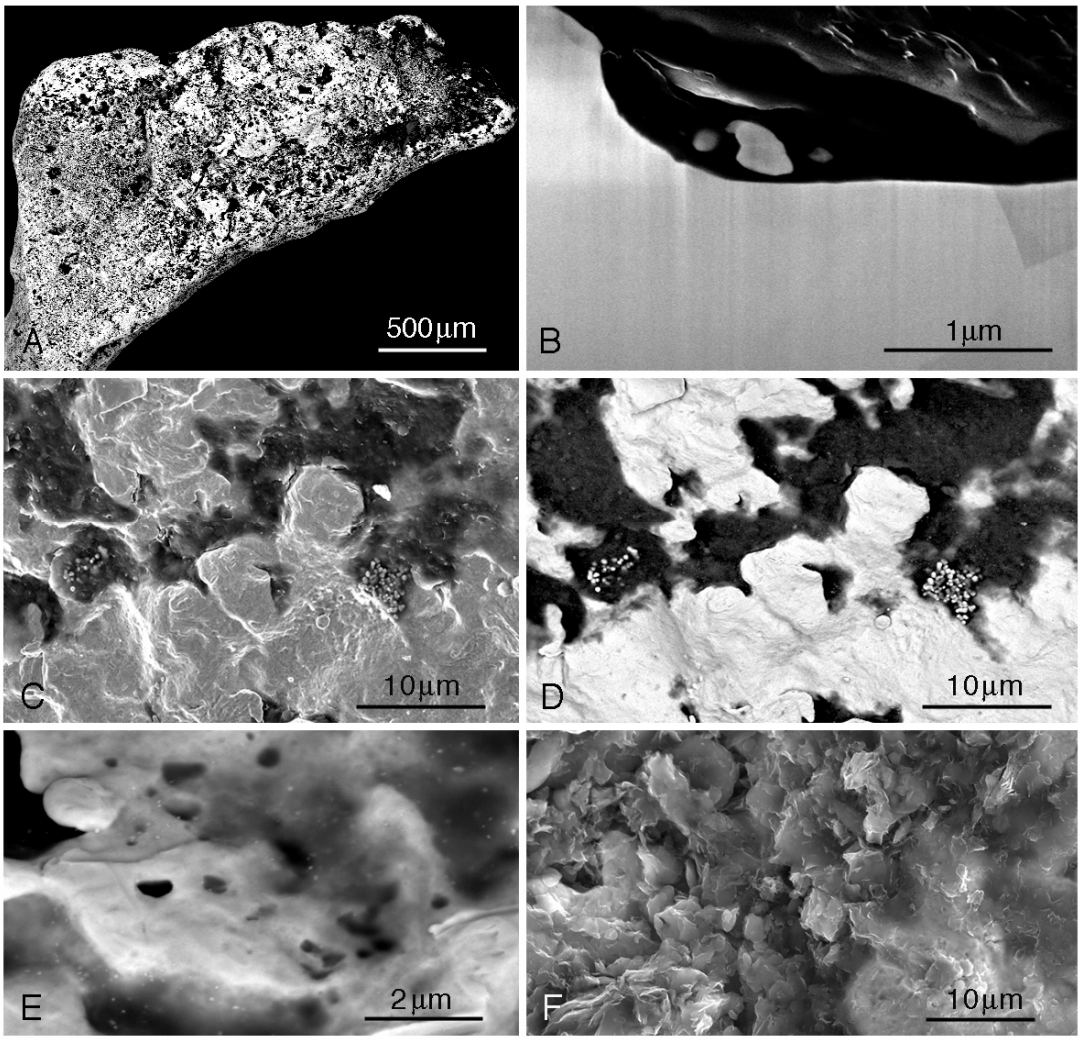

Figure 4.10. Morphology and features of the grains collected within a calcrete channel near the Donegal workings in the Lawlers tenement. (A) BSE micrograph showing rounded morphology and striations. (B) SEM micrograph showing the contrast between the coarse bulk gold and the nanoparticulate gold dispersed throughout the polymorphic layer. (C,D) Images in both secondary (C) and BSE (D) modes showing the contrast between bulk and nanoparticulate gold dispersed throughout the polymorphic layer. Nano-particulate and spheroidal gold occur in the polymorphic layer that lies within the dissolution pits and natural valleys of the grains. (E) BSE micrograph of dissolution pits and fine gold structures distributed across the grain. (F) SEM micrograph showing the vermiform structure of the siliclastic material on the surface of the grain.

Coreshed Alluvium grains range between 1 and 1.5 mm in diameter, with irregular morphology and rounding of surfaces (Figure 4.11A). Microprobe analyses reveals that the cores of the grains are comprised of on average 3.0 [0, 5.5] wt.% silver and 96.7 [94.4, 100.0] wt.% gold; traces of copper, iron and silicon were also detected. The core of the grains is comprised of crystals several microns in size with polycrystalline, µm-sized subgrains towards the rims (Figure 4.11B). Backscatter electron imaging and X-ray imaging revealed that most grains feature a silver-free rim (up to 10 µm thickness). The surfaces displayed extensive damage, including flattening, gouging, and striations (Figure 4.11C, black arrows). Abundant bacteriomorphic budding features (Figure 4.11C; insert, D; yellow arrow) cover the grains. In addition, abundant gold nano-particles and µ-crystals are dispersed throughout a polymorphic layer comprised of silicon, aluminum, carbon and oxygen that covers the surface of the grains, especially in pits and voids (Figure 4.11C-F). These gold particles range from tens, but, more typically hundreds, of nm with some reaching up to two µm in diameter (Figure 4.11C-F). The particles show a range in morphology, including rare triangular plates (Figure 4.11D; white arrow), pentagonal dipyramids (Figure 4.11C; Insert, white arrow), and abundant spheroids (Figure 4.11C), as well as complex crystalline aggregates (Figure 4.11C-F). FIB-milling revealed that the gold particles are dispersed right throughout the polymorphic layer (Figure 4.11E-F). The aggregates of gold nano- and micro-particles form chains of buds, in which each bud appears to have nucleated from the

previous bud (Figure 4.11D, yellow arrow). FIB-milling also revealed dissolution pits underneath the siliciclastic material (Figure 4.11E,F).

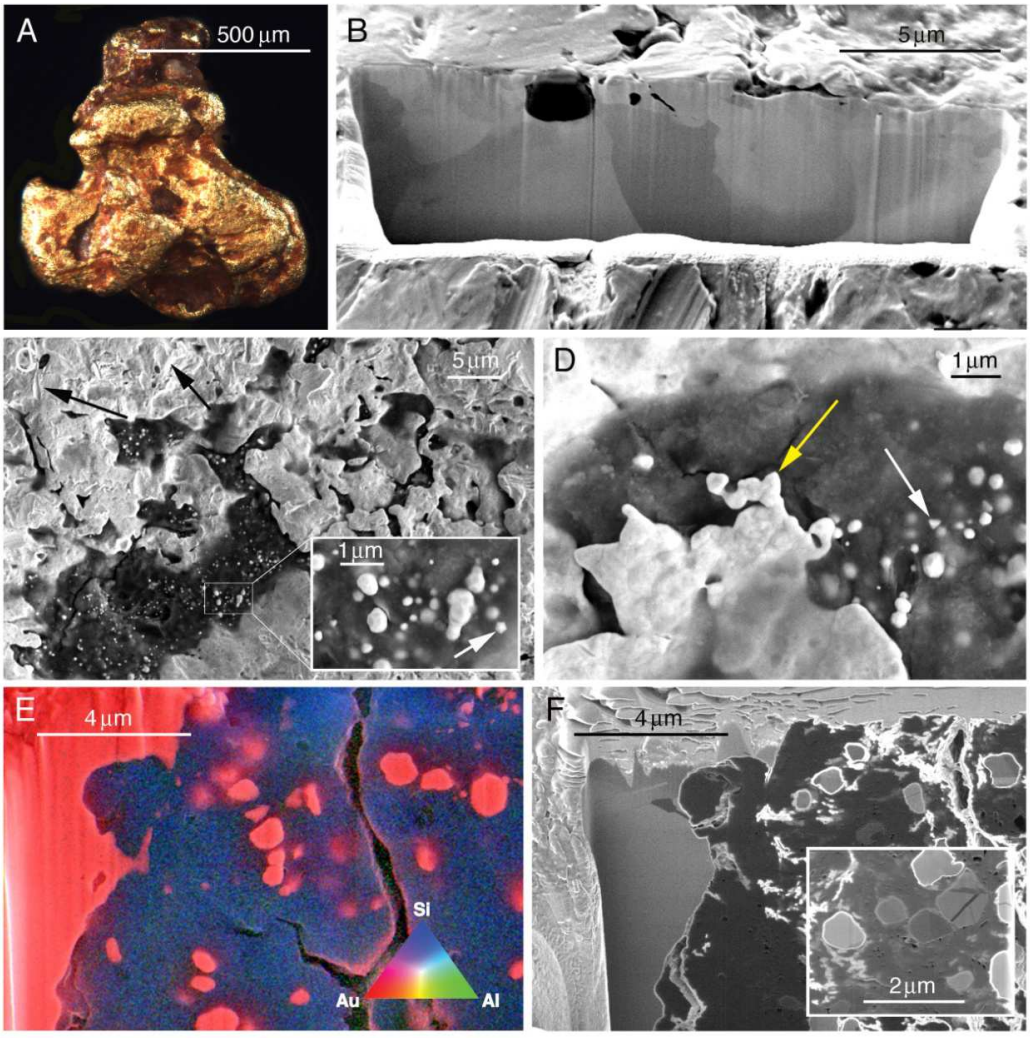

Figure 4.11. Morphology and features of the grains collected from the Coreshed Alluvium, Lawlers tenement. (A) Optical micrograph showing a typical grain with rounded morphology. (B) FIB-SEM micrograph revealing the bulk texture. (C) SEM micrograph of grain surface showing damage from physical transport and spherical gold nano- and micro-particles dispersed throughout a layer of polymorphic material. Inset showing the crystalline, spheroidal nature of the gold nano-particles. (D) SEM micrograph of the grain surface with nano-particles dispersed throughout the polymorphic material. (E) EDS X-ray map showing gold (Au; red), aluminum (Al; green), and silicon (Si; blue). (F) Secondary ion image showing the extent to which the gold nanoparticles are dispersed throughout the polymorphic material and the smaller crystallinity compared to the bulk gold.

All distal grains show a rich history of dissolution (Figure 4.10E, and 4.11C,E,F) and re-precipitation (Figure 4.10C-E and 4.11C-F) with abundant dissolution features, *e.g.*, etched pits occurring directly adjacent to precipitation features, and agglomeration of gold nano-particles and µ-crystals (Figure 4.10E, 4.11E,F). The grains comprise a primary core overlain by secondary gold. A polymorphic layer of carbonaceous materials and minerals, interpreted as residual biofilm, covers large areas of the grains, especially in topographically low-lying regions. In these layers, which are more extensive than on the elluvial and colluvial (proximal) grains, nano-particulate gold, aggregates of gold nano-particles, µ-crystals and bacterioform gold are abundant (Figure 4.10C,D and 4.11C-F). We suggest that this increase in gold mobility, at the local grain scale, reflects time and/or distance traveled from source, as well as the increased availability of water in the alluvial setting *versus* the elluvial and colluvial settings. This increased water availability sustains biological activity and viable biofilms for longer periods, relative to neighboring elluvial/colluvial settings.

Donegal Calcrete grains are associated with a valley-type calcrete, which forms as a result of biological processes (Reith *et al*., 2009a). In calcrete settings the formation of gold-in-calcrete anomalies is mediated by resident plant- and microbial communities (Lintern *et al.*, 2006; Reith *et al*., 2009a), hence a strong influence of microbial processes on the transformation of the gold grains is expected. Gold grains from calcrete at the Challenger gold deposit in South Australia are entirely secondary, and

displayed complex aggregated crystals, budding bacteriomorphic structures, similar to morphotypes detected on grains from Donegal calcrete (Lintern *et al.*, 2006). Dissolution features were also observed on Challenger grains, these were similar in morphology to the pits and pores detected on Donegal calcrete grains (Figure 4.10E).

4.4.3. Biofilms: key-catalysts for the supergene transformation of gold grains

Similar to sites (*i.e.*, Kilkivan) on the eastern seaboard of Australia, which receive in excess of 1000 mm of rainfall per annum, viable and residual biofilms were detected on gold grains at semi-arid and arid Australian sites. Biofilm formation is a process that gives rise to multiple cell types, each with a range of gene expression patterns that correspond to the diversity of biofilm micro-niches. This allows the population to withstand a diverse range of environmental stresses, including heavy metal toxicity (Harrison *et al.*, 2007). Biofilm populations are better protected from heavy metal toxicity compared to planktonic cells via the combined action of chemical, physical and physiological processes (Harrison *et al*., 2007). In particular extracellular polymeric substances, resulting from excretions, shedding of cell surface materials, lyses of cells and adsorption of organic constituents, aid biofilm development by enabling cell aggregation and adhesion to substratum, and

provide protection from desiccation and resistance to toxic heavy metals (Pal and Paul, 2008).

Laboratory studies have shown that bacterial biofilms are capable of mobilizing gold from gold surfaces (Reith and McPhail, 2006; Fairbrother *et al*. 2009). Dissolution of gold leads to the formation of cyto-toxic Au-complexes, which are reductively precipitated by other biofilm bacteria leading to the formation of gold nano-particles and µ-crystals observed in this and previous studies (Reith *et al.*, 2006, 2010). The Gram-negative bacterium *C. metallidurans*, which has been detected on gold grains from the three Australian sites, appears to play a special role in the cycling of gold within a biofilm (Reith *et al*., 2006, 2010). *Cupriavidus metallidurans* is capable of actively reducing aqueous Au-complexes and forming spherical nano-particles via gold-specific biochemical mechanisms (Reith *et al.*, 2009b). All grains from Lively's Find were covered by a microbial biofilm that was up to 10 µm thick and consisted of rod-like 1-4 µm sized bacterial cells covered in exopolymeric substances, which resembled those observed in earlier studies closely (Figure 4.9D,E; Reith *et al.*, 2006, 2010). Here microbial biofilms were associated with abundant nano-particulate, µ-crystalline and bacterioform secondary gold embedded in a polymorphic layer of secondary clay-, iron-, and silicate minerals (Reith *et al*., 2006, 2010). On the grains from Lively's Find, nano-particulate and µ-crystalline gold is also associated with the biofilms, and is especially plentiful at the contact between the biofilm and the primary gold. Spherical nano-particles as

well as octahedral gold platelets (Lengke *et al.*, 2006a; Lengke and Southam, 2007) have also been formed within biofilms consisting of thiosulfate-oxidizing-, sulfate reducing-, or cyano-bacteria (Lengke and Southam, 2005, 2006). Over time, these gold nano-particles were released from cells and deposited at cell surfaces (Lengke and Southam, 2006, 2007). Ultimately, nano-particles of gold contribute to the formation of µm-scale octahedral gold crystals, framboid-like structures (~1.5-µm) and mm-scale gold foils (Lengke and Southam, 2006, 2007).

One of the most important pre-requisites for biofilms to form is the availability of water (Costerton *et al.*, 1995), but the results from Lively's Find show that abundant gold-precipitating biofilms can form in arid settings. In July 2007, the Arkaroola region was within a long draught period (below average yearly precipitation since 2000), and received 31.5 mm during the 3 months before sampling, which was enough to form and sustain the biofilms (Bureau of Meteorology, 2011b). In the presence of water, the formation of biofilms occurs rapidly on coarse surfaces with irregular features; hence, gold grains in the supergene environment provide an ideal surface for the formation of biofilms. Dunne (2002) described the two-phase process for bacterial adhesion to a surface during biofilm formation, *i.e.,* the docking and locking stages. During the docking stage microorganisms get into close proximity (< 1 nm) to surfaces via motility or a stream of fluid flowing over the surface. The docking stage is complete when the net sum of forces between the two surfaces is overcome (Dunne, 2002). This is followed by the locking

stage in which the loosely bound organisms produce exopolysaccharides resulting in irreversible binding of these organisms to the surface. Once matured the biofilms will only be removed via physical or chemical abrasion (Dunne, 2002). However, drying and desiccation of biofilms will occur in the seasonal absence of water especially under the conditions experienced in arid settings, leading to the formation of carbonaceous residuals on surfaces, *e.g.*, our gold grains. The fossilization of biofilms occurs via cell walls, cytoplasm, and extracellular polysaccharides acting as nucleation sites for biomineralization (Westall *et al*., 1995). This nucleation can lead to the biofilm residues being encrusted by minerals as the organic matter degrades (Westall *et al*., 2001). Biofilms replaced by minerals are reported as taking on many different forms from spherules, “sausage”-shaped rods, rice grain structures, subrounded-suboval, filaments and spindles, similar to those observed on grains from Lawlers and Old Pirate (Westall *et al.*, 2001). Hence, while no viable biofilms were observed on gold grains from Lawlers and Old Pirate, ample evidence of past biofilm activities, such as iron-minerals, spherical gold nano-particulates and spheroidal gold µ-crystals were observed. The presence of polymorphic layers of organics and secondary minerals derived from the biomineralization or biofilm residues points to a transient nature of biofilm formation on these grains. While overall grain morphologies, *i.e.*, angularity and progressive rounding, of placer grains appears to be dominantly driven by physical processes occurring during transport, the chemical composition of grains, especially the rims, and

occurrence of secondary gold are linked to biogeochemical processes mediated by extended exposure to biofilm activity, rather than distance travelled from source. The study of gold grains from arid Australian sites has shown that supergene transformations occur under arid conditions. Microbial biofilms are likely to play a fundamental role in catalyzing these transformations in arid conditions. This demonstrates that the model of gold cycling and gold grain formation is valid in arid environments. Under arid conditions, biofilm growth is episodic, and the rates of gold cycling in arid environments is likely to be controlled by the periods of biofilm growth, with desiccation leading to the release of mobile nano-particulate gold in the environment. As biofilms have a limited lifespan (interrupted by drying out events), formation of nano-particles within the biofilms appears to occur over a period of months. However, further research needs to be undertaken to characterize the biofilm communities and biochemical processes important for gold cycling in the arid zone.

4.4.4. Application to mineral exploration

Transported gold grains are commonly used in mineral exploration for gold to pinpoint a primary source (Hough *et al*., 2007). For example, Chapman *et al*., (2011) used a combination of composition and inclusion mineralogy in placer gold grains to illuminate their relationship to sources and styles of mineralization in the Yukon Territory, Canada. The placer gold inventory

derived from this study led to the identification of the characteristics of populations of placer grains contributing to economically important placers. Knight *et al*. (1999) studied the relationship between distance travelled in fluvial systems and gold grain shape and rimming. The roundness and flatness of gold grains increased rapidly over the first five kilometers of transport from the source. This, coupled with the observed development of gold-rich rims, allowed for the separation of gold grains into the classification of proximal and distal to a likely source (Knight *et al*., 1999). However, Hough *et al*. (2007) noted that the morphology of grains, and in particular those found in stream sediments, is not diagnostic for origin or distance, but rather provides a record of the supergene transformations the grains have undergone. Our study confirms these findings and provides a biogeochemical process model for the initial and subsequent stages of gold grain transformations in arid environments. In combination with geological and physicochemical conditions, this model provides a baseline for the interpretation of macro- and micro-morphologies as well as chemical compositions of gold grains from arid sites in Australia.

Chapter 5: Conclusions - *Cupriavidus metallidurans* plays a key role in the formation of secondary gold structures on grains found in the Australian regolith

Previous chapters have shown that *C. metallidurans* will take up and precipitate Au(I)-complexes that bear a striking resemblance to formations found on detrital grains from arid Australian sites and thus *C. metallidurans*, and biofilms on these grains, are found to play a driving role in the genesis of authigenic supergene gold. In this final chapter, the conclusions of this Ph.D. research are drawn and an outlook is given into the type of studies that need to be undertaken to further understand the processes of supergene gold grain development. Additionally, the future applications of this research in mineral processing are discussed.

5.1. Uptake of environmentally relevant Au(I)-complexes, *by Cupriavidus metallidurans* and the effects of cell state.

If gold biomineralization by *C. metallidurans* is to be shown, the ability to take up gold must be demonstrated. This was tested by exposing different cell states (viable, inactive and sterile) of *C. metallidurans* to Au(I)-complexes over a range of pH and exposure times. By using biologically active versus inactive cells, active and passive mechanisms of gold uptake were definable. To determine uptake, gold content (and cell numbers) in these solutions was measured before and after exposure. Although CFU numbers (mL^{-1}) were greatest in full media, at the exposure times investigated bacterial uptake of gold, over sorption to organics in the growth media, was only observable in minimal media. In MME, across the pH range investigated, both viable cells and non-metabolizing controls were found to be taking up gold.

Conclusion 1

Viable cells of *C. metallidurans* take up more gold than the comparably rapid adsorption in inactive and sterile cells or abiotic controls under the same conditions.

Conclusion 2

Increasing the duration of viable *C. metallidurans* cell exposure to Au(I)-complexes results in an increased amount of gold uptake.

Conclusion 3

Uptake of gold by viable *C. metallidurans* cells is most observable with Au(I)-thiosulfate compared with Au(I)-thiomalate and Au(I)-cyanide.

Conclusion 4

Microbial uptake from Au(I)-complexes, by viable *C. metallidurans* cells suggests an active mechanism.

Conclusion 5

Uptake of gold from Au(I)-complexes by viable *C. metallidurans* is highest at pH 7.

Conclusion 6

At low pH conditions, gold retention is greatest in sterile cells and occurs much faster than uptake driven by viable cells.

Conclusion 7

Retention of gold by the organics in controls is a rapid (*i.e.*, < 6 hrs) mechanism and is not seen to increase with prolonged exposure.

5.2. *Cupriavidus metallidurans* mediated precipitation of Au(I)-complexes in supergene settings

As *C. metallidurans* was found to grow on gold grains in the supergene, column experiments loosely emulating supergene settings were conducted. These column experiments were designed to assess the ability of biofilms of *C. metallidurans* to biomineralize gold in the regolith. Following the growth of *C. metallidurans* biofilms on sand grains and subsequent treatment to obtain active versus inactive biofilms, gold was introduced to the columns over 84 days via increasing concentrations of Au(I)-thiosulfate in peptone meat extract. Via the use of longer exposure times than in initial uptake experiments, solutions collected periodically during the experiment showed viable cells were taking up practically all gold introduced to the columns and forming colloidal gold particles. At the end of the experiment microscopy showed the biomineralization of gold by *C. metallidurans* biofilms resulted in the formation of bacteriomorphic gold aggregates, composed of nano-particles that encapsulated void areas the size and shape of bacterial cells, also observed in a polymorphic layer covering gold grains collected from Kilkivan. In contrast, although gold was taken up in the controls, it was lower than that in the viable biofilms, and no precipitates formed.

Conclusion 8

Viable *C. metallidurans* biofilms on sand grains actively take up ~100 % of the gold from Au(I)-complexes under the conditions investigated.

Conclusion 9

The biofilm growth allows viable cells of *C. metallidurans* to take up more gold from solutions than planktonic cells and inactive or abiotic controls.

Conclusion 10

Viable cells of *C. metallidurans* growing in biofilms will precipitate gold nano-particles that will aggregate into micron-sized formations.

Conclusion 11

Gold particles precipitated by *C. metallidurans* biofilms can act as nuclei for further aggregation, ultimately leading to encapsulation and replacement of cells.

Conclusion 12

Precipitates similar to those formed by viable *C. metallidurans* biofilms are also found on grains collected from supergene Australia.

5.3. Biomineralization and the accumulative effect of microbial surface processes on placer grains in Australia

To determine and effectively model the likely role of microbial biofilms catalyzing supergene gold grain genesis and transformations in Australian supergene environments, grains from arid environments were characterized for comparison. Using a combination of composition and inclusion mineralogy, along with the study of morphology of source and placer gold grains, the relationship between the two was elucidated. Evidence of past biofilm activities, such as iron-minerals, spherical gold nano-particulates and spheroidal gold µ-crystals were found on the surface of the grains. The presence of mechanical damage, gold-rich rims, aggregating polymorphic layers, authigenic gold nanoparticles and the increasing incidence of these, allowed for the separation of gold grains into the classification of proximal and distal to a likely source respectively, but more importantly to extended biofilm exposure. The presence of polymorphic layers of organics and secondary minerals derived from biomineralization or biofilm residues highlights the transient nature of biofilm formation on Australian supergene grains.

Thus a biogeochemical process model for the initial and subsequent stages of supergene gold grain transformations from a likely source was achieved for arid environments that integrate a primary origin with secondary mobilization and aggregation processes. These secondary morphologies are

the result of gold/silver dissolution and gold precipitation acting simultaneously. Complexed gold is re-precipitated and forms secondary metallic gold via a number of biogenic and abiogenic processes. The greater part of this secondary gold precipitation occurs as nano-particles which are then transformed to µ-crystalline gold via aggregation and re-crystallization.

Nano-particulate, spheroidal and bacterioform structures are common in biofilms on gold grains from these localities, demonstrating that bacteria contribute to the formation of secondary nano-particulate and spheroidal gold.

Conclusion 13

The morphology of supergene gold grains, the presence of polymorphic layers and nanoparticulate gold and dissolution pits therein, provide a record of supergene transformations of gold in the Australian regolith.

Conclusion 14

Nanoparticulate gold and aggregations thereof are present in the polymorphic, biofilm-like material on supergene gold grains from arid Australia.

Conclusion 15

The presence of polymorphic layers on arid supergene gold grains are likely remnants of biofilms.

5.4. An updated model for the microbially mediated formation of gold grains in the Australian regolith

The results of this Ph.D. lead to the formation of the model as summarized in Figure 5.1.. This model links the individual processes of biological and abiotic gold solubilization, transport, precipitation and authigenic bacteriomorph gold formations constituting the biogeochemical nature of supergene gold grain formation and gold anomaly distribution in the Australian regolith. The model and conclusions are based on the results of uptake and column experiments conducted in conjunction with microscopy studies of gold grains from arid Australian settings, demonstrating the progressive nature of supergene processes in gold grain formation. The model presented (Figure 5.1.) builds on the existing unified model for the formation of nano-particulate and secondary gold (Figure 1.3.) by providing direct evidence of the ability of *C. metallidurans* to take-up and precipitate environmentally relevant Au(I)-complexes and comparing the morphology and composition of resultant precipitates to secondary gold features on supergene grains collected from Australian sites.

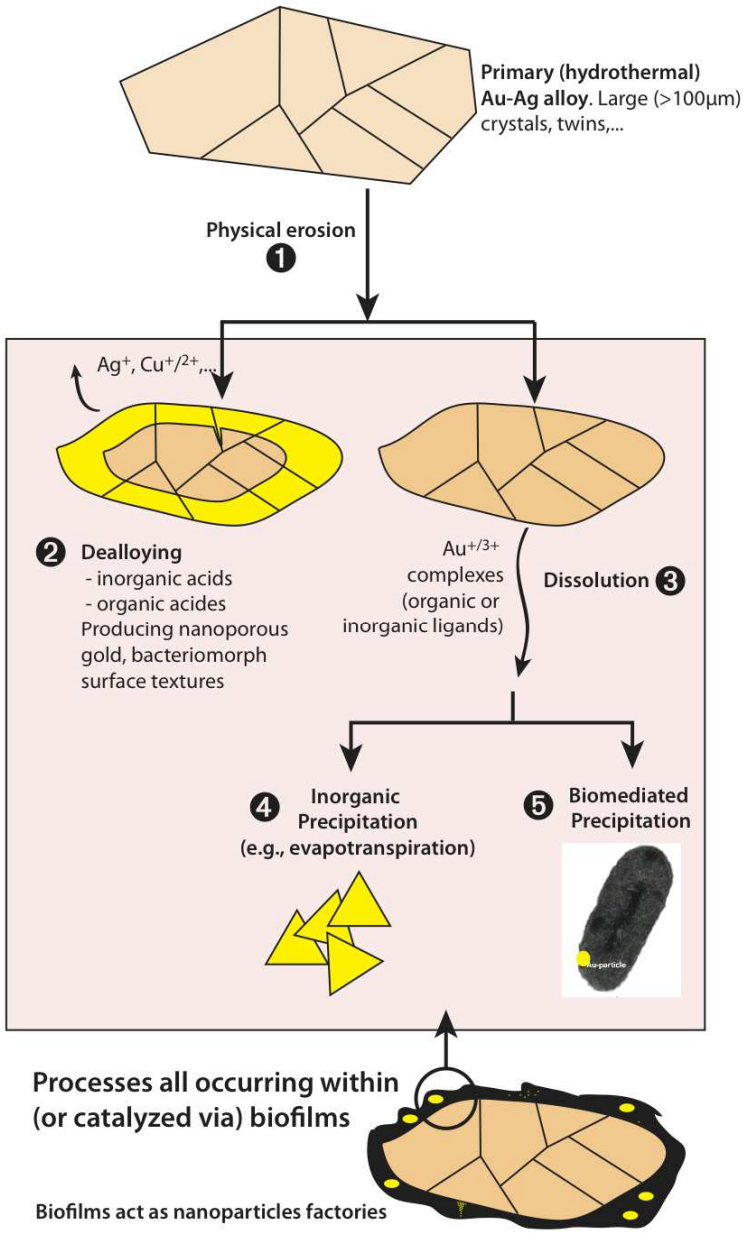

Figure 5.1. Model of processes responsible for the transformation of gold grains in supergene environments. Modified after Reith *et al*. (2010) and Hough *et al*. (2011); bright yellow is high fineness gold (> 95 wt.% gold), orange is gold-silver alloy, black is biofilm.

In this model gold grains originate as primary gold and are present in the supergene due to weathering and erosion of host materials (1. in Figure 5.1.). Secondary gold of high purity and very fine crystallinity *i.e.*, nano- and

µ-particles, triangular plate gold, sheet-like gold, bacterioform gold and wire gold, occurs on the surface of primary grains or as small grains. These morphologies are the result of gold/silver dissolution and gold precipitation acting simultaneously (2 in Figure 5.1). Soluble gold in surface waters form via interaction with ligands such as halides, thiosulfate, organic acids and cyanide (3 in Figure 5.1). Microorganisms release organic acids promoting de-alloying, similarly cyanide-producing organisms are capable of producing the ligands for gold dissolution, complexation and transport. Complexed gold is re-precipitated and forms secondary metallic gold via a number of biogenic and abiogenic processes (4 and 5 in Figure 5.1.). Secondary gold precipitation typically occurs as nano-particles, which aggregate forming µ-crystalline gold. These secondary processes are apparently accumulative with distance from source of origin, significantly transforming the gold grain surfaces.

5.5. Applications and limitations of the proposed model and future research directions

The main results of this Ph.D. research show: 1) the ability of *C. metallidurans* to form biofilms that precipitate Au(I)-complexes; 2) the likely role of *C. metallidurans* in the genesis and supergene transformations of gold grains in the Australian regolith in arid environments; 3) the coupled nature of dissolution, the formation of Au-complexes and the precipitation of gold at both the scale of individual grains and potentially, the regolith at large. Establishing these relationships for *C. metallidurans*, having been found to be growing on grains from the Australian regolith, is a critical step towards understanding the geomicrobiological nature of supergene gold. However, questions still remain to be answered if further understanding is to be achieved. Among these are;

- What other organisms might be able to drive supergene gold biomineralization?
- Which organisms might be responsible for other parts of the proposed model?
- What are the kinetics of gold solubilization and precipitation in the regolith?
- How long does it take for authigenic secondary structures to form on supergene gold grains in the regolith?

- Can the effect of transport and progressive bacterial surface transformations be further elucidated?
- Is the model unique to Australian supergene grains?
- What are the contributions of abiotic mechanisms on the formation of gold grains?
- What are the prevalent Au-complexes that form following solubilization, biotic or otherwise, of gold at the scale of the regolith or individual grains?

In order to begin to answer these questions, a number of further studies will have to be undertaken. The results of this study show that the genesis and formation of secondary structures on supergene gold grains can be driven by biotic mechanisms by demonstrating the uptake and precipitation of gold by a bacterium that is present around mineralization in (Australian) supergene environments. The biomineralization capability of *C. metallidurans* in differing geological environments, as well as the ability of other bacteria to adequately perform this role, is unknown. The timescale at which the biological genesis and transformation of gold occurs is also undetermined. Similarly the ratio of abiotic versus biotic mechanisms in the solubilization of gold and the precipitation of resultant Au-complexes in the formation of supergene gold is undefined. The work presented here can be enhanced by additional experiments that will allow for some of the questions, posed earlier in this section, to be resolved.

Biomass measurement, electron microscopy, kinetic experiments and synchrotron technology allow further definition of gold uptake by *C. metallidurans.* Metabolically active cells increase in number during the experiment, evidenced by an increase $CFU.mL^{-1}$, resulting in an increase in biomass which is not replicated in experiments with inactive and sterile cells. Measuring cell mass at the end of incubations in metabolically active and biotic controls, allows for the normalization of gold uptake to cell mass, accounting for increases in biomass over the duration of the experiment and allowing stronger conclusions to be drawn on the presence of active mechanisms of gold uptake over simple sorption to cell wall material. Transmission electron microscopy of ultra-thin sections of *C. metallidurans* cells, prepared at the end of experimentation, coupled with EDX analysis would allow for the determination of the presence of metallic gold precipitates formed by bacterial uptake. Although a purple coloration (indicative of the presence of precipitates of 100 nm colloidal gold; Edwards and Thomas, 2007) was not obvious in the experiments presented here (Chapter 2.), the use of TEM allows for the determination of *C. metallidurans* biomineralization potential at these conditions. Synchrotron X-ray fluorescence measurements can be used to determine the distribution and concentration of any gold precipitates via quantitative elemental imaging. The concentration of gold in individual cells can be mapped while showing the distribution of other elements (to $ng.cm^{-2}$) expected to be present in bacterial cells (*i.e.*, Ca, Cu, Fe, S and Zn; Rouf, 1964). Reith *et al*., (2009b) demonstrated that X-ray

fluorescence (XRF) can be used to determine that gold precipitates, formed via Au(III)-complexes exposed to *C. metallidurans,* were associated with the cell envelope and more numerous and larger than those associated with the cytoplasm. From XRF maps, Reith *et al*., (2009b) deduced that *C.metallidurans* cells precipitate gold in the periplasm and confirmed this by TEM.

Kinetic experiments and spectroscopy have the capacity to demonstrate the extent of gold uptake from solution over time, and XANES can be used to track valence state transformations and binding environments. By investigating the rate of reactions in uptake experiments, Kenney *et al*., (2012) demonstrated that increasing amounts of gold (from Au(III)-chloride) was removed from solution over time for non-metabolizing cells of two common soil bacteria (*B. subtilis and P. Putida*). The use of kinetic experiments and XANES allowed Kenney *et al*., (2012) to determine that gold reduction was occurring rapidly and extensively upon interaction with cell wall functional groups, with speciation of Au-complexes and bacterial surface controlling the rate of gold removal from solution. Similarly, Reith *et al*. (2009b) used kinetic experiments with metabolically active *C. metallidurans* cells incubated with 50 μM Au(III) over 1 min to 144 hours to confirm a two-stage reduction for Au(III)-complexes. The experiments conducted by Reith *et al*., (2009b) measured XANES after *C. metallidurans* cells were exposed to Au(III) in PME and showed that 100 % of accumulated gold was present as Au(I)-S after 6 hours which fell to 53 % after 72 hours (accompanied by 28.8

% metallic gold and 18.3 % Au(I)-C). After 144 hours exposure 37.3-55.1 % of gold associated with individual cells was present as carbon-bound gold whilst the remainder was metallic gold (Reith *et al*., 2009b). Due to the complex mathematical models required to fit measured XANES spectrum, to obtain reliable results, sufficiently long counting periods are required (typically 0.5–1.5 hours per sampling point). If true kinetic experimentation, to further elucidate the speciation of Au(I)-complexes during the uptake of gold by *C. metallidurans* is to be achieved, XANES measurement must be rapid, accurate and reliable. Recently the time consuming data collection of XANES (compared to the rapid initial bacterial uptake of gold) has been overcome by the use of a simplified model of data collection and evaluation (Bielewski *et al*., 2009). Plutonium oxidation states on a particle from a nuclear weapon test site were measured and analyzed using a single straight line segment through the slope of the absorption edge and was proven to be a valid method (via comparison to conventional fitting of XANES spectra; Bielewski *et al*., 2009). Extending the application of this method, fast XANES coupled with kinetic experiments will allow for the conclusive determination of changes in speciation as they occur, further defining the mechanisms of Au(I)-complexes by *C. metallidurans*.

Transcriptome microarray determines gene expression resultant from external environmental conditions. Analysis of *C. metallidurans* gene expression when exposed to Au(I/III)-complexes was very recently determined and the genes in the genome of *C. metallidurans* that are up- or

down-regulated by the presence of Au(I)-complexes under conditions similar to studied here (Wiesemann *et al*., 2013).

The combination of these techniques will allow for the mechanisms of gold uptake by *C. metallidurans* to be thoroughly determined. Study of the speciation and kinetics of Au-complexes during uptake and the distribution of resultant gold precipitates throughout cells will not only lead to an improvement understanding of biomineralization potential for *C. metallidurans* but allows further investigation of optimal parameters for biomineralization via more eloquent experiments.

The column experiments presented in this thesis, conclusively showed the ability of active biofilms of *C. metallidurans* to take up Au(I)-thiosulfate, over non-metabolizing cells and abiotic controls. However these experiments can be improved by increasing complexity. Titration burettes and sand grains allow for a supergene or sediment environment to be loosely emulated within the laboratory, allowing the study of *C. metallidurans* biomineralization ability, whilst controlling relevant parameters. The use of more complicated matrix material within the columns and investigation of microbial consortia biomineralization, will allow for the gap between the laboratory and the supergene to be closed by more closely approximating the regolith. The inclusion of minerals, clays and soils likely to be encountered in the regolith around mineralization in column experiments will allow for the multifaceted biomineralization processes to be studied in more detail via the determination of total gold uptake along with uptake and retention by different fractions

within the columns. Selective sequential extractions have been used for the determination of gold mobilization in soils and deeper regolith materials and thus the association of gold within operationally defined fractions (Reith *et al*., 2005). Selective sequential extractions involve the use of progressively more potent chemical reagents, typically ranging from deionized water for water soluble fractions through to reagents such as hydrochloric acid for crystalline oxide fractions (with appropriate reagents used for fractions such as clays, carbonates and organics should they be present). The use of materials such as clays, carbonates, organics and crystalline oxides coupled with sequential extractions will allow for the determination of gold association to fractions within columns. The use of more complex column experiments has the capability to provide a more detailed approximation of the regolith from which a more detailed model of regolith mechanisms of gold uptake may be determined.

The biomineralization of gold by bacteria present on gold grains in the regolith has been demonstrated in this thesis for *C. metallidurans*. If other organisms (techniques for identification are described on page 158) are to be shown to be capable of driving biomineralization, via the uptake of Au(I/III)-complexes, the ability of active cells must be demonstrated over passive sorption to control. A combination of ICPMS, SXRF, XANES, SEM and TEM can be used to determine the ability of organism to take up Au-complexes, precipitate Au-complexes and determine how the gold is distributed and speciated in the cells. As demonstrated here (Chapter 2 and 3), exposure of

pure cultures to Au-complexes under controlled conditions can determine the ability of an organism to drive biomineralization. Pure cultures do not exist in nature and so the use of bacterial consortium in column experiments is a logical choice in introducing another layer of complexity and thus more closely approximating natural systems. The development of desired microbial consortia involves the enrichment of original sediment/ground-water slurries with amendments of the target contaminants that the desired microbial species are capable of degrading (*i.e.*, Au-complexes). By repeated and sequential dilutions into appropriate culture medium the amount of different types of microbes in the original sediment is reduced until the species remaining are those most likely to be directly or indirectly involved in degradation of these contaminants (aka uptake of gold). This technique has been used to isolate consortia for column experiments to investigate the role of sulphate-reducing bacteria in the precipitation of gold though a quartz grain matrix designed to emulate geologic stratum (Lengke and Southam, 2007). Consortia, isolated from a gold mine and dominated by SRB was found to survive in the presence of Au(I)-thiosulfate and to also precipitate gold more efficiently than abiotic controls (Lengke and Southam, 2007).

Delftia acidovorans has been shown to coexist on DNA-positive gold grains with *C. metallidurans* (Reith *et al*., 2010) and shares similarities in metal resistance (evident by an apparent horizontal transfer of genes; van Houdt *et al*., 2009). *Delftia acidivorans* has been shown to produce a secondary metabolite (delftibactin), precipitating colloidal and octahedral gold

nanoparticles from Au(III)-complexes (Johnston *et al*., 2013). Similar gold forms are found on supergene gold grains (*i.e.*, Chapter 4. and Reith *et al*., 2007; Hough *et al*., 2008) and thus *D. acidivorans* may potentially be another driver of gold biomineralization in the regolith. Column experiments from consortia isolated from the Australian regolith (as well as *C. metallidurans* and *D. acidivorans*) coupled with the methods presented in Chapter 3, can provide the next step in more accurately modelling the formation of supergene gold deposits in the regolith. The development of column experiments to the point where they are closer approximating the regolith environment also extends to the use of cell and nutrient concentrations as observed in the field. Most studies of gold adsorption and nanoparticle formation involve high gold concentrations and supersaturated solutions (e.g., Beveridge and Murray, 1976; Southam and Beveridge, 1994, 1996) and it is unclear if the results of such studies are applicable to the gold:cell ratios observed in the field. Determination of biomineralization at concentrations found in the field will need to be a long term experiment with time frames of months and years rather than days and months (as presented in Chapter 3) in order to allow active cell processes to occur. However as long as nutrients and Au-complexes are provided to the system it is not unreasonable to assume that the cyclical process of reduction and enrichment of elemental gold by bacterial cells will continue as they do in nature. By introducing more complexity to column experiments via the use of additional fractions to the matrix, consortia and concentrations likely to be

found in the regolith, it is possible to more accurately determine mechanisms of supergene gold formation.

The study of supergene gold from the arid Australia showed the presence of biofilms (in the case of Flinders Ranges grains) and polymorphic layers that were dispersed on the surface of grains exposed to the regolith. Dispersed throughout these layers gold nanoparticles, and agglomerations thereof, are present that have also been produced via the biomineralization of Au(I)-thiosulfate complexes by biofilms of *C. metallidurans.* The use of SEM coupled with EDX analysis allowed for the identification and characterization of these layers (as presented in this thesis). However the identification of the species within biofilms depends on molecular techniques (extraction and PCR amplification of target DNA, DGGE, molecular cloning and sequencing combined with DNA-sequence analysis) and can determine the community structures of biofilms associated with gold grains (and how these compare to communities surrounding auriferous soils). 16S ribosomal DNA analysis, amplified via PCR can be used to determine a genetic fingerprint of gold grains and soil communities. Using primers a highly variable region of the 16S rDNA is amplified that is suitable for DGGE. Purified fragments resulting from DGGE can then be cloned (into *E. coli* cells) from which DNA is extracted and sequenced using BLAST software of the GenBank database (National Center for Biotechnology Information, NCBI). These data allow for the construction of phylogenetic trees that allow the placement of gold grain (and soil) organisms into domains. The determination

of biofilm and soil community speciation allows for the identification of possible players in the biomineralization (and solubilization) of gold in the regolith. These methods (16S ribosomal DNA clones) were how bacterial biofilms associated with secondary gold grains, from two sites in tropical Australia, were found to be of the genus *Ralstonia*, bearing 99% similarity to the bacterium *C. metallidurans* (Reith *et al*., 2006). If molecular techniques were used to study the grains presented in Chapter 4, the biofilms and polymorphic layers may reveal bacterial species capable of driving biomineralization (*i.e.*, *C. metallidurans*, *D. acidivorans* or consortia such as SRB). If, for example, these biofilms were shown to be comprised of *C. metallidurans*, given the results of column experiments in Chapter 3, then the presence of nanoparticulate gold within these biofilms could be more conclusively determined to be of a biogeochemical origin.

The applicability of the conclusions presented in this thesis to other regions is undetermined. Grains from Australia, New Zealand, Africa and the Americas have been shown to display secondary gold in a wide variety of morphotypes that are brought on by solubilization and gold precipitation acting simultaneously (Reith *et al.*, 2007; Southam *et al.*, 2009). These include nano- and µ-particles, triangular plate gold, sheet-like gold, bacterioform gold, wire gold as well as purely secondary gold grains (Bischoff 1994, 1997; Reith *et al.*, 2007; Falconer and Craw 2009; Hough *et al.*, 2011). In order to determine if microbial processes play a critical role in the formation of these structures, the transformation of supergene gold grains

and the dispersion of gold in environments on multiple continents and the influences of (bio)geochemical processes on these grains must be evaluated. As in Chapter 4, if this is to be shown, ideally field areas are selected to provide access to primary gold (*i.e.*, preserved within hosting material) and gold grains from related elluvial, colluvial and alluvial settings from localities representative of environments where gold grains are found. By selecting grains from such regions, detrital gold grains from placer settings can be traced back to a likely source of primary mineralization and accumulative transformations identified. As morphology of gold grains alone cannot account for origin (Hough *et al*., 2007) nor biological involvement (Watterson, 1994), field-sterile techniques must be utilized in order to preserve polymorphic layers (Reith *et al.*, 2010) and the integrity of biofilms (Fratesi *et al*., 2004) should they be present. This thesis demonstrates that a combination of microscopy and spectroscopy techniques (OM, FIB-SEM, EDXA, EPMA, PIXE) allow for the characterization of morphology and chemical composition, the determination of the presence of microbial biofilms, polymorphic layers (or remnants thereof) and the occurrence of gold nano-particles and µ-crystals associated with these. Such study of gold grains can determine whether supergene transformations have occurred and if bacteria have played a likely role as defined by the proposed updated model (Figure 5.1.). A recent study suggested that abiogenic processes, *e.g.*, evaporation, control the formation of nano-particles and µ-crystalline gold platelets, and therefore the dispersion of gold in arid environments (Hough *et*

al., 2008). Similarly, mobilization of gold was once believed to be solely abiotic with oxidation and dissolution of gold being attributed to higher concentrations of O_2 in the supergene, abiotic weathering of gold-hosting minerals, mechanical abrasion of gold during alteration and swelling of minerals (Gray, 1998). If the current understanding of the geomicrobiological cycle is going to be improved and contributions of biotic and abiotic processes of solubilization and precipitation determined, then likely mechanisms of Au-complex formation need to be evaluated. In order to achieve this, techniques able to identify speciation of Au-complexes at environmentally relevant concentrations, with appropriate sensitivity, is needed. Recently the development of a high performance liquid chromatography (HPLC)-ICPMS method for the determination of Au(I)-cyanide, Au(I)-thiosulfate, Au(III)-chloro-hydroxyl and Au(III)-bromo-hydroxyl complexes in mine waters and groundwaters was created with detection limits for the gold species from 0.081-0.58 $\mu g.L^{-1}$ (Christine Ta, 2013). This new method of Au-complex analysis shows promise for mineral exploration, in studies on the fate of gold in mine wastes and bioremediation processes, and in studies on the effect of organic matter, microorganisms and minerals on the speciation and thus the biomineralization of gold.

5.6. Future applications of this research

The extraction of gold from low grade ore, that does not justify the higher costs of agitation leaching, is achieved via heap leaching. Cyanide is universally used in this process due to its high selectivity for gold, and silver, over other metals (Marsden and House, 2006). Cyanide concentrations used in practice range from 0.05 to 0.5 gL^{-1} NaCN and using lime, gold recovery approximates 65% (ranging from 50 to 80%) with 0.05 and 0.50 $kg.t^{-1}$ (Pizzaro, *et al*., 1974) of cyanide and lime respectively. The infrastructure involved in these processing plants of heap leaching is costly as there is an inherent risk of cyanide contamination of the immediate environment that must be mitigated. The biosorption of metals is emerging as a low cost and low-tech option for recovery of metals including gold (Mack *et al*., 2007) and successful treatment involves the use of carefully selected consortia such that treatment involves strains that are able to survive and be active in the presence of (toxic) solutions but are also able to degrade the desired components (Van der Gast *et al*., 2002). Although biosorption is typically a term given to the passive sorption and/or complexation of metal ions by biomass (Mack *et al*., 2007), microbes are playing increasingly important roles in commercial mining operations. Microbes can be used to change the redox state of the metal being harvested, rendering it more soluble, or the redox chemistry of metal cations that are then coupled in chemical oxidation or reduction of the harvested metal ion (Rawlings and Silver, 1995). Microbes

can even be used in the solubilization of mineral matrices in which the metal is hosted (Rawlings and Silver, 1995). Bacterial cells are able to produce cyanide, solubilizing gold, precipitate Au-cyanide complexes and detoxify the waste cyanide solutions from gold-mining operations (Knowles, 1976; Niu and Volesky, 1999; Blumer and Haas, 2000; Brinne, 2000; Campbell *et al*., 2001; Carepo *et al*., 2004; Fairbrother *et al*., 2009). The work presented here demonstrates the ability of bacterial cells to replace activated carbon or alternative biomass. With increasing understanding of microbial processes such as biomineralization improving these microbial capabilities for bioleaching applications becomes a possibility.

The conceptual modeling of the biogeochemical process(es) for gold grain transformations in arid supergene environments provides a baseline for the interpretation of macro- and micro-morphologies as well as chemical compositions of gold grains from arid sites in Australia. This identification of the characteristics of placer grains, *i.e.*, composition, morphology, and inclusion mineralogy, allows the classification of gold grains and thus the source and styles of the primary mineralization.

Mechanical damage such as rounding and flattening of gold grains develops rapidly with transport from source. However, morphology of placer grains and the presence of polymorphic layers and biofilms, nanoparticulate gold and aggregates thereof, is not diagnostic for origin or distance, but provides a record of the accumulative supergene transformations the grains have undergone.

References

Ahmad, A., Senapati, S., Khan, M.I., Kumar, R., Ramani, R., Srinivas, V., 2003. Intracellular synthesis of gold nanoparticles by a novel alkalotolerant actinomycete, *Rhodococcus* species. Nanotechnology, 14, 824–828.

Anand, R., 2003. Lawlers District, Western Australia. CRC LEME, CSIRO Exploration and Mining, 6.

Armendariz, V., Herrera, I., Peralta-Videa, J.R., Jose-Yacaman, M., Troiani, H., Santiago, P., Gardea-Torresdey, J.L., 2004. Size controlled gold nanoparticle formation by Avena sativa biomass: use of plants in nanobiotechnology. Journal of nanoparticle research, 6(4), 377-382.

Aspandiar, M., Anand, R., Gray, D., 2008. Review of geochemical dispersion mechanisms through transported regolith. CRC LEME, Open File Report 246.

Australian Bureau of Meteorology, 2011a. Lawlers Climate Statistics, http://www.bom.gov.au/climate/averages/tables/cw_012158.shtml

Australian Bureau of Meteorology, 2011b. Tanami Climate Statistics, http://www.bom.gov.au/climate/averages/tables/cw_015548.shtml

Australian Bureau of Meteorology, 2011c. Arkaroola Climate Statistics, http://www.bom.gov.au/climate/averages/tables/cw_017099.shtml

Aylmore, M.G., Muir, D.M., 2001. Thiosulfate leaching of gold—a review. Minerals Engineering, 14, 135–174.

Baker, W.E., 1973. The role of humic acids from Tasmanian podzolic soils in mineral degradation and metal mobilization. Geochimica et Cosmochimica Acta, 37, 269–281.

Baker, W.E., 1978. The role of humic acids in the transport of gold. Geochimica et Cosmochimica Acta, 42, 645–649.

Bali, R., Siegele, R. Harris, A.T., 2010. Phytoextraction of Au: Uptake, accumulation and cellular distribution in Medicago sativa and Brassica juncea. Chemical Engineering Journal, 156(2), 286-297.

Basile, L.J., Willson, R.C., Sewell, B.T., Benedik, M.J., 2008. Genome mining of cyanide-degrading nitrilases from filamentous fungi. Applied Microbiology and Biotechnology, 80, 427-435.

Beardsmore, T., Allardyce, W., 2002. The Geology, Tectonic Evolution and Gold Mineralization of the Lawlers Region: A Synopsis of Present Knowledge. Barrick Gold of Australia Limited. Technical Report No., 1026.

Benedetti, M., Boulegue, J,. 1991. Mechanism of gold transfer and deposition in a supergene environment. Geochimica et Cosmochimica Acta, 55 1539–1547.

Berners-Price, S., Sadler, P., 1988. Phosphines and metal phosphine complexes: Relationship of chemistry to anticancer and other biological activity, in Bioinorganic Chemistry. Springer Berlin Heidelberg, 27-102.

Beveridge, T.J., Murray, R.G.E., 1976. Uptake and retention of metals by cell walls of *Bacillus subtilis*. Journal of Bacteriology, 127, 1502–1518.

Bielewski, M., Eriksson, M., Himbert, J., Betti, M., Belloni, F., Falkenberg, G., 2009. Fast method of XANES data collection suitable for oxidation state mapping. Journal of Radioanalytical and Nuclear Chemistry, 282(2), 355-359.

Bimboim, H.C. Doly, J., 1979. A rapid alkaline extraction procedure for screening recombinant plasmid DNA. Nucleic Acids Research, 7(6), 1513-1523.

Bischoff, G., 1994. Gold-adsorbing bacteria as colonisers on alluvial placer gold. Neues Jahrbuch fur Geologie und Palaeontologie, P-A., 194, 187-209.

Bischoff, G., 1997. The biological origin of bacterioform gold from Australia. Neues Jahrbuch fur Geologie und Palaeontologie, P-A., 6, 329–338.

Blake, D.H., 1978. The Proterozoic and Palaeozoic rocks of the Granites Tanami region, Western Australia and Northern Territory and interregional correlations. BMR Journal of Australian Geology and Geophysics, 3, 35–42.

Blumer, C., Haas, D., 2000. Mechanism, regulation, and ecological role of bacterial cyanide biosynthesis. Archives of Microbiology, 173, 170-177.

Bonev, I.K., Kerestedjian, T., Atanassova, R., Andrew., C.J., 2002. Morphogenesis and composition of native gold in the Chelopech volcanic-hosted Au-Cu epithermal deposit, Srednogorie zone, Bulgaria. Mineralium Deposita, 37, 614-629.

Borrok, D., Fein, J.B., Tischler, M., O'Loughlin, E., Meyer, H., Liss, M., Kemner, K.M., 2004a. The effect of acidic solutions and growth conditions on the adsorptive properties of bacterial surfaces. Chemical Geology, 09(1-2), 107-119.

Borrok, D.M., Fein, J.B., Kulpa, C.F., 2004b. Cd and proton adsorption onto bacterial consortia grown from industrial wastes and contaminated geologic settings. Environmental Science & Technology, 38(21), 5656-5664.

Bowles, J., 1988. Mechanical and chemical modification of alluvial gold. Bulletin and Proceeding of the Australian Institute of Mining and Metallurgy, 293, 9-11.

Boyanov, M.I., Kelly, S.D., Kemner, K.M., Bunker, B.A., Fein, J.B., Fowle, D.A., 2003. Adsorption of cadmium to *Bacillus subtilis* bacterial cell walls: A pH-dependent X-ray absorption fine structure spectroscopy study. Geochimica et Cosmochimica Acta, 67(18), 3299-3311.

Boyle, R., 1979. The Geochemistry of Gold and Its Deposits, Bulletin - Geological Survey of Canada, 280.

Boyle, 1987. Gold: History and genesis of deposits. Society of economic geologists foundation, 86-15675.
Boyle, R.W., Alexander, W.M., Aslin, G.E.M., 1975. Some observation on the solubility of gold. Paper - Geological Survey of Canada, 26–63.

Brinne, A., 2000. Phylogenetic studies of metal cyanide degrading bacteria in gold mine tailings dams., in Molecular Biotechnology. Uppsala University School of Engineering: Uppsala.

Brown, D.H., Smith, W.E., 1980. The chemistry of the gold drugs used in the treatment of rheumatoid arthritis. Chemical Society Reviews, 9(2), 217-240.

Brugger, J., Long, N., McPhail, D.C., Plimer, I., 2005. An active amagmatic hydrothermal system: The Paralana hot springs, Northern Flinders Ranges, South Australia. Chemical Geology, 222, 35-64.

Bunting, J., Williams, S., 1979. Sir Samuel, 1:250 000 Geological Series-Explanatory Notes. Geological Survey of Western Australia. SG51-13, 40.

Campbell, S., Olson, G., Clark, T., McFeters, G., 2001. Biogenic production of cyanide and its application to gold recovery. Journal of industrial microbiology and biotechnology, 26, 134-139.

Carepo. M., de Azevedo, N., Porto, J., 2004. Identification of *Chromobacterium violaceum* genes with potential biotechnological application in environmental detoxification. Genetics and Molecular research, 3(1), 181-194.

Chapman, R.J., Mortensen, J.K., LeBarge, W.P., 2011. Styles of lode gold mineralization contributing to the placers of the Indian River and Black Hills Creek, Yukon Territory, Canada as deduced from microchemical characterization of placer gold grains. Mineralium Deposita, 46(8), 881-903.

Choi, O., Yu, C.P., Fernandez, E., Hu, Z., 2010. Interactions of nanosilver with *Escherichia coli* cells in planktonic and biofilm cultures. Water Research, 44, 6095-6103.

Clough, D., Craw, D., 1989. Authigenic gold-marcasite association — evidence for nugget growth by chemical accretion in fluvial gravels, Southland, New Zealand. Economic Geology, 84, 953-958.

Coats, R., Blissett, A., 1971. Regional and economic geology of the Mount Painter province. Department of Mines, Geological Survey of South Australia, Bulletin, 43, 426.

Colin, F., Veillard, P., 1991. Behaviour of gold in the lateritc equatorial environment: weathering and surface dispersion of residual gold particles, at Dondo Mobi, Gabon. Applied Geochemistry, 6, 279-290.

Collier, J.B., Plimer, I.R., 2002. Supergene clinobisvanite pseudomorphs after supergene dreyerite from Lively's Mine, Arkaroola, South Australia. Neues Jahrbuch fur Mineralogie-Monatshefte, 401-410.

Costerton, J.W., Lewandowski, Z., Caldwell, D.E., Korber, D.R., Lappin-Scott, H.M., 1995. Microbial Biofilms. Annual Review of Microbiology, 49, 11-45.

Craw, D., Youngson, J., 1993. Eluvial gold placer formation on actively rising mountain ranges, Central Otago, New Zealand. Sedimentary Geology, (85), 623–635.

Das, N., Vimala, R., Karthika, P., 2008. Biosorption of heavy metals –An overview. Indian Journal of Biotechnology, 7, 159-169.

Ding, Y., Kim Y-J., Erlebacher, J., 2004. Nanoporous gold leaf: ancient technology/advanced material. Advanced Materials, 16, 1897 – 1900.

Duineveld, B.M., Rosado, A.S., van Elsas, J.D., van Veen, J.A., 1998. Analysis of the dynamics of bacterial communities in the rhizosphere of the chrysanthemum via denaturing gradient gel electrophoresis and substrate utilization patterns. Applied and Environmental Microbiology, 64, 4950-4957.

Dunne, M., 2002. Bacterial Adhesion: Seen Any Good Biofilms Lately? Clinical Microbiology Reviews, 15(2), 155.

Ebbs, S.D., Kolev, S., Piccinin, R., Woodrow, I.E, Baker, A.J.M, 2010. Solubilization of heavy metals from gold ore by adjuvants used during gold phytomining. Minerals Engineering, 23(10), 819-822.

Edwards, P.P., Thomas, J.M., 2007. Gold in a metallic divided state—from Faraday to present day nanoscience. Angewandte Chemie International Edition, 46, 5480–5486.

Ehrlich, H.L., 1996. How microbes influence mineral growth and dissolution. Chemical Geology, 132(1-4), 5-9.

Ehrlich, H.L., 2002. Geomicrobiology. Marcel Dekker, Inc: New York, USA.

El-Naggara, M.Y., Wangerb, G., Leungc, K., Yuzvinskya, T.D., Southam, G., Yangc, J., Laud, W.M., Nealson, K.H., Gorby, Y.A., 2010. Electrical transport along bacterial nanowires from *Shewanella oneidensis* MR-1. Proceedings of the National Academy of Sciences, 1073, 1-5.

Enders, M.S., Southam, G., Knickerbocker, C., Titley, S.R., 2006. The role of microorganisms in the supergene environment of the Morenci porphyry copper deposit, Greenlee County, Arizona. Economic Geology, 101, 59–70.

Fairbrother, L., Shapter, J., Brugger, J., Southam, G., Pring, A., Reith, F. 2009. Effect of the cyanide-producing bacterium *Chromobacterium violaceum* on ultraflat Au surfaces. Chemical Geology, 265(3-4), 313-320.

Falconer, D., Craw, D., 2009. Supergene gold mobility: a textural and geochemical study from gold placers in southern New Zealand. Economic Geology Special Publication, 14**,** 77-93.

Falconer, D., Craw, D., Youngson, J., Faure, K., 2006. Gold and sulphide minerals in Tertiary quartz pebble conglomerate gold placers, Southland, New Zealand. Ore Geology Reviews, 28, 525-545.

Faramarzi, M.A., Stagars, M., Pensini, E., Krebs, W., Brandl, H., 2004. Metal solubilization from metal-containing solid materials by cyanogenic *Chromobacterium violaceum.* Journal of Biotechnology, 113, 321-326*.*

Faramarzi, M., Brandl, H., 2006. Formation of water-soluble metal cyanide complexes from solid minerals by *Pseudomonas plecoglossicida*. FEMS Microbiology Letters, 259, 47-52.

Farges, F., Sharps, J.A., Brown, Jr G.E., 1991. Local environment around gold(III) in aqueous chloride solutions: an EXAFS spectroscopy study. Geochimica et Cosmochimica Acta, 57, 1243–1252.

Fein, J.B., Daughney, C.J., Yee, N., Davis, T.A. 1997. A chemical equilibrium model for metal adsorption onto bacterial surfaces. Geochimica et Cosmochimica Acta, 61(16), 3319-3328.

Fitz, R.M., Cypionka, H., 1990. Formation of thiosulfate and trithionate during sulfite reduction by washed cells of *Desulfovibrio desulfuricans*. Archives of Microbiology, 154, 400–

Fratesi, S.E., Lynch, F.L., Kirkland, B.L., Brown L.R., 2004. Effects of SEM preparation techniques on the appearance of bacteria and biofilms in the carter sandstone. Journal of Sedimentary Research, 74(6), 858-867.

Freise, F.W., 1931. The transportation of gold by organic underground solutions. Economic Geology, 26, 421–431.

Freyssinet, P., Butt C.R.M., 1988. Morphology and geochemistry of gold in a lateritic profile, Bardoc Mine, Western Australia. CSIRO Division of Exploration Geoscience, CRC LEME Open-file Report 5

Freyssinet, P., Zeegers, H.. Tardy, Y., 1989. Morphology and geochemistry of gold grains in lateritic profiles of southern Mali. Journal of Geochemical Exploration, 32, 17 – 31.

Freyssinet, P., Butt, C.R.M., Morris, R.C., Piantone, P., 2005. Ore-forming processes related to lateritic weathering. Economic Geology 100th Anniversary volume, 681–722.

Friedrich, C.G., Bardischewsky, F., Rother, D., Quentmeier, A., Fischer, J., 2005. Prokaryotic sulfur oxidation. Current Opinion in Microbiology, 8, 1–7.

Gammons, C.H., Yu, Y., Williams-Jones, A.E., 1997. The disproportionation of gold(I) chloride complexes at 25–200 1C. Geochimica et Cosmochimica Acta, 61, 1971–1983.

Gee, A.R., Dudeney, A.W.L., 1988. Adsorption and crystallization of gold on biological surfaces. In: Kelly DP, Norris PR (eds). Biohydrometallurgy. Science & Technology Letters: London, UK. 437–451.

Geslin, C., Llanos, J., Prieur, D., Jeanthon, C., 2001. The manganese and iron superoxide dismutases protect *Escherichia coli* from heavy metal toxicity. Research in Microbiology, 152, 901-905.

Gibson, D., 1986. A Biological Survey of the Tanami Desert in the Northern Territory. Conservation Commission of the Northern Territory. Technical Report, 30, 258.

Girling, C., Peterson, P., 1980. Gold in plants. Gold Bulletin, 13(4), 151-157.

Giusti, L., Smith, D.G.W., 1984. An electron microprobe study of some Alberta placer gold. Tschermaks Mineralogische und Petrographische, 33, 187-902.

Goldhaber, M.B., 1983. Experimental study of metastable sulphur oxyanion formation during pyrite oxidation at pH 6–9 and 30 ^{o}C. American Journal of Science, 283, 193–217.

Goldschmidt. V.M., 1954. Geochemistry. Clarendon Press: Oxford, UK.

Gorby, Y.A., Yanina, S., McLean, J.S., Rosso, K., Moyles, D., Dohnalkova, A., Beveridge, T.J., Chang, I.S., Kim, B.H., Kim, K.S., Culley, D.E., Reed, S.B., Romine, M.F., Saffarini, D.A., Hill, E.A., Shi, L., Elias, D.A., Kennedy, D.W., Pinchuk, G., Watanabe, K., Ishii, S., Logan, B., Nealson, K.H., Fredrickson, J.K., 2006. Electrically conductive bacterial nanowires produced by *Shewanella oneidensis* strain MR-1 and other microorganisms. Proceedings of the National Academy of Sciences, 103, 11358-11363.

Gray, D., 1998. The aqueous chemistry of gold in the weathering environment. Cooperative Research Centre for Landscape Evolution and Mineral Exploration. Open File Report 38 (Wembley West: Australia).

Groen, J., Craig, J., Rimstidt, J., 1990. The gold-rich formation on electrum grains in placers. The Canadian Mineralogist, 28, 207–228.

Hansen, S.K., Rainey, P.B., Haagensen, J.A., Molin, S., 2007. Evolution of species interactions in a biofilm community. Nature, 445, 533–536.

Harrison, J., Ceri, H., Turner, R., 2007. Multimetal resistance and tolerance in microbial biofilms. Nature Reviews Microbiology, 5, 928-938.

Harrison, J.J., Rabiei, M., Turner, R.J., Badry, E.A., Sproule, K.M., Ceri, H., 2006. Metal resistance in *Candida* biofilms. FEMS Microbiology Ecology, 55, 479-91.

He, Y.H., Yuan, J.Y., Su, F.Y., Xing, X.H., Shi, G.Q., 2006. *Bacillus subtilis* assisted assembly of gold nanoparticles into long conductive nodous ribbons. Journal of Physical Chemistry B, 110(36), 17813-17818.

Higham, D.P., Sadler, P.J., Scawen, M.D., 1986. Gold-resistant bacteria: excretion of cysteine-rich protein by *Pseudomanas cepacia* induced by antiarthritic drug. Journal of Inorganic Biochemistry, 28, 253–261.

Hiskey, B.J., Atluri, V.P., 1988. Dissolution chemistry of gold in silver in different lixiviants. Mineral Processing and extractive Metallurgy Review, 4, 95-134.

Horcas, I., Fernández, R., Gómez-Rodríguez, J., Colchero, J., Gómez-Herrero, J., Baro, A., 2007. *W*SXM: A software for scanning probe microscopy and a tool for nanotechnology. Review of Scientific Instruments, 78.

Hough, R., Noble, R., Hitchen, G., Hart, G., Reddy, S., Saunders, M., Clode, P., Vaughan, D., Lowe, J., Gray, D., Anand, R., Butt, C., Verrall, M., 2008. Naturally occurring gold nanoparticles and nanoplates. Geology, 36, 571-574.

Hough, R., Noble, R., Reich, M., 2011. Natural Gold Nanoparticles. Ore Geology Reviews, 42, 55-61.

Hough, R.M., Butt, C.R.M., Reddy, S.M., Verrall, M., 2007. Gold nuggets: supergene or hypogene? Australian Journal of Earth Sciences, 54, 959-964.

Hutchinson, M.F., McIntyre, S., Hobbs R.J., Stein, J.L., Garnett, S., Kinloch, J., 2005. Integrating a global agro-climatic classification with bioregional boundaries in Australia. Global Ecology and Biogeography, 14, 197-212.

Jian, X., Wasinger, E., Lockard, J., Chen, L., He, C., 2009. Highly sensitive and selective gold(I) recognition by a metalloregulator in Ralstonia metallidurans. Journal of the Chemical Society, 131, 10869-10871.

Johnston, C.W., Wyatt, M.A., Li, X., Ibrahim, A., Shuster, J., Southam, G., Magarvey, N.A., 2013. Gold biomineralization by a metallophore from a gold-associated microbe. Nature Chemical Biology, 9(4), 241-243.

Kalinin, Y.A., Kovalev, K.R., Naumov, E.A., Kirillov, M.V., 2009. Gold in the weathering crust at the Suzdal' deposit (Kazakhstan). Russian Geology Geophysics, 50(3), 174-187.

Kampf, A.R., Keller, P.C., 1982. The Colorado quartz mine, Mariposa County, California: a modern source of crystallized gold. The Mineralogical Record, 13, 347–354.

Karthikeyan, S., Beveridge, T., 2002. *Pseudomonas aeruginosa* biofilms react with and precipitate toxic soluble gold. Environmental Microbiology 4, 667-675.

Kashefi, K., Tor, J.M., Nevin, K.P., Lovley, D.R., 2001. Reductive precipitation of gold by dissimilatory Fe(III)-Reducing Bacteria and Archaea. Applied and Environmental Microbiology, 67 (7), 3275-3279.

Keeling, J.R., 1993. Microbial influence in the growth of alluvial gold from Watts Gully, South Australia. Quarterly Geological Notes (Geological Survey of South Australia), 126, 12–19.

Kenney, J.P.L., Song, Z., Bunker, B.A., Fein, J.B., 2012. An experimental study of Au removal from solution by Inactive bacterial cells and their exudates. Geochimica et Cosmochimica Acta, 87, 51-60.

Khoo, K., Ting, Y., 2001. Biosorption of gold by immobilized fungal biomass. Biochemical Engineering Journal, 8, 51 59.

Kirsten, A., Herzberg, M., Voigt, A., Seravalli, J., Grass, G., Scherer, J., Nies, D.H., 2011. Contributions of five secondary metal uptake systems to metal homeostasis of *Cupriavidus metallidurans* CH34. Journal of Bacteriology, 193, 4652–4663.

Knight, J., Morison, S., Mortensen, J., 1999. Relationship between placer gold shape, rimming, and distance of fluvial transport as exemplified by gold from the Klondike district, Yukon Territory, Canada. Economic Geology, 94, 635-648.

Knowles, C., 1976. Microorganisms and cyanide. Bacteriological Reviews, 40, 652-680.

Konishi, Y., Tsukiyama, T., Ohno, K., Saitoh, N., Nomura, T., Nagamine, S., 2006. Intracellular recovery of gold by microbial reduction of $AuCl4^-$ ions using the anaerobic bacterium *Shewanella algae*. Hydrometallurgy, 81, 24-29.

Konisi, Y., Tsukiyama, T., Tachimi, T., Saitoh, N., Nomura, T., Nagamine, S., 2007. Microbial deposition of gold nanoparticles by the metal-reducing bacterium Shewanella algae. Electrochimica Acta, 53, 186-192.

Korobushkina, E.D., Karavaiko, G.I., Korobushkin, I.M., 1983. Biochemistry of gold. In: Hallberg R (ed). Environmental Biogeochemistry Ecological Bulletins, (35), 325–333.

Krauskopf, K.B., 1951. The solubility of gold. Economic Geology, 46, 858–870.

Kuimova, N.G., Pavlova, L.M., 2011. Biogenic gold accumulation in brown coals at the peat stage. Doklady Earth Sciences, 443, 347-352.

Kulkarni, M.G., Stirk, W.A., Southway, C., Papenfus, H.B., Swart, P.A., Lux, A., Vaculík M., Kumar, V. Yadav, S.K., 2009. Plant-mediated synthesis of silver and gold nanoparticles and their applications. Journal of Chemical Technology & Biotechnology, 84(2), 151-157.

Kumar, V., Yadav, S., 2009. Plant-mediated synthesis of silver and gold nanoparticles and their applications. Journal of Chemical Technology and Biotechnology, 84(2), 151-157.

Kunert, J., Stransky, Z., 1988. Thiosulfate production from cystine by the kerarinolytic prokaryote *Streptomyces fradiae*. Archives of Microbiology, 150, 600–601.

Lakin H.W , Curtin, G.C., Hubert, A.E., Shacklette, H.T., Doxtader, G., 1974. Geochemistry of gold in the weathering cycle. U.S. Geological Bulletin, 1330, 80.

Ledrich, M., Stemmler, S., Laval-Gilly, P., Foucaud, L., Falla, J., 2005. Precipitation of silver-thiosulfate complex and immobilization of silver by *Cupriavidus metallidurans* CH34. Biometals, 18, 643-650.

Leicht, W.C., 1982. California gold. The Mineralogical Record, 13, 375–.

Lengke, M., Fleet, M., Southam, G., 2006a. Morphology of Gold Nanoparticles Synthesized by Filamentous Cyanobacteria from Gold(I)-Thiosulfate and Gold(III)-Chloride Complexes. Langmuir, 22, 2780-2787.

Lengke, M., Ravel, B., Fleet, M., Wanger, G., Gordon, R., Southam, G., 2006b. Mechanisms of Gold Bioaccumulation by Filamentous Cyanobacteria from Gold(III)-chloride Complexes. Environmental Science Technology, 40, 6304-6309.

Lengke, M., Southam, G., 2005. The effect of thiosulfate-oxidizing bacteria on the stability of the gold-thiosulfate complex. Geochimica et Cosmochima Acta, 69, 3759-3772.

Lengke, M., Southam, G., 2006. Bioaccumulation of gold by sulfate-reducing bacteria cultured in the presence of gold(I)-thiosulfate complex. Geochimica et Cosmochima Acta, 70, 3646-3661.

Lengke, M., Southam, G., 2007. The Deposition of Elemental Gold from Gold(I)-Thiosulfate Complexes Mediated by Sulfate-Reducing Bacterial Conditions. Society of Economic Geologists, 102, 109-126.

Leybourne, M.I., 2001. Mineralogy and geochemistry of suspended sediments from groundwaters associated with undisturbed Zn-Pb massive sulfide deposits, Bathurst Mining Camp, New Brunswick, Canada. The Canadian Mineralogist, 39, 1597-1616.

Lieber, W., 1982. European gold. The Mineralogical Record, 6, 359–364.

Lintern, M.J., Sheard, M.J., Chivas, A.R., 2006. The source of pedogenic carbonate associated with gold-calcrete anomalies in the western Gawler Craton, South Australia. Chemical Geology, 235(3-4), 299-324.

Lloyd, J.R., 2003. Microbial reduction of metals and radionuclides. FEMS Microbiology Reviews, 27, 411–425.

Lovley, D.R., 1995. Microbial reduction of iron, manganese, and other metals. Advanced Agronomy, 54, 175-231.

Lungwitz, E., 1900. The lixiviation of gold deposits by vegetation. Engineering and Mining Journal, 69, 500-502.

Ma´rquez-Zavalı´a, M.F., Southam, G., Craig, J.R., Galliski, M.A., 2004. Morphological and chemical study of placer gold from the San Luis Range, Argentina. The Canadian Mineralogist, 42, 55–68.

Mack, C., Wilhelmi, B., Duncan, J.R., Burgess, J.E., 2007. Biosorption of precious metals. Biotechnology Advances, 25(3), 264-271.

Madigan, M.T., Martinko, J.M., 2006. Brock—Biology of Microorganisms. Prentice Hall: New York, USA, 11th edn.

Malvankar, N.S., Vargas, M., Nevin, K.P., Franks, A.E., Leang, C., Kim, B-C., Inoue, K., Mester, T., Covalla, S.F., Johnson, J.P., Rotello, V.M., Tuominen, M.T., Lovley, D.R., 2011. Tunable metallic-like conductivity in microbial nanowire networks. Nature Nanotechnology, 6.

Mann, A.W., 1984. Mobility of gold and silver in lateritic weathering profiles: some observations from Western Australia. Economic Geology, 79, 38–50.

Marsden, J.O., House, C.I., 2006. The Chemistry of Gold Extraction (Second Edition). Littleton, CO: Society for Mining, metallurgy and Exploration, Inc., Littleton, Colorado, 651.

McCready, A.J., Parnell, J., Castro, L., 2003. Crystalline placer gold from the Rio Neuquen, Argentina: Implications for the gold budget in placer gold formation. Economic Geology and the Bulletin of the Society of Economic Geologists, 98, 623-633.

McHugh, J.B., 1988. Concentration of gold in natural waters. Journal of Geochemical Exploration, 30, 85–94.

McPhail, D.C., Usher, A., Reith, F., 2006. On the mobility of gold in the regolith: results and implications from experimental studies. In: Fitzpatrick RW, Shand P (eds). Proceeding of the CRC LEME Regolith Symposium. Cooperative Research Centre for Landscape Environments and Mineral Exploration: Australia, 227–229

Mergeay, M., Monchy, S., Vallaeys, T., Auquier, V., Benotmane, A., Bertin, P., Taghavi, S., Dunn, J., van der Lelie, D., Wattiez, R., 2003. *Ralstonia metallidurans*, a bacterium specifically adapted to toxic metals: towards a catalogue of metal-responsive genes. FEMS Microbiology Reviews, 27, 385-410.

Mergeay, M., Nies, D., Schlegel, H.G., Gerits, J., Charles, P., van Gijsegem, F., 1985. *Alcaligenes eutrophus* CH34 is a facultative chemolithotroph with plasmid-bound resistance to heavy metals. Journal of Bacteriology, 162, 328-334.

Michaels, R., Corpe, W., 1964. Cyanide Formation by *Chromobacterium violaceum*. Journal of Bacteriology 89, 106-112.

Miles, A.A., Misra, S.S., Irwin, J.O., 1938. The estimation of the bactericidal power of the blood. Journal of Hygiene 38(6), 732-749.

Mineyev, G.G., 1976. Organisms in the gold migration accumulation cycle. Geokhimiya 13, 577–582.

Mishra, B., Boyanov, M., Bunker, B. A., Kelly, S. D., Kemner, K. M., Fein, J. B., 2010. High- and low-affinity binding sites for Cd on the bacterial cell walls of *Bacillus subtilis* and *Shewanella oneidensis*. Geochimica et Cosmochima Acta, 74, 4219.

Mittelman, M.W., Geesey, G.G., 1985. Copper-binding characteristics of exopolymers from a freshwater-sediment bacterium. Applied Environmental Microbiology, 49, 846-851.

Mohammadnejad, S., Provis, J.L., van Deventer, J.S.J., 2011. Gold sorption by silicates in acidic and alkaline chloride media. International Journal of Mineral Processing, 100, 149–156.

Monchy, S., Vallaeys, T., Bossus, A., Mergeay, M., 2006. Metal transport ATPase genes from *Cupriavidus metallidurans* CH34: a transcriptomic approach. International Journal of Environmental Analytical Chemistry, 86, 677-692.

Moroni, M., Girardi, V.A.V., Ferrari, A., 2001. The, Serra dos Carajas (Para State, Brazil): geological and geochemical indications for a composite mineralising process. Mineralium Deposita, 36(8), 768-785.

Morteani, G., 1999. In: Schmidbaur H (ed). Gold: Progress in Chemistry, Biochemistry and Technology. Wiley and Sons. Chapter 2.

Mossman, D.J., Reimer, T., Durstling, H., 1999. Microbial processes in gold migration and deposition: Modern analogues to ancient deposits. Geoscience Canada, 26(3), 131-140.

Nakagawa, M., Santosh, M., Nambiar, C.G., Matsubara C., 2005. Morphology and Chemistry of Placer Gold from the Attappadi Valley, Southern India. International Association for Gondwana Research. 8(2), 213-222.

Nakajima, A., 2003. Accumulation of gold by microorganisms. World Journal of Microbiology and Biotechnology, 19, 369-374.

Nguyen, T.M.P., Sheng, X.X., Ting, Y.P., Pehkonen S.O., 2008. Biocorrosion of $AISI_30_4$ stainless steel by *Desulfovibrio desulfuricans* in seawater. Industrial & Engineering Chemistry Research, 47, 4703-4711.

Nies, D.H., 1999. Microbial heavy metal resistance. Applied Microbiology Biotechnology, 51, 730-750.

Nies, D., 2000. Heavy metal-resistant bacteria as extremeophiles: molecular physiology and biotechnological use of *Ralstonia sp*. CH34. Extremophiles, 4, 77-82.

Nies, D.H., 2003. Efflux-mediated heavy metal resistance in prokaryotes. FEMS Microbiology Reviews, 27, 313-339.

Nies, D., Mergeay, M., Friedrich, B., Schlegel, H.G., 1987. Cloning of plasmid genes encoding resistance to cadmium, zinc, and cobalt in *Alcaligenes eutrophus* CH34. Journal of Bacteriology, 169, 4865– 4868.

Niu, H., Volesky, B., 1999. Characteristics of gold biosorption from cyanide solution. Journal of chemical technology and biotechnology, 74, 778-784.

Nordstrom, D.K., Southam, G., 1997. Geomicrobiology of sulfide metal oxidation. Reviews in Mineralogy, 35, 361–390.

Pagnanelli, F., Papini, M.P., Toro, L., Trifoni, M., Veglio, F., 2000. Biosorption of metal ions on *Arthrobacter* sp.: Biomass characterization and biosorption modeling. Environmental Science & Technology, 34(13), 2773-2778.

Pal, A., Paul, A.K., 2008. Microbial extracellular polymeric substance; central elements in heavy metal bioremediation. Indian Journal of Microbiology, 48, 49-64.

Pan, P., Wood, S.A., 1991. Gold-Chloride Complexes In Very Acidic Aqueous-Solutions And At Temperatures 25-300-Degrees-C - A Laser Raman-Spectroscopic Study. Geochimica et Cosmochimica Acta, 55(8), 2365-2371.

Parfitt, G.D., Rochester, C.H., 1983. Adsorption from Solution at the Solid/Liquid Interface. Academic Press, New York. 416.

Paterson, D., de Jonge, M.D., Howard, D.L., Lewis, W., McKinlay, J.A., Starritt A., Kusel, M., Ryan, C.G., Kirkham, R., Moorhead, G., Siddons, D.P., 2011. The X-ray Fluorescence Microscopy Beamline at the Australian Synchrotron. American Institute of Physics Conference Proceedings, 1365, 219–222.

Peachey, Y., 1999. Aeromagnetic image interpretation and potential target area definition at Lawlers. Homestake Gold of Australia. Technical Report Number, 871, 11.

Pedersen, K., 1993. The deep subterranean biosphere. Earth-Science Reviews, 34, 243-260.

Peeters, E., Nelis, H., Coenye, T., 2008. Resistance of planktonic and biofilm-grown *Burkholderia cepacia* complex isolates to the transition metal gallium. Journal of Antimicrobial Chemotherapy, 61, 1062-1065.

Petts, A., Hill, S., Worrall, L., 2009. Termite species variations and significance for termitaria biogeochemistry: towards a robust approach for mineral exploration. Geochemistry: Exploration Environment, Analysis, 9, 257-266.

Phillips, G.N., Thomson, D., Kuehn, C.A., 1998. Deep Weathering of Deposits in the Yilgarn and Carlin Gold Provinces. Regolith 1998: New Approaches to an Old Continent. CRC-LEME, 1-22.

Pizzaro, R., Mcbeth, J., Potter, G., 1974. Heap leaching practice at the Carlin Gold Mining Co., Carlin, Nevada. Annual American Institute of Mining, Metallurgical, and Petroleum Engineers Meeting, Dallas, TX, February, 23-28.

Raju, D., Mehta, U.J., Ahmad, A., 2012. Phytosynthesis of intracellular and extracellular gold nanoparticles by living peanut plant (*Arachis hypogaea* L.). Biotechnology and Applied Biochemistry, 59(6), 471-478.

Ran, Y., Fu, J., Rate, A.W., Gilkes, R.J., 2002. Adsorption of Au(I, III) complexes on Fe, Mn oxides and humic acid. Chemical Geology, 185, 33-49.

Rasmussen, U., Svenning, M.M., 1998. Fingerprinting of cyanobacteria based on PCR with primers derived from short and long tandemly repeated repetitive sequences. Applied Environmental Microbiology, 64, 265-272.

Rawlings, D., Silver, S., 1995. Mining with Microbes. Biotechnology, 13, 773-778.

Rawlings, D.E., Johnson, D.B., 2007. The microbiology of biomining: development and optimization of mineral-oxidizing microbial consortia. Microbiology. 153, 315-324.

Reith, F., Etschmann, B., Brewe, D.L., Vogt, S., Brugger, J., 2009a. The distribution of gold in biogenic and abiogenic carbonates. Geochimica et Cosmochimica Acta, 73(13), 1942-1956.

Reith, F., Etschmann, B., Grosse, C., Moors, H., Benotmane, M.A., Monsieurs, P., Grass, G., Doonan, C., Vogt, S., Lai, B., Martinez-Criado, G., George, G.N., Nies, D.H., Mergeay, M., Pring, A., Southam, G., Brugger, J., 2009b. Mechanisms of gold biomineralization in the bacterium *Cupriavidus metallidurans*. Proceedings of the National Academy of Sciences, 106 (42), 17757-17762

Reith, F., Fairbrother, L., Nolze, G., Wilhelmi, O., Clode, P.L., Gregg, A., Parsons, J.E., Wakelin, S.A., Pring, A., Hough, R., Southam, G., Brugger, J.

2010. Nanoparticle factories: Biofilms hold the key to gold dispersion and nugget formation. Geology, 38(9), 843-846.

Reith, F., Lengke, M., Falconer, D., Craw D., Southam, G., 2007. The geomicrobiology of gold. The ISME Journal, 1, 1-18.

Reith, F., McPhail, D., Christy, A., 2005. *Bacillus cereus*, gold and associated elements in soil and other regolith samples from Tomakin Park Gold Mine in southeastern New South Wales, Australia. Journal of Geochemical Exploration, 85, 81-98.

Reith, F., Rogers, S., McPhail, D., Webb, D., 2006. Biomineralization of Gold: Biofilms on Bacterioform Gold. Science, 313, 233-236.

Reith, F., Stewart, L., Wakelin, S.A., 2012. Supergene gold transformation: Secondary and nano-particulate gold from southern New Zealand. Chemical Geology, 320-321, 32-45.

Reith, F., McPhail, D.C., 2006. Effect of resident microbiota on the solubilization of gold in soils from the Tomakin Park Gold Mine, New South Wales, Australia. Geochimica et Cosmochimica Acta, 70, 1421-1438.

Reith, F., McPhail, D.C., 2007. Microbial influences on solubilisation and mobility of gold and arsenic in regolith samples from two gold mines in semi-arid and tropical Australia. Geochimica et Cosmochimica Acta, 71, 1183–1196.

Reith, F., Rogers, S., 2008. Assessment of bacterial communities in auriferous and non-auriferous soils using genetic and functional fingerprinting. Geomicrobiology Journal, 25(3-4), 203-215.

Reith, F., 2005. The geomicrobiology of gold - Interaction of bacteria with gold in Australian soils and deeper regolith materials., in Quaternary and Regolith Sciences, The Australian National University: Canberra, 252.

Rodgers, P.B., Knowles, C.J., 1978. Cyanide Production And Degradation During Growth Of Chromobacterium-Violaceum. Journal of General Microbiology, 108, 261-267.

Rouf, M.A., 1964. Spectrochemical analysis of inorganic elements in bacteria. Journal of Bacteriology, 6, 1545–1549.

Ryan, C.G., 2001. The new CSIRO-GEMOC nuclear microprobe: First results, performance and recent applications. Nuclear Instruments and Methods in Physics Research Section B, 181, 12-19.

Ryan, C.G., Jamieson, D.N., 1993. Dynamic analysis - online quantitative Pixe microanalysis and its use in overlap-resolved elemental mapping. Nuclear Instruments and Methods in Physics Research Section B, 77, 203-214.

Ryan, C.G., Siddons, D.P., Kirkham, R., Dunn, P.A., Kuczewski, A., Moorhead, G., De Geronimo, G., Paterson, D.J., de Jonge, M.D., Hough, R.M., Lintern, M.J., Howard, D.L., Kappen, P., Cleverley, J., 2010. The new Maia detector system: methods for high definition trace element imaging of natural material. In M.A. Denecke, and C.T. Walker, Eds. X-Ray Optics and Microanalysis, Proceedings, 1221, 9-17.

Sand, W., Gehrke, T., Jozsa, P.G., Schippers, A., 2001. (Bio)chemistry of bacterial leaching—direct vs indirect bioleaching. Hydrometallurgy, 59, 159–175.

Sambrook, J., Fritsch, E.F., Maniatis, T., 1989. Molecular cloning: a laboratory manual, 2nd ed. Cold Spring Harbor Laboratory, Cold Spring Harbor, NY.

Savvaidis, I., Karamushka, V.I., Lee, H., Trevors, J.T., 1998. Micro-organism-gold interactions. BioMetals, 11, 69–78.

Schofield, E.J., Ingham, B., Turnbull, A., Toney, M.F, Ryan, M.P., 2008. Strain development in nanoporous metallic foils formed by dealloying. Applied Physics Letters, 92, 3.

Smith, R.M., Martell, A.E., 1976. Critical stability constants. Inorganic Complexes, 4, 86-87.

Sneath, P.H.A 1972. Identification methods applied to Chromobacterium. In “Identification methods for microbiologists”. EDS Skinner, F.A., and Lovelock, D.W. Academic press, London, 15-20.

Song, Z., Kenney, J.P.L., Fein, J.B., Bunker, B.A., 2012. An X-ray Absorption Fine Structure study of Au adsorbed onto the non-metabolizing cells of two soil bacterial species. Geochimica et Cosmochimica Acta, 86, 103-117.

Southam, G., Beveridge, T.J., 1994. The in vitro formation of placer gold by bacteria. Geochimica et Cosmochimica Acta, 58, 4227-4230.

Southam, G., Beveridge, T.J., 1996. The occurrence of sulfur and phosphorus within bacterially derived crystalline and pseudeocrystalline gold formed in vitro. Geochimica et Cosmochimica Acta, 60, 4369–4376.

Southam, G., Fyfe, W.S., Beveridge, T.J., 2000. The immobilization of free ionic gold and asparagine-complexed ionic gold by *Sporosarcina ureae*: the importance of organo-gold complexes in gold transport. Minerals and Metallurgic Processing Journal, 17, 129–132.

Southam, G., Lengke, M.F., Fairbrother, L., Reith, F., 2009. The Biogeochemistry of Gold. Elements 5(5), 303-307.

Southam, G., Saunders, J., 2005. The Geomicrobiology of Ore Deposits. Economic Geology and the Bulletin of the Society of Economic Geologists, 100, 1067-1084.

Stoffregen, R., 1986. Observation on the behaviour of gold during supegene oxidation at Summitville, Colorado, USA, and implications for electrum stability in the weathering environment. Applied Geochemistry, 1, 549–558.

Stolz, J.F., Oremland, R.S., 1999. Bacterial respiration of arsenic and selenium. FEMS Microbiology Reviews, 23, 615–627.

Stone, A., 1997. Reactions of extracellular organic ligands with dissolved metal ions and mineral surfaces. Reviews in Mineralogy, 35, 309–341.

Stoyanov, J.V., Brown, N.L., 2003. The *Escherichia coli* copper-responsive copA promoter is activated by gold. The Journal of Biological Chemistry, 278, 1407–1410.

Ta, C., 2013. The speciation of gold in mine wastes and natural waters. School of Chemistry and Physical Sciences, Faculty of Science and Engineering. Flinders University of South Australia: 134.

Tebo, B.M., Johnson, H.A., McCarthy, J.K., Templeton, A.S., 2005. Geomicrobiology of manganese(II)-oxidation. Trends in Microbiology, 13, 421–428.

Tebo, B.M., Obraztsova, A.Y., 1998. Sulfate-reducing bacterium grows with Cr(VI), U(VI), Mn(IV), and Fe(III) as electron acceptors. FEMS Microbiology Letters, 162, 193–198.

Tsuruta, T., 2004. Biosorption and recycling of gold using various microorganisms. The Journal of General and Applied Microbiology, 50, 221-228.

Usher, A., McPhail, D.C., Brugger, J., 2009. A spectrophotometric study of aqueous Au(III) halide-hydroxy complexes at 25˚C. Geochimica et Cosmochimica Acta, 73, 3359-3380.

Van der Gast, C.J., Knowles, C.J., Starkey, M., Thompson, I.P., 2002. Selection of microbial consortia for treating metal-working fluids. Journal of Industrial Microbiology & Biotechnology, 29(1), 20-27.

van Houdt, R., Monchy, S., Leys, N., Mergeay, M., 2009. New mobile genetic elements in *Cupriavidus metallidurans* CH34, their possible roles and occurrence in other bacteria. Antonie Van Leeuwenhoek, 96, 205–226.

Varshal, G.M., Velyukhanova, T.K., Baranova, N.N., 1984. The geochemical role of gold(III) fulvate complexes. Geochemistry International, 19, 94–98.

Vlassopoulos, D., Wood, S.A., Mucci, A., 1990a. Gold speciation in natural waters: I. Solubility and hydrolysis reactions of gold in aqueous solution. Geochimica et Cosmochima Acta, 54, 3–12.

Vlassopoulos, D., Wood, S., Mucci, A., 1990b. Gold speciation in natural waters: II. The importance of organic complexing-Experiments with some simple model ligands. Geochimica et Cosmochima Acta, 54, 1575-1586.

Wakelin, S.A., Colloff, M.J., Kookana, R.S., 2008. Effect of wastewater treatment plant effluent on microbial function and community structure in the sediment of a freshwater stream with variable seasonal flow. Applied Environmental Microbiology, 74, 2659–2668.

Watterson, J.R., 1992. Preliminary evidence for the involvement of budding bacteria in the origin of alaskan placer gold - reply. Geology, 21(3), 280-280.

Watterson, J.R., 1994. Artifacts resembling budding bacteria produced in placer-gold amalgams by nitric acid leaching. Geology, 22, 1144-1146.

Webster, J.G., 1986. The solubility of gold and silver in the system Au-Ag-S-O2-H2O at 25 1C and 1 atm. Geochimica et Cosmochima Acta, 50, 1837–1845.

Webster, J.G., Mann, A.W., 1984. The influence of climate, geomorphology and primary geology on the supergene migration of gold and silver. Journal of Geochemical Exploration, 22, 21–42.

Westall, F., Boni, L., Guerzoni, E., 1995. The Experimental Silicification of Microorganisms. Palaeontology, 30, 495-528.

Westall, F., de Wit, M.J., Dann, J., van der Gaast, S., de Ronde, C.E.J., Gerneke, D., 2001. Early Archean fossil bacteria and biofilms in hydrothermally-influenced sediments from the Barberton greenstone belt, South Africa. Precambrian Research, 106, 93-116.

Wiesemann, N., Mohr, J., Grosse, C., M. Herzberg, M., Hause, G., Reith, F., Nies, D.H., 2013. Influence of Copper Resistance Determinants on Gold Transformation by *Cupriavidus metallidurans* Strain CH34. Journal of Bacteriology, 195(10), 2298-2308.

Wilford, J., 2003. Granites-Tanami Region, Northern Territory. CSIRO LEME, Geoscience Australia, 1-5.

Wilson, A.F., 1984. Origin of quartz-free gold nuggets and supergene gold found in laterites and soils - A review and some new observations. The Australian Journal of Earth Sciences, 31, 303-316.

Wilson-Corral, V., Anderson, C., Rodriguez-Lopez, M., Arenas-Vargas, M., Lopez-Perez, J., 2013., Phytoextraction of gold and copper from mine tailings with *Helianthus annuus* L. and *Kalanchoe serrata* L. Minerals Engineering, 24(13), 1488-1494.

Witkiewicz, P.L., Shaw, C.F., 1981. Oxidative cleavage of peptide and protein disulphide bonds by gold(III): a mechanism for gold toxicity. Journal of the Chemical Society, Chemical Communications, 21, 1111–1114.

Workentine, M.L., Harrison, J.J., Stenroos, P.U., Ceri, H., Turner, R.J., 2008. *Pseudomonas fluorescens* view of the periodic table. Environmental Microbiology, 10, 238-250.

Wulser, P.A., Brugger, J., Foden, J., Pfeiffer, H.R., 2011. The Sandstone-hosted Beverley Uranium Deposit, Lake Frome basin, South Australia: Mineralogy, Geochemistry and Time-Constrained Model for its Genesis. Economic Geology, 106, 835-867.

Wygralak, A., Mernagh, T., Fraser, G., Huston, D., Denton, G., McInnes, B., Crispe, A., Vandenberg L., 2001. Gold mineral systems in the Tanami region. AGSO Research Newsletter, 34, 2-14.

Yee, N., Fein, J. 2001. Cd adsorption onto bacterial surfaces: A universal adsorption edge? Geochimica et Cosmochimica Acta, 65(13), 2037-2042.

Youngson, J., Craw, D., 1993. Gold nugget growth during tectonically induced sedimentary recycling, Otago, New Zealand. Sedimentary Geology, 84, 71–88.

Youngson J., Craw D., 1995. Evolution of placer gold deposits during regional uplift, Central Otago, New Zealand. Economic Geology, 90, 731-745.